

**Newcastle**  
University

**Identifying Components of the TGF  $\beta$ -1 Pathway in  
Renal Fibrosis**

**Thesis submitted in partial fulfilment of the requirement of the degree of  
Doctor of Philosophy**

**Victoria Gemma Shuttleworth**

**Institute of Cellular Medicine**

**Faculty of Medical Sciences**

**Newcastle University**

**November 2018**



## Abstract

Chronic Kidney Disease (CKD) is characterised by the expression of alpha smooth muscle actin ( $\alpha$ -SMA) and Collagen from the aberrant infiltration and proliferation of myofibroblasts. This results in renal fibrosis and ultimately end stage renal disease (ESRD). CKD is a growing health problem resulting in significant costs to the NHS, making the identification of novel therapeutic targets for the treatment of CKD a key clinical priority.

Transforming growth factor  $\beta$ -1 (TGF  $\beta$ -1) plays a critical role in the persistent activation of myofibroblasts leading to fibrosis. TGF  $\beta$ -1 signals through transmembrane serine-threonine kinase type I and II receptors to phosphorylate SMAD3, a downstream intracellular receptor-regulated SMAD protein (R-SMAD). Upon phosphorylation, activated SMAD3 translocates to the nucleus to regulate the transcription of fibrotic genes such as  $\alpha$ -SMA and Collagen. Studies have shown SMAD3 to have an important role in fibrosis.

This work sought to identify novel components of TGF  $\beta$ -1 signalling in order to increase our understanding of the pathway and identify potential therapeutic targets to treat CKD. This was achieved through siRNA and compound screening in renal cells.

Here, three novel components of the TGF  $\beta$ -1 pathway are described. SET9, a lysine methyltransferase and Aurora Kinase A, a serine/threonine kinase were shown to interact with SMAD3 to upregulate its transcriptional activity. Inhibitors of SET9 and Aurora Kinase A were shown to have anti-fibrotic activities by reducing TGF  $\beta$ -1 signalling. Additionally, SETDB1, a different lysine methyltransferase was also shown to interact with SMAD3, acting as a brake on TGF  $\beta$ -1 signalling. Identification of novel components of TGF  $\beta$ -1 signalling in renal fibrosis will aid our understanding of the mechanisms of fibrosis to develop novel therapeutics for the treatment of CKD.

## **Acknowledgements**

I would like to thank my two supervisors Dr. Ian Logan and Prof. Neil Sheerin for all of their support throughout my PhD. The time they sacrificed and the guidance and knowledge they provided me with enabled me to learn and progress through my PhD. Their patience and continuous support allowed me to thoroughly enjoy my PhD years.

I would like to give thanks to the following people for their help and contribution towards this work. Jess Ng for her contribution to the small molecule inhibitor screen, Dr Ana Moles for her expertise with the UUO mouse study and Prof. Fiona Oakley for her expertise with the CCl<sub>4</sub> mouse study and HSC isolation.

I would also like to thank the other members of the kidney group Aldi Simutorang, Lucy Bates, Rishab Kapoor and Wisnu Tirtayasa for their kindness, support and expertise in the lab.

I would like to thank Glaxo Smith Kline (GSK) and Northern Counties Kidney Research Fund (NCKRF) for funding my PhD, as without their contributions this work would not have been possible.

Lastly, I am most thankful to my parents Joanne and Brendan and my son Hugo. Without you I would not have been able to achieve this PhD, you have sacrificed so much to enable me to reach my goal, for which I am sincerely grateful.

# Table of Contents

Abstract.....	iii
Acknowledgements .....	iv
List of Tables .....	ix
List of Figures.....	x
List of Abbreviations .....	xii
Chapter 1. Introduction.....	1
1.1 General Anatomy of the Kidney .....	1
1.1.1 General Structure and Function of the Kidney .....	1
1.1.2 The Nephron.....	1
1.2 Chronic Kidney Disease .....	3
1.2.1 Definition of Fibrosis .....	3
1.2.2 Renal Fibrosis in Chronic Kidney Disease .....	3
1.2.3 Chronic Kidney Disease: Definition and Disease Staging.....	4
1.2.4 Epidemiology, Risk and Costs of CKD .....	5
1.2.5 Aetiology of CKD .....	5
1.2.6 Management of CKD .....	6
1.3 Contribution of Cell Types to Renal Fibrosis .....	8
1.3.1 Renal Tubular Epithelial Cells .....	8
1.3.2 Fibroblasts .....	8
1.3.3 Origins of Myofibroblasts in Renal Fibrosis.....	9
1.4 Experimental Models of Renal Fibrosis and CKD .....	12
1.4.1 Cellular Models of CKD .....	12
1.4.2 Whole Organism Models of CKD.....	12
1.4.3 Limitations of CKD Models to Human Disease .....	13
1.5 TGF $\beta$ Signalling .....	13
1.5.1 The TGF $\beta$ Superfamily .....	13
1.5.2 The TGF $\beta$ -1 Signalling Pathway .....	15
1.5.3 The Role of TGF $\beta$ -1 in Human Disease .....	16
1.5.4 The Role of TGF $\beta$ -1 in Renal Fibrosis .....	17
1.6 SMAD Signalling .....	18
1.6.1 The SMAD Signalling Protein Family.....	18
1.6.2 The SMAD3 Transcription Factor .....	19
1.6.3 The Role of SMAD3 in Renal Fibrosis.....	20

1.7 Lysine Methyltransferases .....	21
1.7.1 The SET-domain Lysine Methyltransferase Family .....	21
1.7.3 SET9.....	22
1.7.4 SETDB1 .....	23
1.7.5 SET9 and SETDB1 in Human Disease.....	23
1.8 Aurora Kinase Signalling.....	24
1.8.1 The Aurora Kinase Protein Family .....	24
1.8.2 The Role Aurora Kinases in Human Disease.....	25
1.9 Aims.....	25
Chapter 2: Materials and Methods .....	26
2.1 Risk Assessment .....	26
2.2 Mammalian Cell Culture and Compounds .....	26
2.2.1 Mammalian Cell Culture.....	26
2.2.2 Cell Subculturing .....	27
2.2.3 Cell Storage.....	27
2.2.4 Compounds .....	27
2.3 Plasmids .....	28
2.4 siRNA and DNA Plasmid Transfection .....	28
2.4.1 siRNA Transfection .....	28
2.4.2 Plasmid DNA transfection .....	29
2.4.3 Stable cell cloning.....	29
2.4.4 Methyltransferase siRNA Screen.....	30
2.5 Isolation of Primary Renal Fibroblast (PRF) Cells.....	30
2.6 SDS-poly acrylamide gel electrophoresis (SDS-PAGE) and Western blotting (WB) ...	31
2.6.1 SDS-PAGE.....	31
2.6.2 Western Blotting (WB) .....	31
2.7 Bacterial Transformation, Plasmid DNA Isolation and Gel Electrophoresis .....	33
2.7.1 Bacterial transformation of plasmid DNA .....	33
2.7.2 Amplification of transformed DNA .....	33
2.7.3 Plasmid DNA Extraction.....	33
2.7.4 Agarose Gel Electrophoresis.....	33
2.8 Protein Purification .....	34
2.9 Nuclear and Cytoplasmic Extractions.....	34
2.10 Immunoprecipitation: Cell Lysates, Purified Proteins and Nuclear Cell Fractions.....	35
2.10.1 Immunoprecipitation from Cell Lysates .....	35
2.10.2 Immunoprecipitation with Nuclear Cell fractions.....	35

2.10.3 Immunoprecipitation with Purified Proteins .....	35
2.11 Proliferation Assay .....	36
2.12 Protein Half-Life Assay .....	36
2.13 Ubiquitylation .....	36
2.14 Immunofluorescence.....	36
2.15 Luciferase Reporter Assay .....	37
2.15.1 Cell Transfection .....	37
2.15.2 Luciferase Assay .....	37
2.15.3 BCA Assay .....	37
2.16 Wound Healing Assay .....	38
2.17 Collagen Contractility Assay .....	38
2.18 Chromatin Immunoprecipitation (ChIP).....	38
2.19 <i>In Vitro</i> kinase reactions .....	39
2.20 Flow cytometry .....	39
2.21 Unilateral Ureteral Obstruction (UUO) Model of Renal Fibrosis .....	39
2.22 Immunohistochemistry .....	40
2.22.1 Immunohistochemistry: $\alpha$ -SMA, Phospho-SMAD3, Phospho-Aurora A, Collagen I and III.....	40
2.22.2 Picro-Sirius Red .....	41
2.22.3 Masson's Trichrome.....	41
2.22.4 Imaging and analysis .....	41
2.22.5 Acute CCl <sub>4</sub> Liver Injury Model.....	42
2.22.6 $\alpha$ -SMA Immunohistochemistry .....	42
2.23 Isolation of Stellate Cells .....	42
2.23.1 Obtaining the Liver from the Mouse.....	42
2.23.2 Processing the Liver to Isolate Hepatic Stellate Cells (HSC) .....	42
2.24 Statistical Analyses .....	43
Chapter 3. SMAD3:SET9 Interaction in the TGF $\beta$ -1 Signalling Pathway .....	44
3.1 Introduction and Objectives .....	44
3.2 Results.....	46
3.2.1 SMAD3 Interacts with SET9 .....	46
3.2.2 SMAD3 Interacts with SET9 Through its NL Domain .....	47
3.2.3 SET9 Regulates SMAD3 Nuclear Import and Protein Turnover.....	49
3.2.4 Characterisation of Mouse Embryonic Cell Lines (MEFs).....	53
3.2.5 SET9 is Required for Fibroblast Migration in Wound Healing Assays.....	55
3.2.6 SET9 is Required for Collagen Contractility Mediated by Fibroblasts .....	59

3.2.7 Isolation and Characterisation of Primary Human Renal Fibroblasts (PRFs) .....	60
3.2.8 Treatment of PRFs with SET9 Inhibitor Reduces Expression of Pro-Fibrotic Markers .....	63
3.2.9 Treatment with SET9 Inhibitor Reduced Wound Healing and Collagen Contractility of PRFs.....	63
3.2.10 SET9 Regulates TGF $\beta$ -1-driven $\alpha$ -SMA Expression.....	66
3.3 Discussion.....	68
Chapter 4. The Role of Methyltransferase SETDB1 in TGF $\beta$ -1/SMAD3 Signalling in Renal Fibroblasts .....	74
4.1 Introduction and Objectives.....	74
4.2 Results.....	75
4.2.1 Methyltransferase siRNA Library Screen.....	75
4.2.2 SETDB1 Co-localises and Interacts with SMAD3 .....	80
4.2.3 SETDB1 Silencing Results in Increased Expression of SMAD3 and Pro-Fibrotic Markers .....	82
4.2.4 SETDB1 Silencing Enhances Wound Healing and Collagen Contractility of PRFs .....	84
4.3 Discussion.....	87
Chapter 5. Aurora Kinase A Promotes Renal Fibrosis through TGF $\beta$ -1 Signalling in Myofibroblasts.....	91
5.1 Introduction.....	91
5.2 Results.....	92
5.2.1 Aurora Kinase Inhibitors Selectively Reduce Proliferation, Induce Apoptosis and Prevent Myofibroblasts Differentiation of Human Primary Renal Fibroblasts .....	92
5.2.2 AURKA Phosphorylates SMAD3 in Response to TGF $\beta$ -1 .....	98
5.2.3 MK-5108 Inhibits Renal Fibrosis in Mice .....	101
5.2.4 MK-5108 Reduces $\alpha$ -SMA Accumulation in Liver Injury in Mice.....	104
5.3 Discussion.....	106
Chapter 6. Final Discussion.....	109
6.1 Overall Discussion.....	109
6.2 Future Directions .....	114
List of Publications and Presentations.....	116
Published Manuscripts .....	116
Manuscripts in Preparation for Publication .....	116
Oral and Poster Presentations .....	116
Appendix .....	117
Bibliography .....	119

## **List of Tables**

Table 1.1 Classification of CKD

Table 2.1 siRNA Sequences and their Gene Target

Table 2.2 Antibodies used for Western Blotting (WB), Immunoprecipitation (IP), Immunofluorescence (IF), Immunohistochemistry (IHC) and Chromatin Immunoprecipitation (ChIP).

Table 4.1 Methyltransferase siRNA Library

Table 4.2. Methyltransferase siRNA Screen Z-Score hits

## List of Figures

Figure 1.1 General Anatomy of the Kidney

Figure 1.2 Structure of the Nephron

Figure 1.3 Source of Fibroblasts

Figure 1.4 TGF  $\beta$ -1/SMAD Signalling Pathway

Figure 1.5 Classification of the SMAD Family of Proteins

Figure 1.6 Structure of SMAD3

Figure 3.1 Methylation Targets for SET9

Figure 3.2 SET9 Interacts with SMAD3

Figure 3.3 SET9 Regulates SMAD3 Nuclear Import and Protein Turnover

Figure 3.4 SET9 Regulates SMAD3 Ubiquitylation

Figure 3.5 Phenotypes of SMAD3 and SET9  $+/+$  and  $-/-$  MEF cells

Figure 3.6 Expression of Pro-Fibrotic Markers in SET9  $+/+$  and  $-/-$  MEF Cells

Figure 3.7 SET9 Regulates TGF  $\beta$ -1-driven Transformation and Wound Healing

Figure 3.8 The Effect of SMAD3 and SET9 on Wound Healing in MEF Cells

Figure 3.9 SET9 Regulates TGF  $\beta$ -1-driven Collagen Contractility and Fibrotic Gene Expression.

Figure 3.10 Isolating and Characterising Primary Renal Fibroblasts.

Figure 3.11 Treatment of PRFs with a SET9 Inhibitor Significantly Reduces Expression of Pro-Fibrotic Markers

Figure 3.12 SET9 Regulates TGF  $\beta$ -1-driven  $\alpha$ -SMA Expression

Figure 4.1 Methyltransferase siRNA Library Screen

Figure 4.2 SETDB1 co-localises and interacts with SMAD3

Figure 4.3 SETDB1 Silencing Results in Increased Expression of SMAD3 and Pro-Fibrotic Markers.

Figure 4.4 SETDB1 Silencing Enhanced Wound Healing and Collagen Contractility of PRFs

Figure 5.1 Aurora Kinase Inhibitors Cause Selective Apoptosis in Primary Renal Fibroblasts

Figure 5.2 Aurora Kinase Inhibitors Inhibit Proliferation and Transdifferentiation in Primary Renal Fibroblasts

Figure 5.3 Aurora Kinase A Phosphorylates SMAD3

Figure 5.4 MK-5108 Attenuates Renal Fibrosis after Ureteric Obstruction

Figure 5.5 MK-5108 Prevents  $\alpha$ -SMA Accumulation and HSC Proliferation in CCl<sub>4</sub> Mice

Figure 6.1. Illustration of Novel Roles Identified for SET9, SETDB1 and Aurora Kinase A in the TGF  $\beta$ -1/SMAD3 Signalling Pathway in Renal Fibrosis

Appendix Figure 1. Immunofluorescence Negative Control Slides

## List of Abbreviations

ACEi	Angiotensin-converting enzyme inhibitors
AR	Androgen receptor
ARB	Angiotensin II receptor blockers
ALK	Activin-like kinase
AURK	Aurora kinase
BCA	Bicinchoninic acid assay
BM	Basal medium
BM	Bone marrow
BMDC	Bone marrow-derived cells
BMP	Bone morphogenetic proteins
BSA	Bovine serum albumin
CIP	Calf intestinal phosphatase
ChIP	Chromatin immunoprecipitation
CKD	Chronic kidney disease
CKD	Cyclin-dependent kinases
COLI	Collagen I
COLIII	Collagen III
Co-SMAD	Co-regulatory SMAD
CTGF	Connective tissue growth factor
CVD	Cardiovascular disease
CXH	Cycloheximide
DCT	Distal convoluted tubule

DBD	DNA binding domain
DNA	Deoxyribonucleic acid
ECM	Extracellular matrix
EMT	Epithelial-to-mesenchymal transition
EndMT	Endothelial-Mesenchymal Transition
ER	Estrogen receptor
ERK	Extracellular-signal-regulated kinase
ESRF	End-stage renal failure
ET-1	Endothelin-1
ETR-A	Endothelin receptor-A
FBS	Foetal bovine serum
FM	Full medium
FN1	Fibronectin-1
FSP1	Fibroblast-specific protein 1
GFR	Glomerular filtration rate
GS	Glycine serine
HD	Huntington's disease
HEF1	Human enhancer of filament 1
HDAC	Histone deacetylase
HP1	Histone Protein 1
HSC	Hepatic Stellate Cells
HKMT	Histone lysine methyltransferase
IHC	Immunohistochemistry
IP	Immunoprecipitation

I-SMAD	Inhibitory SMAD
JAK2	Janus Kinase 2
JNK	JUN N-terminal Kinase
LAP	Latency-associated peptide
MAPK	Mitogen-activated protein kinases
MEF	Mouse embryonic fibroblasts
MH1	Mad homology 1
MH2	Mad homology 2
MMP	Matrix metalloproteinases
MS	Marfan syndrome
MUT	Mutant
NFκB	Nuclear factor kappa-light-chain-enhancer of activated B cells
NG2	Neuron-glia antigen 2
NLS	Nuclear localisation sequence
PAI-1	Plasminogen activator inhibitor-1
PCAF	p300/CBP-associated factor
PCT	Proximal convoluted tubule
PDGFR	Platelet-derived growth factor receptor
PRF	Primary renal fibroblasts
PRMT1	Protein arginine methyltransferase 1
PTC	Proximal tubular cells
RFP	Red fluorescent protein
R-PFI-2	(R)-PFI hydrochloride
R-SMAD	Receptor-activated SMAD

SMAD	Sma Mothers against decapentaplegia
Smurf	Smad ubiquitination regulatory factor 1
SDS-PAGE	SDS-poly acrylamide gel electrophoresis
SETDB1	SET domain, bifurcated 1
siRNA	Small interfering RNA
SNP	Single nucleotide polymorphism
STZ	Streptozotocin
TAF10	Transcription initiation factor TFIID subunit 10
TGF $\beta$	Transforming growth factor $\beta$
TGF $\beta$ -1	Transforming growth factor $\beta$ -1
TGF $\beta$ R	Transforming growth factor $\beta$ receptor
THMC	Transformed Human Mesangial Cells
UUO	Unilateral ureter obstruction
WB	Western blotting
WT	Wild-type
ZO-1	Zonula occludens-1
$\alpha$ -SMA	Alpha-smooth muscle actin

# Chapter 1. Introduction

## 1.1 General Anatomy of the Kidney

### *1.1.1 General Structure and Function of the Kidney*

The kidneys are paired bean-shaped organs located on the posterior abdominal wall either side of the vertebral column between T12-L3, with the right kidney usually positioned slightly lower than the left. They weigh between 135-150g each and are typically 10-12cm in length and 5-7cm in width. The kidney is divided into two distinct sections; the cortex and the medulla. The medulla is composed of renal pyramids which are separated by renal columns of cortical tissue (Preuss, 1993). Figure 1.1 outlines the general anatomy of the kidney.

The kidneys play a vital homeostatic role within the body including; filtration and excretion of circulating metabolic waste products (urea and ammonium), acid-base balance, and fluid and electrolyte homeostasis. The by-product of these homeostatic processes is urine. The kidneys also have endocrine functions including blood pressure regulation via the renin-angiotensin-aldosterone system, erythrocyte production via erythropoietin production, and bone mineralisation via Vitamin D activation.

### *1.1.2 The Nephron*

The nephron is the functional unit of the kidney (Figure 1.2). It is composed of the renal corpuscle containing the glomerulus and Bowman's capsule. The glomerulus is a network of capillaries that filters blood supplied by the afferent arteriole, across the Bowman's capsule, into the proximal convoluted tubule (PCT). Together, the glomerular endothelium, the glomerular basement membrane and epithelial podocytes selectively filter water and solutes depending on their size and charge. The PCT then reabsorbs water, glucose and electrolytes from this initial filtrate. The blood which has been filtered by the glomerulus passes through the efferent glomerular arteriole where it then descends into the renal pyramids. The tubular system is composed of the PCT, loop of Henle, the distal convoluted tubule (DCT) and the collecting duct. In the PCT, reabsorption of electrolytes and nutrients from the tubule is facilitated by endoluminal microvilli that form a brush border, thereby increasing the surface area available for reabsorption. In the downstream loop of Henle, urine is concentrated via an intricate counter-current mechanism. Further downstream in the DCT, urine electrolytes are again modified prior to arrival of urine at the collecting duct the principle role of which is water resorption. Urine then passes to the renal pelvis, then the ureters and finally the urinary bladder that controls excretion (Preuss, 1993).

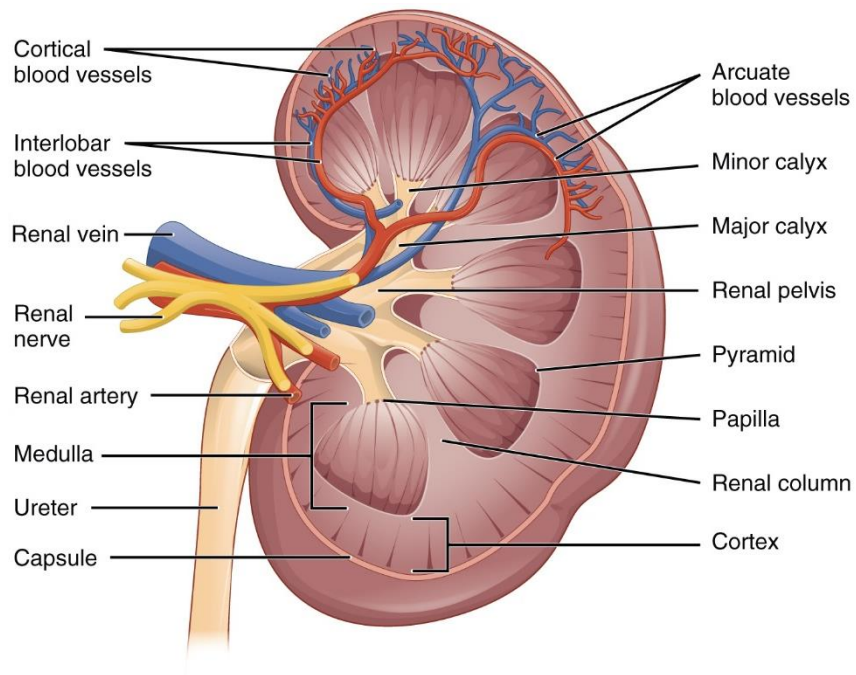


**Figure 1.1 General Anatomy of the Kidney.** Illustration of main anatomical structures of the kidney. Image taken from (Drake et al., 2009).

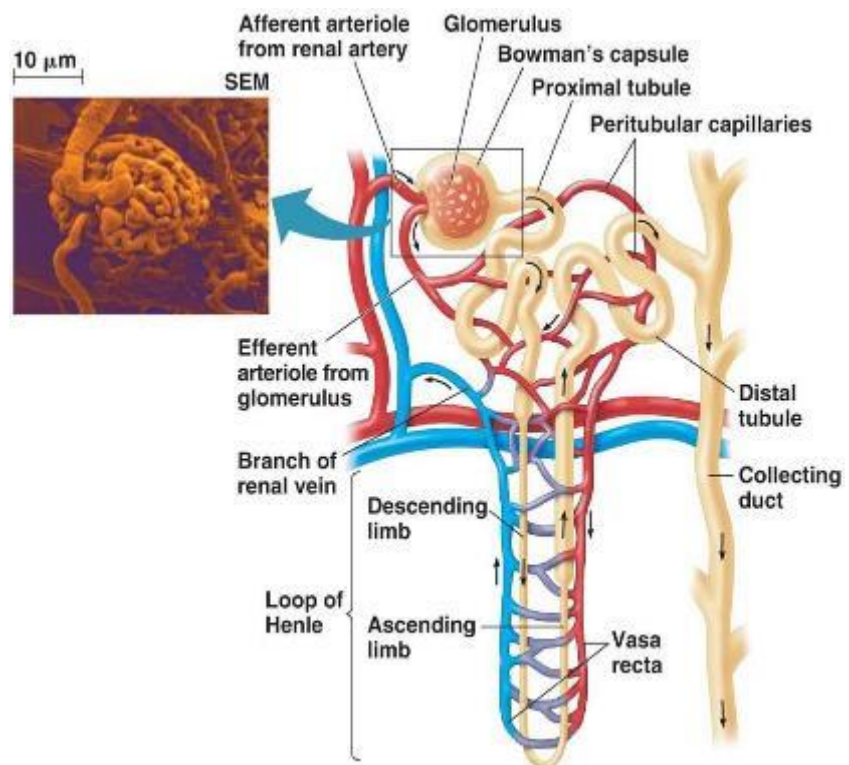


**Figure 1.2 Structure of the Nephron.** Illustration of the nephron structure. Image taken from (Drake et al., 2009).

## **1.2 Chronic Kidney Disease**

### ***1.2.1 Definition of Fibrosis***

Fibrosis, colloquially termed scarring, is the excessive deposition of extracellular matrix (ECM), primarily composed of Collagen proteins, by activated fibroblasts. Activation of these fibroblasts to myofibroblasts is characterised by increased Collagen contractility and cell motility, facilitated by intracellular cytoskeletal proteins such as alpha-smooth muscle actin ( $\alpha$ -SMA) which are overexpressed in fibrosis. Fibrosis can occur in numerous organs including the heart, lungs, kidney, liver and skin and can be thought of as a “wound healing response that has gone out of control” (Wynn, 2007). Tissue injury can result from acute or chronic infections, autoimmunity or mechanical trauma. Injured tissues require repair, a biological process essential for survival, to restore architecture and regain function. The repair process has a regenerative phase in which damaged tissue is replaced by the original cell type and a fibrosis phase in which damaged tissue is replaced by connective tissue. In normal tissue repair, an inflammatory response results in the appearance of myofibroblasts and inflammatory cells to initiate tissue regeneration which then comes to a halt once the damaged tissue is repaired. Although initially beneficial, the fibrosis phase can become pathogenic if inappropriately sustained, through aberrant myofibroblast activation leading to dysregulated ECM deposition and remodelling and the formation of permanent scar tissue. This scar tissue replaces normal renal tissue compromising organ function and ultimately leads to organ failure (Eddy, 2014).

A major factor implicated in fibrosis is transforming growth factor  $\beta$ -1 (TGF  $\beta$ -1). The TGF  $\beta$  superfamily comprises signalling molecules involved in physiological processes such as proliferation, embryogenesis and homeostasis, but also human disease (Massague, 2012). TGF  $\beta$ -1, the prototypical member of this superfamily, has long been known to have an important role in the pathological response to wound healing and fibrotic diseases (Gordon and Blobe, 2008), as discussed further in section 1.5.

### ***1.2.2 Renal Fibrosis in Chronic Kidney Disease***

Fibrosis is the histological end-point of almost all forms of chronic kidney disease (CKD). Excessive accumulation of ECM results in the formation of permanent scar tissue, replacing normal renal parenchyma, leading to reduced renal function and, eventually organ failure; end-stage renal disease (ESRD) requiring dialysis or transplantation. Renal fibrosis can occur in all the major compartments of the kidney including the glomerulus (termed

glomerulosclerosis), the tubulointerstitium (termed tubulointerstitial fibrosis) and the vasculature (Strutz and Zeisberg, 2006). Once established, renal fibrosis is irreversible.

The earliest identifiable histological feature of CKD is the aberrant accumulation of myofibroblasts, the cells that mediate fibrosis (Meran and Steadman, 2011). TGF  $\beta$ -1 stimulates fibroblast migration to the site of tissue injury where they become activated and differentiate into myofibroblasts. A defining feature of myofibroblasts is their expression of  $\alpha$ -SMA, a classical fibrotic marker (Bottinger and Bitzer, 2002; Massague, 2012). Upon TGF  $\beta$ -1 stimulation,  $\alpha$ -SMA is incorporated into stress fibres conferring myofibroblasts with their contractile activity (Hinz *et al.*, 2001). Myofibroblasts also produce the fibrillary Collagen-rich ECM upon TGF  $\beta$ -1 stimulation. The contractile force created by the  $\alpha$ -SMA-containing stress fibres can be transmitted to the surrounding ECM resulting in ECM reorganisation and wound contraction (Tomasek *et al.*, 2002). In fibrotic diseases such as CKD, persistent TGF  $\beta$ -1 stimulation and myofibroblast activation results in ongoing fibrosis and progressive organ failure.

### ***1.2.3 Chronic Kidney Disease: Definition and Disease Staging***

The definition of Chronic Kidney Disease (CKD) defined by the global KDIGO organisation is glomerular filtration rate (GFR)  $<60\text{mL}/\text{min}/1.73\text{m}^2$  for more than 3 months, with or without kidney damage or structural or functional abnormalities of the kidney for more than 3 months, with or without reduced GFR defined by pathological abnormalities or markers of kidney damage including blood or urine composition abnormalities or abnormalities in imaging tests (Levey *et al.*, 2005).

As detailed in Table 1.1, CKD can be classified into 5 stages according to kidney function defined by GFR. Early detection and treatment of CKD can allow intervention to slow disease progression but early detection is challenging due to a paucity of reliable disease markers. CKD is often associated with underlying causes such as hypertension, diabetes and glomerulonephritis. Secondary complications such as cardiovascular disease, anaemia and hypertension make it difficult to estimate the severity of CKD based upon GFR alone.

Stage	Description	GFR (mL/min/1.73m <sup>2</sup> )
1	Kidney damage with normal or increased GFR	≥90
2	Kidney damage with mild reduction in GFR	60-89
3	Moderate reduction in GFR	30-59
4	Severe reduction in GFR	15-29
5	Kidney failure (ESRF)	<15 (or dialysis)

**Table 1.1 Classification of CKD.** CKD can be classified into 5 stages based on kidney function GFR. 1 denoting some kidney damage but with normal GFR to 5 denoting kidney failure requiring dialysis, according to the National Kidney Foundation.

#### ***1.2.4 Epidemiology, Risk and Costs of CKD***

CKD is a growing public health issue. In England in 2008/09 there were 1,739,443 people aged 18 and over who were registered with CKD (stages 3-5). Prevalence rates continue to increase as result of an ageing population and an increasing incidence of Type II diabetes mellitus (Arnold *et al.*, 2015). The cost of CKD to the NHS in England alone in 2009–10 was estimated at £1.45 billion accounting for around 1.3% of all NHS spending in that year. Epidemiological data has revealed that CKD sufferers are far more likely to be need further hospital admissions than non CKD sufferers, with associated costs for the NHS (Arnold *et al.*, 2015).

More globally, CKD is also a growing health problem with recent reports identifying a significant increase in mortality due to CKD from 1990 to 2013 in a survey of 188 countries (GBD 2013 Mortality and Causes of Death Collaborators, 2015).

#### ***1.2.5 Aetiology of CKD***

CKD is a multifactorial disease known to have many underlying causes such as hypertension, glomerulonephritis and diabetes as well as being associated with complications such as cardiovascular diseases, bone disorders and anaemia. The kidney's role in vital homeostatic functions such as regulation of blood pressure and electrolyte balance highlights the

importance of their role in systemic complications of disease. Significant single-nucleotide polymorphism (SNP) associations in *UMOD*, *SHROOM3* and *GATM* loci have previously been associated with an increased risk of CKD (Kottgen et al., 2009; Chambers et al., 2010). The findings of these common genetic variants provide insight into mechanisms underlying CKD and offer the potential to develop new therapeutic strategies for CKD management, although to date this has not been achieved.

### ***1.2.6 Management of CKD***

Management of ESRF remains limited to either dialysis or transplantation. Measures to prevent ESRF include weight control, diet and exercise and blood pressure control. However, the evidence for these interventions remains relatively weak. To date, only angiotensin-converting enzyme inhibitors (ACEi) and angiotensin II receptor blockers (ARBs) have proved effective in clinical trials in retarding the progression of CKD (Turner *et al.*, 2012). These two agents remain the primary treatment of CKD but at best can only slow the progression of the disease.

The clinical focus is therefore towards early detection and management of risk factors for progressive CKD. The pro-fibrotic role of TGF  $\beta$ -1 has been widely described in the literature in several species, organs and models of renal injury (Meng *et al.*, 2016; Vega *et al.*, 2016). TGF  $\beta$ -1 inhibition has been the focus of much research, with the use of blocking antibodies, small molecule inhibitors and gene disruption, but only very few of these approaches have proved that TGF  $\beta$ -1 can be successfully targeted (Klinkhammer *et al.*, 2017).

Inhibition of TGF  $\beta$ -1 by the neutralizing human monoclonal antibody fresolimumab has been tested in Phase I and II clinical trials. In Phase II trials in glomerulosclerosis patients, fresolimumab showed promising results with improved GFR compared to placebo which could be a result of retardation of fibrosis (Klinkhammer *et al.*, 2017; Vincenti *et al.*, 2017).

Connective tissue growth factor (CTGF) is a pro-fibrotic matricellular protein downstream of TGF  $\beta$ . Upregulated CTGF expression is seen in kidneys with renal fibrosis. Reduction of CTGF by antisense treatment has proven effective in murine models of kidney disease, significantly reducing renal tubulointerstitial fibrosis (Dubey *et al.*, 1997). Phase I and II clinical trials using a monoclonal anti-CTGF antibody were found to reduce albuminuria but the Phase II trial was prematurely terminated due to poor efficacy of the compound (Adler *et al.*, 2010).

Because renal fibrosis is partly caused by increased Collagen synthesis and reduced Collagen degradation, other research has focussed on a search for therapeutics that increase Collagen degradation. Pirfenidone, a synthetic oral compound with anti-fibrotic properties has been licensed for the treatment of pulmonary fibrosis. It is thought to disrupt TGF  $\beta$ -1 signalling by interfering with gene promotor activity, thereby reducing ECM production and indirectly increasing Collagen degradation, although the exact mechanisms are unknown (RamachandraRao *et al.*, 2009). Pirfenidone has shown some success in animal models (Vega *et al.*, 2016) but in CKD patients it has produced varied results. In diabetic nephropathy Phase II trials of low dose Pirfenidone increased GFR compared to placebo but was poorly tolerated (Sharma *et al.*, 2011) and was shown to cause a slight but possibly beneficial increase in GFR in patients with glomerulosclerosis (Cho *et al.*, 2007). Larger clinical trials are required to determine the benefit of Pirfenidone in CKD.

Endothelin-1 (ET-1) receptor blockers are promising therapeutics for the treatment of renal fibrosis. ET-1 is involved in renal fibrosis whereupon it binds to its receptor endothelin receptor-A (ETR-A) which promotes renal vasoconstriction resulting in greater glomerular pressure and ischemia leading to renal fibrosis and also promotes inflammation and activation of the renin angiotensin system (Dhaun *et al.*, 2006). ETR-A blockers were developed and used in Phase I and II clinical trials which led to significantly lower proteinuria and blood pressure in diabetic and CKD patients (Black *et al.*, 2007). A Phase III clinical trial with over 4000 patients is now ongoing which will provide further critical data including renal and cardiovascular end-points (Egido *et al.*, 2017).

Although there has been a lot of focus on identifying novel therapeutic targets in renal fibrosis and CKD there are still few promising potential candidates that are likely to be used clinically. Many treatments show promise in animal models but then produce disappointing results in clinical trials. We are still awaiting clinical data concerning some promising therapeutics such as Pirfenidone. The discovery of new biomarkers for renal fibrosis and CKD would also be very useful in developing more promising treatments in addition to the use of GFR and proteinuria which only partially correlate with the progression of CKD.

There is still an inherent need for the discovery of novel therapeutic targets and markers of fibrosis for the detection of CKD and prevention of ESRF and cardiovascular end-points resulting from CKD.

### **1.3 Contribution of Cell Types to Renal Fibrosis**

#### ***1.3.1 Renal Tubular Epithelial Cells***

In fibrosis, renal tubular epithelial cells are lost due to cell death or undergo epithelial-to-mesenchymal transition (EMT) resulting in the loss of epithelial cell markers and an increase in the expression of mesenchymal markers. Renal tubular epithelial cell dedifferentiation may play an important role in fibrosis progression and may also contribute by secreting pro-fibrotic cytokines and growth factors, in models of CKD (Duffield, 2014). TGF  $\beta$ -1 has a vital role in fibrosis, promoting cell death and dedifferentiation of tubular epithelial cells and inducing the increased deposition of ECM (Kang *et al.*, 2015). Nevertheless, the role of tubular cells in fibrosis remains debated (Liu, 2004).

#### ***1.3.2 Fibroblasts***

Fibroblasts in the kidney are located within the interstitial space where they maintain a steady level of ECM to maintain the organs structural integrity. Damage to the kidney results in the production of factors such as cytokines, growth factors and mechanical forces that activate fibroblasts to become myofibroblasts (Kessler *et al.*, 2001). Myofibroblasts are characterised phenotypically by a large nucleolus, cytoplasmic  $\alpha$ -SMA stress fibres and prominent rough endoplasmic reticulum. They are a non-uniform cell population and display heterogenous phenotypes depending on their location, even within single organs (Sorrell and Caplan, 2009). Being the principle source of ECM synthesis in fibrosis, makes myofibroblasts a key target in research to identify anti-fibrotic therapeutics to inhibit ECM production. Aside from  $\alpha$ -SMA, other markers used to identify fibroblasts include, Vimentin and Fibroblast-specific protein 1 (FSP1) but none of these are specific to fibroblasts alone so identification and analysis of fibroblasts is challenging due to the lack of a common specific marker. To further complicate matters, ageing fibroblasts are thought to differ in their phenotypes and proliferative capacity. The evolving heterogeneity of fibroblasts further hinders the development of fibroblast specific-markers (Zeisberg and Kalluri, 2013). Nevertheless, the number of myofibroblasts present, as indicated by  $\alpha$ -SMA expression correlates with renal disease progression (Hewitson and Becker, 1995).

TGF  $\beta$ -1 induces the differentiation of fibroblasts to activated myofibroblasts leading to Collagen matrix remodelling. TGF  $\beta$ -1 increases the ability of fibroblasts to migrate and adhere to Collagen fibres and increases their expression of the contractile protein  $\alpha$ -SMA. The increased expression of  $\alpha$ -SMA enhances intracellular tension leading to Collagen contraction

and wound healing by myofibroblasts, important mechanisms in ECM remodelling in fibrosis (Kondo *et al.*, 2004).

### ***1.3.3 Origins of Myofibroblasts in Renal Fibrosis***

The origin of myofibroblasts in renal fibrosis is a hot topic of research and has been an intense source of debate for many years. Myofibroblasts have been proposed to originate from several sources including proliferation from local resident fibroblasts, EMT, Endothelial-Mesenchymal Transition (EndMT), from bone marrow (BM)-derived cells and from pericytes (Figure 1.3) (LeBleu and Kalluri, 2011; Sun *et al.*, 2016).

A commonly accepted theory of their origin is from the activation of renal interstitial fibroblasts (Liu, 2004). Previous research showed that tubular epithelial cells could express fibroblastic markers such as FSP1 during fibrogenesis. This led to the hypothesis that fibroblasts could be derived from epithelial-to-mesenchymal transition (EMT) (Strutz *et al.*, 1995).

EMT is characterised by the loss of epithelial markers, such as E-cadherin and the acquisition of mesenchymal features, such as  $\alpha$ -SMA and Vimentin expression, enhanced cell motility and invasion and production of Fibronectin and Collagen I (Kalluri and Neilson, 2003). TGF  $\beta$ -1 is a potent inducer of EMT *in vitro* (Fan *et al.*, 1999). In nephrectomised rats the stressed tubular epithelial cells become increasingly positive for  $\alpha$ -SMA with time after nephrectomy with simultaneous disruption of the basement membrane, supporting a model in which epithelial cells undergo EMT and migrate to the interstitium (Ng *et al.*, 1998). In the adult kidney, mature tubular epithelial cells undergo EMT which has been found to be significant in the pathogenesis of renal interstitial fibrosis, as it has been suggested that this is the origin of a significant proportion of interstitial fibroblasts in diseased kidneys (Liu, 2004). A study using transgenic reporter mice quantitatively determined EMT contribution in unilateral ureter obstruction mouse model (UUO), providing evidence that EMT contributed to 36% of fibroblast origin. This finding determines that EMT plays a much greater role in renal fibrosis than previously thought (Iwano *et al.*, 2002). Furthermore, selective blockade of EMT in a whole animal model showed myofibroblast accumulation was actually reversed (Yang *et al.*, 2002a), suggesting that EMT has an important role in renal fibrosis in the whole animal. On the contrary, another study demonstrated the contribution of EMT to myofibroblast accumulation was very low and therefore is insignificant in renal fibrosis (LeBleu *et al.*, 2013). More research is therefore needed to determine the true contribution of EMT in renal fibrosis.

EndMT is a process similar to EMT with the loss of endothelial cell markers and the acquisition of mesenchymal cell markers. This process has been shown to be important in several disease models of fibrosis. A study using a transgenic mouse line with traceable endothelial lineage in 3 models of renal fibrosis; UUO, streptozotocin (STZ)-induced diabetic nephropathy and a model for Alport disease, found myofibroblasts expressed  $\alpha$ -SMA and the endothelial marker CD31, suggesting an endothelial origin for at least some fibroblasts (Zeisberg *et al.*, 2008). Additionally, a similar study using another endothelial lineage-traceable mouse line and confocal microscopy revealed that 23% and 25% of myofibroblast accumulation in the renal interstitium were of endothelial origin in models of STZ-induced diabetic nephropathy and UUO, respectively (Li *et al.*, 2010). Blockade of TGF  $\beta$ /SMAD signalling to inhibit EndMT demonstrated a decrease in renal fibrosis and reduced disease progression in both UUO and STZ-induced diabetic nephropathy (Li *et al.*, 2009). These studies indicate a potentially significant contribution for EndMT in the accumulation of myofibroblasts in several disease models of renal fibrosis. To confirm this contribution, improved endothelial tracing needs to be established.

Pericytes have recently been suggested as another source of myofibroblasts. Pericytes are ECM-producing stromal cells that surround the interstitial capillary endothelium. A study used lineage tracking and cell ablation in a mouse model of renal fibrosis to identify a subset of mesenchymal-like pericytes as progenitors of myofibroblasts. The pericytes identified proliferated within the interstitium and acquired  $\alpha$ -SMA expression identifying them as myofibroblasts. Pericytes and their involvement in myofibroblast accumulation in renal fibrosis is a highly debated subject due to the lack of specific cellular markers. Pericytes express some common markers that are also found on fibroblasts such as Platelet-derived growth factor receptor 2 (PDGFR2) (Kramann *et al.*, 2015). In contrast, LeBleu *et al.* performed a study to determine the origin of myofibroblasts in renal fibrosis using genetic mouse models and cell tracking. They found that the majority of pericytes did not express  $\alpha$ -SMA and considering the cells did express  $\alpha$ -SMA, only a small number were positive for PDGFR and NG2 expression. Furthermore, when PDGFR and NG2 cells were depleted in the UUO model there was no significant reduction in fibrosis, suggesting that the role of pericytes in myofibroblast accumulation in renal fibrosis is insignificant. LeBleu *et al.* discovered myofibroblast accumulation originated from 2 major sources; 50% originated from proliferation of local resident fibroblasts and 35% from bone marrow-derived cells (BMDC). EndMT and EMT contributed to a lesser extent of 10% and 5% respectively. The study revealed that BMDC can differentiate into myofibroblasts in the presence of TGF  $\beta$ -1

promoting their differentiation and migration. Loss of TGF  $\beta$ R2 prevented the cells from differentiating into myofibroblasts, further highlighting a crucial role of TGF  $\beta$ -1 (LeBleu and Kalluri, 2011). These results demonstrate that the accumulation of myofibroblasts involves several methods and therefore treatments such as anti-proliferative drugs will only partially reduce myofibroblast accumulation and fibrosis in the kidney. As TGF  $\beta$ -1 is known to also be involved in the proliferation of fibroblasts, studies targeting the TGF  $\beta$ -1 pathway have been useful in reducing myofibroblast accumulation in renal fibrosis.

BMDC, another potential source of myofibroblasts could migrate into the kidney in response to injury. A study in a UUO mouse model of renal fibrosis transplanted with bone marrow that expressed red fluorescent protein (RFP) under the regulation of an  $\alpha$ -SMA promoter identified around 35% of myofibroblasts were of bone marrow origin, demonstrating a substantial contribution to myofibroblast accumulation in renal fibrosis (LeBleu *et al.*, 2013).

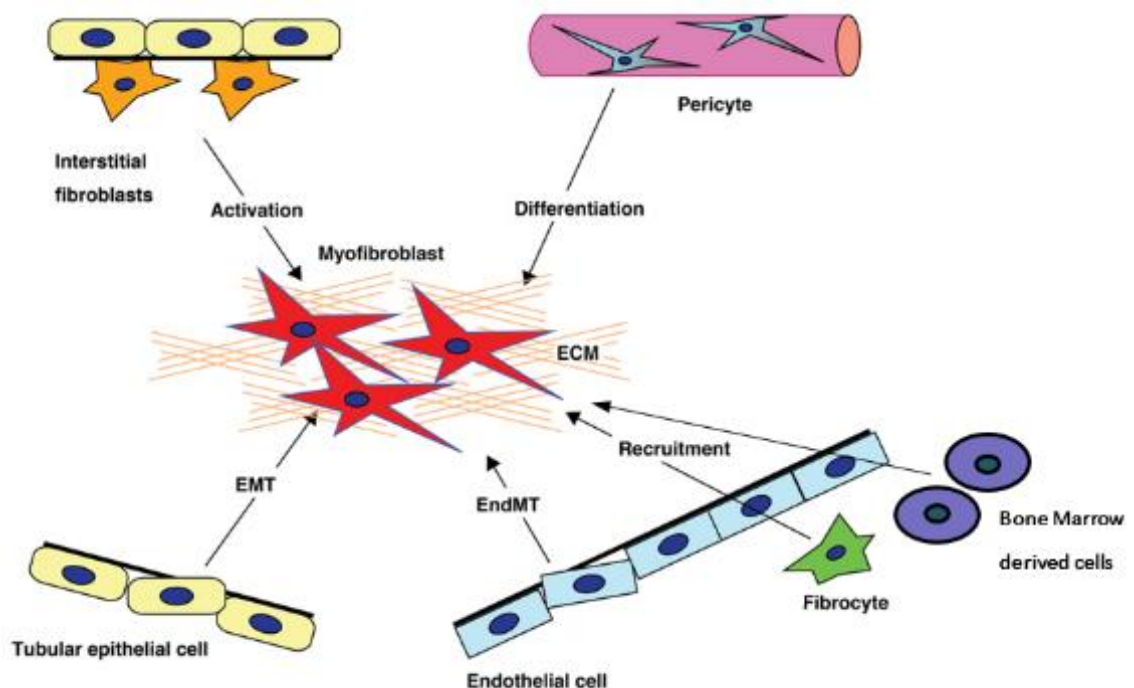


**Figure 1.3. Source of Fibroblasts in Fibrosis.** In fibrosis, fibroblasts are derived from several sources including resident fibroblasts, fibrocytes, pericytes, BMDC, EMT and EndMT. Adapted from (Kanasaki *et al.*, 2013).

## **1.4 Experimental Models of Renal Fibrosis and CKD**

### ***1.4.1 Cellular Models of CKD***

In order to investigate the mechanisms responsible for renal fibrosis, a number of immortalised cell lines are available which represent various models of fibrosis. Each have their advantages as well as limitations. These models include, but are not limited to, HK C-8, Human Mesangial Cells (THMC) and Mouse Embryonic Fibroblast (MEF) cells.

HK C-8 cells are proximal tubular epithelial cells derived from humans. A useful cell model to study human renal function and the mechanisms renal fibrosis as tubular cell dedifferentiation via EMT is thought to be a source of fibroblasts in tubulointerstitial fibrosis.

THMC are perivascular cells which originate from the glomerulus (Sraer *et al.*, 1996). These cells represent an *in vitro* model of glomerular pathologies and are useful cell line to study the effect of fibrosis.

MEF cells are derived from mouse embryos that present typical features of fibroblasts. Genes of interest can be knocked out of these cells to study their function in fibrosis.

In addition to immortalised cell line models, renal fibrosis can be modelled using Primary Renal Fibroblasts (PRFs); fibroblasts isolated directly from human cortical kidney tissue providing a primary model of tubulointerstitial fibrosis when treated with TGF  $\beta$ -1. These cells are arguably the most suitable cellular model for studying renal fibrosis as they have not undergone the process of immortalisation. One limitation of many primary cells studies is that there is a limited quantity of tissue and the life-span of primary cultures can be relatively short..

### ***1.4.2 Whole Organism Models of CKD***

The development of *in vivo* animal models to mimic renal disease is important to provide a better understanding of the pathways and mechanisms involved in renal fibrosis and for testing potential drug candidates.

UUO is the best characterised experimental model of chronic renal disease. Surgically-induced UUO in rodents produces progressive renal fibrosis similar to that seen in most human disease. The duration and severity can be manipulated in this model and obstruction can be reversed by release of ligature. UUO is induced by a single surgical ligation of one ureter (Klahr and Pukerson, 1994) and results in the gradual development of tubular injury and cell death, macrophage and T cell infiltration and the accumulation of myofibroblasts

leading to ECM deposition and subsequently renal tubulointerstitial fibrosis (Chevalier *et al.*, 2009). This model most closely resembles obstructive nephropathy in humans, which is the commonest cause of ESRD in the paediatric population.

### ***1.4.3 Limitations of CKD Models to Human Disease***

Cell and animal models provide us with an opportunity to increase our understanding of the mechanisms of disease and to develop and test novel therapeutics. Whilst they exhibit similarities to human disease, they do not precisely replicate human disease and so there will always be limitations to these models. For example, working with primary and immortalised cell lines that are far removed from their normal environment limits the cross-talk between cells and signalling pathways that occur in their normal conditions, potentially limiting their natural response.

Genetic engineering allows us to manipulate animal models to present a particular genotype/phenotype to mimic human disease for the development of new therapeutics but the limitations to these animal models include the disease developing artificially (surgically, genetically engineered) therefore not representing all the disease features or not closely resembling the human disease. Cellular and animal models should therefore be used with caution and ideally not in isolation. Using more than one model might overcome some of these limitations.

## **1.5 TGF $\beta$ Signalling**

### ***1.5.1 The TGF $\beta$ Superfamily***

The Transforming growth factor  $\beta$  (TGF  $\beta$ ) superfamily are well characterised and multifunctional secreted growth factors. The superfamily includes TGF  $\beta$ s (1-3), inhibins (A and B), bone morphogenetic proteins (BMPs 1-20) and activins (A and B) (Gordon and Blobe, 2008). The TGF  $\beta$  superfamily are ubiquitously expressed and almost every cell in the human body expresses and responds to at least one member of this superfamily (Siegel and Massague, 2003). They therefore play a role in a diverse range of biological activities, including cell proliferation and differentiation, wound healing and tissue homeostasis, apoptosis and angiogenesis. Alterations in the TGF  $\beta$  superfamily pathways can result in human disease such as connective tissue disorders, fibrosis, and cancer (Schmierer and Hill, 2007).

It was clear from when TGF  $\beta$  was first discovered that it had diverse and even opposing effects depending on the cell type and context. A fairly simple pathway was discovered consisting of TGF  $\beta$  receptors (TGF  $\beta$ Rs) and SMAD proteins which function as signal transducers and substrates for the TGF  $\beta$ Rs. However this simple pathway was found to lead to a vast range of effects in many biological processes (Massague, 2012). Many other regulators and related pathways have since been identified, indicating the complexity of this signalling pathway.

A family of TGF  $\beta$  receptors are positioned at the cell membrane. In response to TGF  $\beta$  ligands, cellular responses are transduced via these transmembrane serine/threonine kinase type I and type II receptors, together with a group of intracellular modulators (SMAD proteins) which constitute the cellular machinery responsible for detecting and responding to TGF  $\beta$ . There are three types of contextual determinants that can regulate the transcriptional response of TGF  $\beta$  signalling; 1. Many signal transduction factors can control TGF  $\beta$  ligand binding to the receptors and subsequently the receptors to SMAD proteins. 2. Transcription factors that bind to activated SMADs can determine which genes are targeted and whether transcription of those genes are negatively or positively regulated. 3. The epigenetic state of the cell can provide either an active 'open chromatin' (accessible to binding of SMAD complexes) or repressive 'closed chromatin' (silenced state and closed to SMAD complex binding) (Massague, 2012).

Ligands of the TGF  $\beta$  superfamily initiate cell signalling by binding to cell surface serine/threonine receptors, type I (activin like kinase (ALK) 1-7) receptors and type II TGF  $\beta$  receptors. Increasing numbers of co-receptors have been identified that are thought to regulate ligand binding to the type I and II receptors. Type II receptors are constitutively active serine/threonine kinases and upon ligand binding adopt conformational changes to recruit and interact with a type I receptor to form an active receptor complex (Shi and Massague, 2003). The type II receptor phosphorylates the glycine serine (GS) rich domain of the type I receptor activating its serine/threonine kinase activity. The Type I receptor transduces its cellular effects by directly phosphorylating a conserved family of transcriptional mediators, known as SMADs. Phosphorylation of 2 receptor-activated SMAD (R-SMADs) results in formation of an active complex with SMAD4, a common SMAD, this complex is then translocated to the nucleus where it can interact with transcription factors, co-activators and co-repressors to regulate the transcription of target genes (Heldin *et al.*, 1997; Shi and Massague, 2003).

TGF  $\beta$  signalling occurs predominantly through SMAD-mediated pathways, but other signalling molecules are also involved, including extracellular-signal-regulated kinase (ERK), p38 and JUN N-terminal Kinase (JNK), all of which are mitogen activated protein kinase (MAPK) pathways (Derynck and Zhang, 2003; Miyazono *et al.*, 2005). This cross-talk with other signalling pathways highlights the complexity of TGF  $\beta$  superfamily signalling and the diverse cellular effects the TGF  $\beta$  superfamily can mediate.

### ***1.5.2 The TGF $\beta$ -1 Signalling Pathway***

Cells synthesise and secrete TGF  $\beta$ -1 into the ECM in an inactive form containing mature TGF  $\beta$ -1 and a signal peptide, the latency-associated peptide (LAP). Cleavage of LAP induced by environmental conditions and proteases (plasmin, cathepsin D, furin convertase and MMP2 and 9) or mechanical disruption of the complex results in TGF  $\beta$ -1 release and binding to its receptor (Lyons *et al.*, 1988).

Phosphorylation of type I receptor allows the recruitment of intracellular SMAD3. The activated receptor I phosphorylates a conserved Ser-X-Ser motif (x = any amino acid) within the C-terminal domain of SMAD3, generating an acidic tail, thereby allowing for binding of SMAD4. Phosphorylated SMAD3 oligomerises with SMAD4 and the complex translocates to the nucleus to regulate transcription of pro-fibrotic SMAD3 target genes, such as *ACTA2* which encodes  $\alpha$ -SMA (Hu *et al.*, 2003). Within the nucleus, SMAD4 can enhance SMAD3 transcriptional activity by acting as a co-factor. The final result is an increase in expression of SMAD3 target genes, in response to TGF  $\beta$ -1 (Liu *et al.*, 2012) (Figure 1.4). SMAD7 is an inhibitory SMAD which acts to negatively regulate TGF  $\beta$ -1 signalling by complexing with TGF $\beta$  RI to inhibit phosphorylation of R-SMADs (Nakao *et al.*, 1997). Smad ubiquitination regulatory factor 1 (Smurf 1) and Smurf 2 are E3 ubiquitin ligases which degrade SMADs and can complex with SMAD7 to degrade TGF $\beta$  R1, acting to regulate the signalling pathway (Ebisawa *et al.*, 2001; Ma *et al.*, 2018).

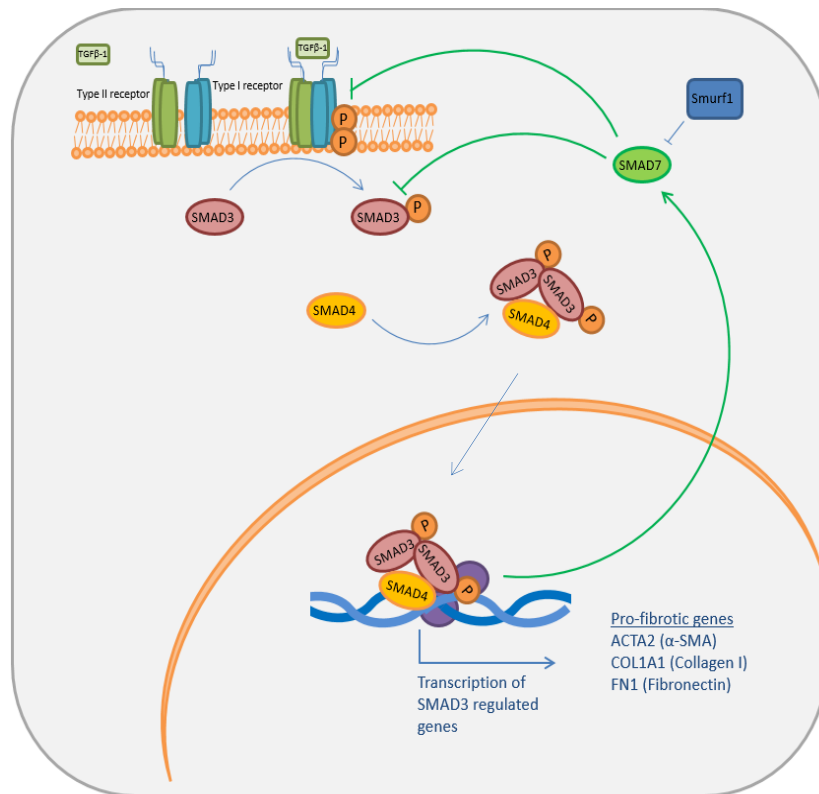


**Figure 1.4. TGF  $\beta$ -1/SMAD Signalling Pathway.** TGF  $\beta$ -1 signalling pathway mediated via cell surface membrane receptors and downstream SMAD mediators to allow transcription of target genes.

### 1.5.3 The Role of TGF $\beta$ -1 in Human Disease

TGF  $\beta$ -1 signalling is a critical regulator of essential cellular processes and many human diseases arise from disruption of this signalling pathway resulting in its aberrant activation or inhibition (Gordon and Blobel, 2008).

#### *Cardiovascular disease (CVD)*

TGF  $\beta$ -1 is a predominant ligand expressed in CVD, demonstrated in *TGF $\beta$ 1*<sup>-/-</sup> mice which die early through excessive systemic inflammatory response resulting in the infiltration of lymphocytes and macrophages into the heart (Kulkarni and Karlsson, 1993).

#### *Connective tissue diseases*

Marfan syndrome (MS) is a multisystem connective tissue disease, clinically characterised by cardiac, skeletal and vision abnormalities. Mutations have been identified in TGF $\beta$  RI and II in MS patients affecting the kinase domains of the receptors resulting in loss of function (LeMaire *et al.*, 2007).

#### *Cancer*

TGF  $\beta$ 's role in cancer is diverse, acting as a tumour suppressor early on in carcinogenesis but later switching to a tumour promoter. TGF  $\beta$  signalling and its role in human cancer is evident as demonstrated by the mutations in the TGF  $\beta$  signalling components, identified in hereditary and sporadic cancers (Elliott and Blobe, 2005).

#### *Breast Cancer*

Several alterations in the TGF  $\beta$  signalling pathway has been discovered in breast cancer and TGF  $\beta$  is well known to regulate normal mammary growth and development. A thymine to cytosine polymorphism in the coding sequence of the *TGF  $\beta$ 1* gene resulting in a leucine to proline amino acid substitution has been shown to lead to higher TGF  $\beta$ -1 levels resulting in an increased risk of breast cancer (Ziv *et al.*, 2001).

#### *Fibrosis*

TGF  $\beta$ -1 is known to have an important role in the pathological response to tissue wounding, resulting in the development and progression of fibrosis. The aberrant deposition of ECM in organs such as the skin, liver, lungs and kidneys leads to loss of organ function and eventually organ failure. TGF  $\beta$ -1 is a major regulator of ECM formation and remodelling and its excessive signalling has been well defined in the pathogenesis of many fibrotic diseases (Verrecchia and Mauviel, 2007a).

#### ***1.5.4 The Role of TGF $\beta$ -1 in Renal Fibrosis***

TGF  $\beta$ -1 plays a central role in wound healing and tissue remodelling but also in the development of tissue fibrosis, including renal fibrosis. Overexpression of TGF  $\beta$ -1 from the albumin promoter is enough to directly cause renal fibrosis, indicating the critical role of TGF  $\beta$ -1 (Liu *et al.*, 2006).

Injury to tissue initiates a repair process in which TGF  $\beta$ -1 expression is upregulated by parenchymal cells and infiltrating cells such as lymphoid cells and macrophages. Further production of TGF  $\beta$ -1 is caused by extracellular signalling molecules angiotensin II and thromboxane and within injured tissue plasmin, thrombospondin and reactive oxygen species activate latent TGF  $\beta$ -1 production. Furthermore, TGF  $\beta$ -1 feedback loops via the autocrine and paracrine signalling also increase TGF  $\beta$ -1 production. The aberrant upregulation and accumulation of TGF  $\beta$ -1 acts to increase ECM synthesis and reduce ECM degradation consequently resulting in tissue fibrosis.

The ECM serves important cellular functions such as structural support, cellular adhesion and barriers against fluids. The ECM provides specialised tissue functions within each tissue type and these specialised functions are accomplished by TGF  $\beta$ -1 regulated expression of specific matrix proteins. For example, within the kidney the interstitial matrix consists of Collagen I and III, Fibronectin and Tenascin.

Under normal tissue repair, TGF  $\beta$ -1 controls enzymes that regulate ECM synthesis including matrix metalloproteinases (MMP) and plasmin. Under pathological conditions SMAD3 is highly activated whereas SMAD7 is degraded by Smurf 1 and 2 via ubiquitin-dependent degradation (Ebisawa *et al.*, 2001). This results in reduced TGF  $\beta$ I receptor degradation, amplified TGF  $\beta$ -1 signalling and increased transcription of SMAD3 target genes and activation of myofibroblasts leading to excessive expression of ECM proteins such as  $\alpha$ -SMA, Collagen I and Fibronectin (Ebisawa *et al.*, 2001; Verrecchia and Mauviel, 2007b; Lan, 2011; Meng *et al.*, 2015b).

## **1.6 SMAD Signalling**

### ***1.6.1 The SMAD Signalling Protein Family***

The SMAD are a family of proteins similar to the gene products of the *Drosophila* gene 'mothers against decapentaplegic' (Mad) and the *C. elegans* gene Sma. SMADs are signal transducers and transcription factors that mediate multiple signalling pathways. There are 8 known human SMAD proteins that can be divided into 3 subgroups based on structure and function (Figure 1.5). The first subgroup, receptor-activated SMADs (R-SMADs) are direct substrates of the TGF  $\beta$  kinase receptors. The second subgroup interact with R-SMADs and contribute to signalling co-regulatory SMADs (co-SMADs). The third subgroup are inhibitory SMADs (I-SMADs) which act as negative regulators by inhibiting SMAD activation. R-SMAD 1, 5 and 8 are mediators of the BMP receptor signalling, whereas R-SMAD 2 and 3 are mediators of TGF  $\beta$  and activin receptor signalling. SMAD4 is a shared co-SMAD which participates in both TGF  $\beta$ /activin and BMP signalling pathways by associating with R-SMADs after receptor activation. SMAD4 is required for R-SMAD signalling function (Watanabe *et al.*, 1997; Kretzschmar and Massague, 1998; Massague *et al.*, 2005). SMAD 6 and 7 are inhibitory SMADs; SMAD7 negatively regulates SMAD3 and TGF $\beta$  Rs via degradation (Kavsak *et al.*, 2000).

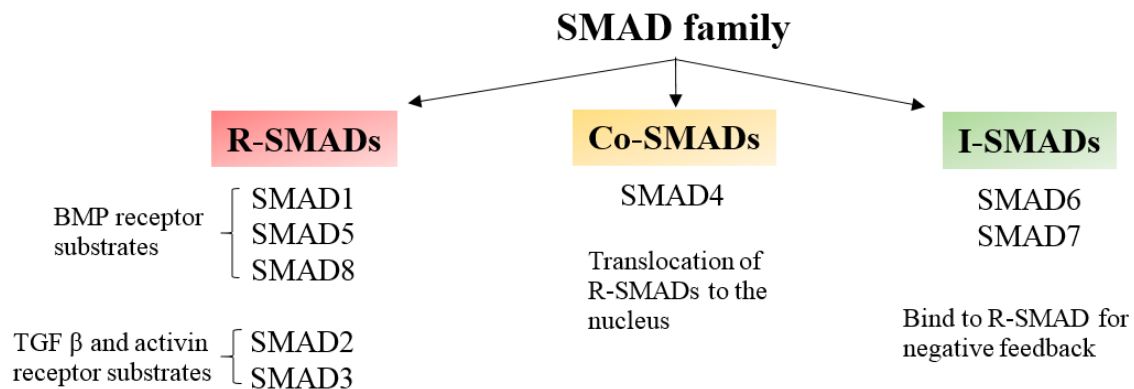


**Figure 1.5. Classification of the SMAD Family of Proteins.** The SMAD family of proteins are classified into 3 subgroups; receptor-activated SMADs (R-SMADs), co-SMADs and inhibitors SMADs (I-SMADs). They each have distinct roles within the TGFβ signalling pathway.

### ***1.6.2 The SMAD3 Transcription Factor***

SMAD3 is a 48kDa protein with two globular domains coupled by a linker domain (Figure 1.6). The amino terminal Mad Homology 1 (MH1) domain of SMAD3 contains a β-hairpin structure that mediates direct DNA binding, this structure is conserved in all R-SMADs and SMAD4.

The linker domain is a proline rich, flexible and unstructured region with phosphorylation sites for kinases such as MAPKs and cyclin-dependent kinases (CDKs) suggesting a function in integrating cross-talk from other signalling pathways. The carboxy terminal Mad Homology 2 (MH2) domain is highly conserved and facilitates protein-protein interaction. The MH2 domain also contains a region of hydrophobic patches, referred to as the “hydrophobic corridor”, a location for various interactions such as with DNA-binding co-factors (Kretzschmar and Massague, 1998; Schmierer and Hill, 2007; Massague, 2012).

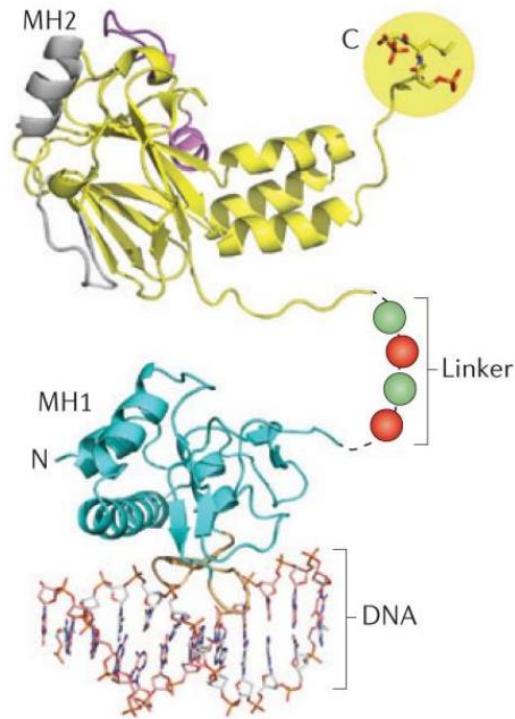


**Figure 1.6. Structure of SMAD3.** SMAD3 consists of MH1 and MH2 domains that are joined by a linker region. The TGF  $\beta$ RI phosphorylates SMAD3 at the C terminal sequence Ser-X-Ser (where X can be any amino acid). The linker can be phosphorylated by CDKs, MAPKs (green) and glycogen synthase kinase 3 (GSK3) (red). The phosphorylated linker creates docking sites for regulators of SMAD3. The N terminal domain binds DNA (Massague, 2012).

### 1.6.3 The Role of SMAD3 in Renal Fibrosis

SMAD3 has an important role in renal fibrosis; SMAD3 knockout mice are resistant to tubulointerstitial renal fibrosis in the UUO model of obstructive nephropathy (Sato *et al.*, 2003; Inazaki *et al.*, 2004) and resistant to glomerular sclerosis caused by induction of type 1 diabetes with streptozotocin (Fujimoto *et al.*, 2003).

Additionally, SMAD3 knockout mice are resistant to fibrosis in other organs including bleomycin-induced pulmonary fibrosis (Zhao *et al.*, 2002), radiation-induced skin fibrosis (Flanders *et al.*, 2002), angiotensin II-induced cardiac fibrosis (Chung *et al.*, 2010) and carbon tetrachloride-induced liver fibrosis (Schnabl *et al.*, 2001).

Furthermore, overexpression of SMAD7, a negative regulatory protein of TGF  $\beta$ -1/SMAD3 pathway inhibits SMAD3, consequently protecting against renal fibrosis in various animal models (Dooley *et al.*, 2003; Lan *et al.*, 2003; Wang *et al.*, 2005).

Treatment with halofuginone, a SMAD3 inhibitor reduces renal fibrosis in rats (Benchetrit *et al.*, 2007) and reduces fibrosis in other organs (Pines, 2008). Collectively, all of these data

show that inhibition of SMAD3 would have clinical utility in the treatment of fibrosis. However, no SMAD3 inhibitory compounds have been developed for clinical application to-date.

This necessitates a more thorough evaluation of SMAD3 signalling in response to pro-fibrotic signals in the kidney and other organs, to determine whether SMAD3 can be inhibited in an alternative and possibly indirect manner. This will involve identification of factors that are needed for the regulation of SMAD3, and an evaluation of such factors as targets in fibrosis.

## **1.7 Lysine Methyltransferases**

### ***1.7.1 The SET-domain Lysine Methyltransferase Family***

DNA is stored in the form of chromatin in the nucleus of eukaryotic cells. Chromatin consists of nucleosomes composed of 146bp of DNA wrapped around 2 of each of the core histones H2A, H2B, H3 and H4 (Luger *et al.*, 1997). The unstructured N-terminal tails of the core histones protrude from the nucleosomes and play a critical role in organising the structure and accessibility of the nucleosomal DNA (Angelov *et al.*, 2001). Two types of chromatin have been defined: heterochromatin, a compressed and transcriptionally silent structure and euchromatin, a more open, transcriptionally active arrangement (Grunstein *et al.*, 1995). Histone tails undergo post-translational modifications including methylation, acetylation, phosphorylation and ubiquitination that modulate the structure and ‘openness’ of chromatin to allow access for transcription factors and regulate the expression of genes (Strahl and Allis, 2000). Acetylation of histone tails has been well studied and is generally known to convert chromatin to an open, transcriptionally active form. More recently, the focus of epigenetic research has been to determine the effects of other types of covalent modifications of chromatin, including methylation, particularly of histones H3 and H4. Histones are well known to be substrates of methylation (Murray, 1964), lysines 4, 9, 27 and 36 of H3 and lysine 20 of H4 have been identified as preferential sites of methylation (Strahl *et al.*, 2001; Xu *et al.*, 2001).

Histone methylation by the SET-domain lysine methyltransferase family of proteins transfers a methyl group from *S*-adenosyl-L-methionine (AdoMet) to the amino group of a lysine residue on histones or other proteins, leaving a methylated lysine residue and the co-factor byproduct *S*-adenosyl-L-homocysteine (AdoHcy) (Nishioka *et al.*, 2002; Dillon *et al.*, 2005).

A major focus of research has been the study of lysine methylation in histones, which identified SUV39H1 as the first histone lysine methyltransferase (HKMT) which targets

lysine 9 of H3 (H3K9), correlating with transcriptional repression. Subsequently, many other lysine methyltransferases have been identified, the majority of which target lysines within histone tails. Furthermore, the HKMTs that methylate histone tail lysines all contain a SET domain, a conserved catalytic domain of 130 amino acids. The SET domain was found to be conserved in the PEV modifier SU(VAR)3-9, the Polycomb-group protein E(Z), and the trithorax-group protein TRX (Jenuwein *et al.*, 1998). Crystal structures reveal the structure of the SET domain is folded in such a way that the two most conserved motifs within the domain (RFINHCXPN and ELXFDY) are brought together forming an active site which is conveniently located next to the peptide-binding cleft and where the methyl donor will bind (Dillon *et al.*, 2005). Studies have demonstrated that the cysteine-rich N- and C- terminal flanking regions (pre- and post-) to the SET domain are also required for enzymatic activity (Rea *et al.*, 2000). Lysine histone methylation can also result in transcriptional activation, such as the methylation of H3K4 which correlates with acetylation, also known to regulate the transcriptional activation of chromatin. SET9 has been identified as a lysine methyltransferase specific for the methylation of K4 of H3 causing transcriptional activation (Nishioka *et al.*, 2002).

### **1.7.3 SET9**

SET9, originally isolated from human cells, specifically mono-methylates lysine 4 of histone H3 (H3-K4) in a SET-domain-dependent manner to up-regulate transcriptional activation. This methylation of H3K4 inhibits acetylation of K4 and causes displacement of the histone deacetylase NuRD and also prevents H3-K9 methylation by SUV39h1 (Nishioka *et al.*, 2002).

Monomethylation of H3K9 by SET9 has been shown to mediate ECM gene expression and silencing SET9 attenuates TGF  $\beta$ -1 mediated ECM gene expression (Sun *et al.*, 2010), indicating a potential role in renal fibrosis.

Further studies have shown that SET9 not only methylates histones but also non-histone proteins including p53 (Chuikov *et al.*, 2004), TAF10 (Kouskouti *et al.*, 2004), and androgen receptor (AR) (Gaughan *et al.*, 2011) regulating their transcriptional activity. Furthermore, SET9 has been shown to have some involvement in the TGF  $\beta$ -1/SMAD signalling pathway; SET9 methylates the inhibitory SMAD7, targeting it for proteasomal degradation, resulting in upregulation of TGF  $\beta$ -1/SMAD signalling (Elkouris *et al.*, 2016).

#### **1.7.4 SETDB1**

ESET (SETDB1) was originally identified as a functional partner of the transcription factor ERG (Yang *et al.*, 2002b). Identification of conserved SET, pre- and post-SET domains suggested histone methyltransferase activity of ESET (Rea *et al.*, 2000). The human homolog of ESET was identified as SETDB1 (SET domain, bifurcated 1) and was shown to specifically methylate lysine 9 of histone 3 (H3K9). SETDB1 has been shown to co-localise with HP1, a heterochromatin protein to play an important role in euchromatic gene silencing and transcriptional repression (Schultz *et al.*, 2002).

SETDB1 has been associated with SMAD3; in response to TGF  $\beta$ -1, SMAD3 recruits SETDB1 to the Snai1 promoter where it initiates H3K9 methylation which in turn represses H3K9 acetylation. SETDB1 therefore regulates SMAD3 activity by alterations to methylation and acetylation at the SNAI1 gene, attenuating Snai1 expression, the driver of EMT. In response to TGF  $\beta$ -1, cells downregulate SETDB1 expression during EMT. (Du *et al.*, 2018).

#### **1.7.5 SET9 and SETDB1 in Human Disease**

Epigenetic alterations resulting in altered chromatin could play a key role in the pathogenesis of Huntington's disease (HD). Chromatin remodeling and neuronal gene transcriptional dysfunction have been strongly correlated to HD pathogenesis (Ryu *et al.*, 2006). Expression of SETDB1 and levels of trimethylated H3K9 have been shown to be elevated in HD patients therefore identifying SETDB1 as a target for treatment in HD (Ryu *et al.*, 2006).

Recent reports show that SETDB1 has also been associated with gene silencing in cancer. Increased SETDB1 expression has been shown to play a role in tumorigenesis, promoting tumour cell proliferation and tumour growth (Sun *et al.*, 2015). Mammary epithelial cells downregulate SETDB1 expression allowing the cells to progress through EMT by attenuating the SMAD3-SETDB1 complex-mediated repression of Snai1. Breast cancer cells that are able to invade surrounding tissue exhibit decreased expression of SETDB1, evidence that SETDB1 suppresses metastasis.

Similarly, a SET9 feedback loop has been identified where SET9 regulates the stability of DNA methyltransferase-1 protein which in turn represses SET9 promoter transcriptional activity with Snai1 has been shown to play a role in modulating breast cancer metastasis; silencing of SET9 allowed cells to progress through EMT, favouring the generation of cancer stem cells. SET9 levels were lower in samples from patients with cancer recurrence compared

to samples from patients in remission, indicating a role for SET9 as a tumour suppressor in breast cancer (Montenegro *et al.*, 2016).

These studies demonstrate the involvement of both SET9 and SETDB1 in EMT and subsequently in diseases such as breast cancer. They also raise the possibility that both of these methyltransferases and their epigenetic modulation be involved in other pathways and diseases.

SET9 expression is upregulated in prostate cancer cells, where it has a pro-proliferative and anti-apoptotic role. SET9 has been found to interact with and methylate the androgen receptor (AR) enhancing its transcriptional activity by facilitating its recruitment to target genes (Gaughan *et al.*, 2011). SET9 has also been shown to methylate the estrogen receptor (ER) to stabilise the protein and enhance its transcriptional activity. An ER mutation strongly associated with breast cancer at K303 demonstrated an increase in SET9 methylation at K302 in vitro. Similarly, SETDB1 has been shown to form a complex with and methylate p53 in cancer cell lines (Fei *et al.*, 2015). These studies demonstrate an alternative but equally important role for SET9 and SETDB1 interacting with non-histone proteins to regulate their transcriptional activity. This led us to examine what roles these methyltransferases could play in TGF  $\beta$ -1/SMAD signalling in renal fibrosis.

## **1.8 Aurora Kinase Signalling**

### ***1.8.1 The Aurora Kinase Protein Family***

The Aurora Kinase (AURK) family, consisting of Aurora A, B and C in humans are closely related serine-threonine protein kinases, involved in the regulation of the mitotic phase of the cell cycle (Vader and Lens, 2008). The function of each AURK is related to their localisation at particular points during the cell cycle. Aurora A (AURKA) is important for cell cycle progression, particularly entry into mitosis and is localised at the centrosome during interphase and at the spindle during mitosis (Stenoien *et al.*, 2003; Seki *et al.*, 2008). AURKA is also involved in centrosome assembly and maturation as well as spindle formation (Sardon *et al.*, 2008). Aurora Kinase B (AURKB) is localised to the chromosomes where it is responsible for chromosome condensation and chromosome attachment to the mitotic spindle, as well as cytokinesis (Welburn *et al.*, 2010). Much less is known about AURKC; it is thought to be involved in meiosis.

The AURKs role in the cell cycle is well characterised but their mechanism of action still remains poorly understood. Their small number of known substrates give little indication of

their role and therefore identification of other AURK substrates is important in determining their functions.

### ***1.8.2 The Role Aurora Kinases in Human Disease***

AURKA is located on chromosome 20q13.2 known to be frequently amplified in tumours and cancer cell lines (Katayama et al., 2003). AURKA overexpression results in centrosome amplification, colony formation and tumour growth due to dysregulation in mitosis (Bischoff et al., 1998). AURKB overexpression leads to failed cytokinesis and is thought to also be involved in tumourigenesis as it has been shown to be overexpressed in some tumour types but its role is less clear as AURKB is located on chromosome 17p12.1, a region that has not yet been associated with amplification in tumours (Katayama et al., 2003). Both AURKA and AURKB being implicated in tumourigenesis has enabled the exploration of AURK inhibitors as targets for anticancer treatments (Damodaran et al., 2017).

### **1.9 Aims**

The aims of this research were to:

1. Validate a previously identified potential therapeutic target in CKD, SET9 and determine its role in TGF  $\beta$ -1/SMAD3 in renal fibrosis.
2. Screen a library of methyltransferase siRNAs to identify additional enzymes which may play an important role in the regulation of TGF  $\beta$ -1 signalling in renal fibrosis.
3. Establish an effective technique for isolating Primary Renal Fibroblasts to provide a more relevant primary cell model.
4. Use the primary cell model to screen a library small molecule inhibitors to determine their effect on cell proliferation and validate any attractive compounds.

## Chapter 2: Materials and Methods

### 2.1 Risk Assessment

All experiments were performed in compliance with Biological Control of Substances Hazardous to Health (BIOCOSH) and Control of Substances Hazardous to Health (COSHH) regulations. All laboratory work was conducted in accordance with Institutional rules and regulations.

### 2.2 Mammalian Cell Culture and Compounds

#### 2.2.1 Mammalian Cell Culture

HK C-8 cells are an immortalised human renal proximal tubular epithelial cell line purchased from ATCC. THMC cells are an immortalised human renal mesangial cell line contributed by Prof. Jill Norman, University College London. Skin Fibroblast cells are an immortalised cell line acquired from Dermatology Department at Newcastle University. SET9 MEFs were obtained from Guiseppe Testa (IFOM IEO, Milan) whereas SMAD3 MEFs were obtained from Prof. Erwin Bottinger (Mt. Sinai School of Medicine, New York City). Primary Renal Fibroblast cell lines were purchased from DV Biologics (Palo Alto, CA) or isolated in-house (section 2.5).

HK C-8 and THMC cells were maintained in DMEM F12 (LZBE12-719F, Lonza) supplemented with 10% (v/v) foetal bovine serum (FBS) (Lonza) and 1% (v/v) 10,000 units penicillin and 10 mg streptomycin/ml (Sigma Aldrich). pCAGA12-luc reporter stably transfected HKC8 cells were maintained in DMEM F12 supplemented with 10% (v/v) FBS, 1% (v/v) penicillin streptomycin and 300 $\mu$ M hygromycin B from *Streptomyces hygroscopicus* (Sigma). All MEF cells and skin fibroblast cells were maintained in DMEM (LZBE12-604F Lonza) supplemented with 10% (v/v) FBS and 1% (v/v) penicillin streptomycin (Sigma Aldrich). Primary renal fibroblasts (isolated in-house or purchased) were maintained in I Gro Fibroblast Cellutions Medium (DV Biologics) supplemented with 10% (v/v) FBS (Lonza) and 1% (v/v) penicillin streptomycin (Sigma Aldrich).

DMEM F12 fully supplemented with 10% (v/v) foetal bovine serum (Lonza) and 1% (v/v) penicillin streptomycin (Sigma), hereby referred to as full media (FM). DMEM F12 supplemented with only penicillin streptomycin (Sigma), hereby referred to as basal media (BM). DMEM F12 supplemented with 0.5% (v/v) foetal bovine serum (Lonza) and 1% (v/v) penicillin streptomycin (Sigma), hereby referred to as full media (0.5% serum starved).

### **2.2.2 Cell Subculturing**

Cell culture was carried out in a BioMat class II microbiological safety cabinet. To passage cells, culture media was removed from the culture flask and cells gently washed two times with phosphate buffered saline (PBS) (Sigma Aldrich) and incubated with 1 x Trypsin-EDTA (Sigma Aldrich) solution at 37°C for 2-3 minutes until cell detachment. Trypsin was neutralised by the addition of an equal volume of FM to the flask and the cell suspension was transferred to a sterile universal tube (Star Lab) and centrifuged at 400 x g for 5 minutes. The supernatant was removed and cell pellet was resuspended in FM and seeded into new flasks at a 1:3 dilution. In-house mycoplasma tests were carried out every 2 months using a Mycoplasma Detection Kit (R&D Systems).

### **2.2.3 Cell Storage**

Cells were resuspended to  $1 \times 10^6$  per ml of freezing media (FBS containing 10% dimethyl sulfoxide (DMSO) (Sigma Aldrich)) and divided into 1ml aliquots in cryogenic tubes (Thermo Scientific) before being stored in a Mr Frosty™ Container (Thermo Scientific) at -80°C. For long-term storage (>2months) cells were transferred to liquid nitrogen after 24 hours at -80°C. To animate cells, the cryogenic tubes of cells were taken from liquid nitrogen and thawed in a 37°C water bath then added to pre-warmed FM in a culture flasks. Once cells had adhered, the culture medium was changed to fresh FM.

### **2.2.4 Compounds**

Transforming Growth Factor beta 1 (TGF  $\beta$ -1)

Transforming Growth Factor beta 1 (TGF  $\beta$ -1), a potent growth factor, was purchased in lyophilised form from R & D Systems, reconstituted in 20  $\mu$ g/ml in sterile 4 mM HCl containing 1 mg/ml human or bovine serum albumin at 20  $\mu$ g/ml and stored in aliquots at -80°C.

(R)-PFI hydrochloride

(R)-PFI hydrochloride (Chemical Name: (1R)-1-[[3-(Trifluoromethyl)phenyl]methyl]-2-oxo-2-(1-pyrrolidinyl)ethyl]1,2,3,4-tetrahydro-6-isoquinolinesulfonamide hydrochloride) (R-PFI-2), a potent and selective SET9 histone lysine methyltransferase inhibitor, was purchased from R & D Systems in powder form, reconstituted in DMSO (Sigma Aldrich) at 100mM and stored at -20°C.

## Cycloheximide (CHX)

Cycloheximide (CHX) (Chemical Name: 3-[2-(3,5-Dimethyl-2-oxocyclohexyl)-2-hydroxyethyl]glutarimide), is an antibiotic produced by *S. griseus*. Its main biological activity is translation inhibition in eukaryotes resulting in cell growth arrest (Schneider-Poetsch *et al.*, 2010). CHX was purchased from Sigma Aldrich in powder form and resuspended in DMSO at 100µg/ml.

## MG-132

MG-132 (chemical name: benzyl (S)-4-methyl-1-1((S)-4-methyl-1-((S)-4-methyl-1-oxopentan-2-ylamino)-1-oxopentan-2-ylamino)-1-oxopentan-2-ylcarbamate), a membrane permeable proteasome inhibitor, was purchased as a ready-made solution in DMSO at a concentration of 10 mM (Sigma Aldrich) and stored at -20°C.

## MK-5108

MK-5108 is a potent Aurora Kinase A inhibitor and was purchased from Selleck Chem and resuspended in DMSO then used at a concentration of 30-50µM in HK C-8 cells and in UUO mice at 45mg/kg body weight in 1% methylcellulose, administered by daily oral gavage.

## SB505124

SB505124 is an ALK5 inhibitor, a potent selective inhibitor of TGF βRI kinase, was purchased from Tocris. SB505124 was used at 5µM in PRF cells.

## **2.3 Plasmids**

pCAGA12-luc plasmid was acquired from Caroline Hill (The Francis Crick Institute, London). The FLAG-tagged SET9 wild-type (FLAG-SET9<sub>WT</sub>) and mutant (FLAG-SET9<sub>H297A</sub>) plasmids were contributed by Dr Danny Reinberg (Howard Hughes Medical Institute, New York). SMAD3 C (1-211) and SMAD3 NL (199-425) plasmid vectors were purchased from Addgene.

## **2.4 siRNA and DNA Plasmid Transfection**

### **2.4.1 siRNA Transfection**

Cells were transfected using Lipofectamine® RNAiMAX transfection reagent (Life Technologies) according to the manufacturer's guidelines. siRNA sequences used are shown in Table 2.1. Transfection mixtures were prepared by adding the required volume of siRNA

at a final concentration of 25-50nM and transfection reagent in a 1:3 volume ratio, respectively, to basal medium (without antibiotics). The transfection mixture was incubated at room temperature for 20 minutes then added directly to seeded cells (forward transfection) or to a dish or well with cells subsequently seeded on top of the transfection mix (reverse transfection). Transfections were incubated for 24-96 hours at 37°C to obtain optimal gene knockdown. Efficient gene knockdown was then determined by Western Blotting.

siRNA Target	siRNA Sense Sequence
Scrambled (non-targeting siRNA)	UUCUCCGAACGUGUCACGU
SET9	GTAATCCGTCATCGTCCAGGTGC
SETDB1	Dharmacon M-020070-00
Aurora Kinase A	Sigma SIHK0140
Aurora Kinase B	Sigma SIHK0145

**Table 2.1 siRNA Sequences and their Gene Target**

#### ***2.4.2 Plasmid DNA transfection***

Mammalian expression plasmids were transfected using Lipofectamine LTX reagent (Life Technologies), by forward transfection. Transfection mixtures were prepared by adding 3µl of LTX reagent to every 1µg of plasmid in basal media (200 µl/well of 6-well plate, 0.5 ml/90mm plate, 1 ml/150mm plate). The LTX reagent and plasmid mixture was incubated at room temperature for 20 minutes then added dropwise to 60-70% confluent cells in culture medium. Transfected cells were incubated for 48-72 hours before harvesting.

#### ***2.4.3 Stable cell cloning***

HKC8 cells were used to create a stable cell line expressing pCAGA12-luc due to their ease of transfection and their intact TGF β-1 signalling pathway. The cells were transfected with 1µg of pDR2 carrier plasmid containing Hygromycin B (Sigma Aldrich) selection marker and 10µg of pCAGA12-luc plasmid using Lipofectamine transfection reagent (Life Technologies). 48 hours post-transfection, cells were cultured in FM containing hygromycin B selection at concentrations of 400µg/ml with subsequent media changes every 4-5 days. After two weeks, colonies arose from cells maintained in 400µg/ml selection. Colonies were selected and maintained in FM containing 300µg/ml hygromycin B. They were then tested for

luciferase induction in the presence of TGF  $\beta$ -1. A single clone with absent luciferase expression in the absence of TGF  $\beta$ -1, exhibiting a high luciferase count in the presence of exogenous TGF  $\beta$ -1 was selected for further experimentation.

#### ***2.4.4 Methyltransferase siRNA Screen***

HK C-8 cells were stably transfected with the TGF  $\beta$ -1 responsive CAGA-luc reporter plasmid then reverse transfected with either control SCR siRNA or a library of 50 methyltransferase siRNAs at a final concentration of 25 nM. The siRNA library contained three pooled specific siRNAs to each of the 50 methyltransferases selected to be investigated, contributed by Dr. Luke Gaughan (Northern Institute for Cancer Research, Newcastle). An untransfected control  $-/+$  TGF  $\beta$ -1 was also included. Each pool of siRNA was performed in quadruplicate. The cells were treated with 1ng/ml TGF  $\beta$ -1 for 24 hours, a luciferase assay was subsequently performed, correcting for protein quantity using a BCA assay.

#### **2.5 Isolation of Primary Renal Fibroblast (PRF) Cells**

Human PRFs were isolated from human nephrectomy kidney specimens. Tissues were derived from human nephrectomised kidney segments or sections from kidneys deemed unsuitable for transplantation (rejected due to donor reasons). Ethical approval was obtained from the National Research Ethics Committee, East Midland, UK for work on gene and protein expression in the kidney.

An outgrowth method as described by (Tan and Hewitson, 2016) was used to isolate the PRFs from dissected cortical tissue which was plated directed onto a scratched cell culture dish. The tissue was then maintained in high glucose enriched media RMPI 1640 (Sigma Aldrich), supplemented with 10% (v/v) FBS and 1% (v/v) penicillin streptomycin (Sigma), for 14 days, with media changes every 3-4 days. Once cells started to grow out, the tissue was gently removed. The cells were trypsinised once they reached a monolayer of 75% confluency and transferred to culture flasks until confluent. To characterise cell morphology by scanning electron microscopy, cells were fixed in 2% glutaraldehyde for 2 hours and before addition of mounting medium and imaging of the cells to look for spindle-shaped cell morphology. The cells were also characterised by immunofluorescence to identify the expression of fibroblast markers alpha-smooth muscle actin ( $\alpha$ -SMA), fibronectin and Collagen I, Collagen III and S100 and the absence of an epithelial cell markers, E-cadherin and K-cadherin. Once characterised, the cells were used to study their response in proliferation assays, siRNA knockdowns, wound healing and collagen contractility assays. Cell proliferation arrested after

passage 4 and the cells changed phenotype, consequently, isolated PRF cells were not used beyond passage 3.

## **2.6 SDS-poly acrylamide gel electrophoresis (SDS-PAGE) and Western blotting (WB)**

### **2.6.1 SDS-PAGE**

Cell lysates were prepared by adding SDS sample buffer (125 mM Tris-HCl, pH 6.8, 5% SDS, 10% glycerol, 10%  $\beta$ -mercaptoethanol and 0.01% bromophenol blue) directly to cells washed with PBS. The cell lysates were then boiled for 10 minutes at 100°C before being loaded on to a precast NuPAGE Novex® 4-12% Bis-Tris Protein Gel (Life Technologies). SeeBlue® Plus2 Pre-stained Protein Standard (Life Technologies) was loaded alongside the samples to determine the molecular weight of the proteins. Proteins were separated by XCell SureLock® Mini-Cell (ThermoFisher) filled with 1x MOPS running buffer (10 x buffer: 52.3g MOPS, 30.3g Tris Base, 5g SDS, 1.5g EDTA made up to 500 ml ddH<sub>2</sub>O) at a constant voltage of 160V.

### **2.6.2 Western Blotting (WB)**

Following protein separation by gel electrophoresis, proteins were electrotransferred to PDVF membrane (Hybond, Amersham) using the XCell II™ Blot Module, with the inner chamber filled with 1x transfer buffer (10x buffer: 30.3g Tris base, 144g Glycine, made up to 1l ddH<sub>2</sub>O) and the outer chamber filled with water, at a constant voltage of 30V for 90 minutes. For molecular weight proteins >150 the Fisherbrand™ TV100-EBK Electroblotter was filled with transfer buffer and set at a constant voltage of 25V overnight at room temperature (RT). The blots were blocked in 1x Tris-Buffered Saline (TBS) (10x stock containing 87.6g NaCl, 12.1g Tris, made up to 1l ddH<sub>2</sub>O pH8.0) containing 5% bovine serum albumin (BSA) (Sigma Aldrich) for 1h at RT. Primary antibodies were diluted between 1:500 to 1:2000 in 1 x TBS containing 1% BSA overnight at 4°C. Blots were washed for 3 x 5 minutes in 0.1% tween-TBS with gentle rocking then incubated in secondary antibodies (rabbit anti-mouse, mouse anti-rabbit, mouse anti-goat horseradish peroxidase-conjugated, Dako) diluted 1:1000 in 1x TBS containing 1% BSA for 1h at RT. After 2x 5 minute washes in 1x 0.1% Tween-TBS and 1x 5 minute wash in 1x TBS with gentle rocking, the blots were developed with ECL reagents (Pierce) and were exposed on X-ray film (Agfa). Protein bands were then quantified using Image J.

<b>Antibody</b>	<b>Species</b>	<b>Supplier</b>	<b>Applications</b>
SMAD3	Rabbit	Abcam	IP, IF, WB, IHC, CHIP
SMAD3	Mouse	Sigma	IP, IF, WB
SMAD2/3	Rabbit	Cell Signaling	IF, WB
SMAD2 S20	Goat	Santa Cruz	IF, WB
P-SMAD2/3	Rabbit	Cell Signaling	IF, WB, IP
P-SMAD32/3 ser423/425	Rabbit	Santa Cruz	WB, IP
SET9	Mouse	Millipore	IP, IF, WB
SET9 (S4E5)	Mouse	Santa Cruz	WB
SET9	Rabbit	Cell signaling	IP, WB, CHIP
FLAG M2	Mouse	Sigma	IP, IF, WB
GAPDH	Mouse	Sigma	WB
GAPDH	Rabbit	Sigma	WB
PARP 1	Mouse	Sigma	WB
HDAC1	Goat	Sigma	WB
Collagen I	Rabbit	Abcam	IF, WB, IHC
Collagen I	Mouse	Sigma	IF, WB
Collagen I	Rabbit	Novis	IF, WB
Collagen III	Rabbit	Abcam	IF, WB, IHC
$\alpha$ -SMA	Rabbit	Abcam	IF, WB, IHC, CHIP
$\alpha$ -SMA	Mouse	Sigma	IF, WB
Fibronectin	Rabbit	Sigma	IF, WB
PAI-1	Rabbit	Abcam	IF, WB
S100	Rabbit	Abcam	IF, WB
Vimentin V9	Rabbit	Abcam	IF, WB
E-cadherin	Mouse	Sigma	IF, WB
ESET G4	Mouse	Santa Cruz	IP, IF, WB
ESET H300	Rabbit	Santa Cruz	IP, IF, WB
ESET	Mouse	Abcam	IP, IF, WB
SMYD2 C20	Goat	Santa Cruz	IP, IF, WB
MLL C20	Goat	Santa Cruz	IP, IF, WB
Aurora Kinase A	Rabbit	Abcam	IP, IF, WB
Aurora Kinase B	Rabbit	Abcam	IP, IF, WB
P-Aurora Kinase A/B	Rabbit	Abcam	WB, IHC
$\alpha$ -Tubulin	Mouse	Sigma	WB
$\alpha$ -Actin	Mouse	Santa Cruz	WB
$\beta$ -Actin	Mouse	Sigma	WB
IgG	Rabbit	Abcam	IP
IgG	Mouse	Sigma	IP
HA tag (agarose)	Goat	Abcam	IF, WB
HA tag (agarose)	Mouse	Abcam	IF, WB
GST	Goat	Abcam	IP, WB
SMAD7	Rabbit	Thermo Fisher	WB
Histone H3	Rabbit	Abcam	WB
P53	Rabbit	Abcam	WB

**Table 2.2 Antibodies used for Western Blotting (WB), Immunoprecipitation (IP), Immunofluorescence (IF), Immunohistochemistry (IHC) and Chromatin Immunoprecipitation (ChIP).**

## **2.7 Bacterial Transformation, Plasmid DNA Isolation and Gel Electrophoresis**

### ***2.7.1 Bacterial transformation of plasmid DNA***

Plasmid DNA was transformed using NEB® 5-alpha Competent *E.coli* chemically competent cells (New England Biolabs). Approximately 500ng of plasmid DNA was added to the competent cells, mixed by gently flicking and incubated on ice for 30 minutes before heat shock at 42°C for 30 seconds. The cells were placed back on ice for 2 minutes before the addition of 500µl SOC outgrowth medium (2% Peptone, 0.5% Yeast Extract, 10mM NaCl, 2.5mM KCl, 10mM MgCl<sub>2</sub>, 10mM MgSO<sub>4</sub>, 20mM Glucose) and incubation at 37°C with agitation for 45 minutes. The cell culture was mixed by gently flicking of the tube then 200µl culture was spread on to pre-warmed LB agar plates (1% (w/v) tryptone, 1% (w/v) NaCl, 0.5% (w/v) Yeast Extract, 1.5% (w/v) agar) containing the antibiotic selection 100 µg/ml ampicillin and incubated at 37°C overnight.

### ***2.7.2 Amplification of transformed DNA***

For DNA maxi prep culture, single colonies were picked from the LB plates and incubated in 4ml LB medium (1% (w/v) NaCl, 1% (w/v) tryptone, 0.5% (w/v) yeast extract) containing the antibiotic selection 100ug/ml ampicillin with 200 rpm agitation at 37°C. After 4 hours the culture was transferred to a conical flask containing 200ml LB medium with antibiotic selection and incubated overnight with 200rpm agitation at 37°C.

### ***2.7.3 Plasmid DNA Extraction***

For maxiprep cultures the ChargeSwitch®-Pro Filter Plasmid Maxiprep Kit (Invitrogen) was used according to the manufacturer's protocol. The kit involved resuspension of the bacterial pellets, cell lysis, filtration of cellular debris, precipitation, washing and elution of plasmid DNA. Resultant purified DNA was resuspended in 500µl Nuclease-free water (Severn Biotech) and DNA concentration measure using the Nanodrop spectrophotometer (Thermo Scientific).

### ***2.7.4 Agarose Gel Electrophoresis***

To ensure successful cloning, purified plasmid DNA were subjected to gel electrophoresis to determine DNA size. Plasmid DNA (500ng) was mixed with 4µl 5x DNA loading buffer (Bioline). Samples were loaded into a 1% Agarose/TAE buffer (40mM Tris, 20mM acetic

acid, 1mM EDTA) gel and run at 100V using Mini-Sub Cell GT Cell system (Bio-Rad) until satisfactory separation was achieved. 1kb ladder (Promega) was loaded alongside the samples as a molecular weight marker. DNA size was visualised on a GBOX Chemi gel doc system (Syngene).

## **2.8 Protein Purification**

GST resin columns were used for GST-tagged protein purification (GE Healthcare). Bacterial cell pellets expressing recombinant proteins were resuspended in 600µl of lysis buffer (PBS containing 1% Triton-X-100) on ice, sonicated and cleared by centrifugation at 1000 x g. Clarified lysates were then transferred to GST spin columns and incubated on ice for 5 minutes. Columns were centrifuged at 1000 x g for 30s and flow-through discarded. 600µl chilled PBS was added to the column and centrifuged again at 1000 x g for 30 seconds, this wash step was repeated. The column was then placed into a fresh tube and 120µl chilled elution buffer (20mM L-glutathione (reduced) in 50mM Tris pH8.0) added to the column and centrifuged at 1000 x g for 30s. The flow-through contained the purified protein.

## **2.9 Nuclear and Cytoplasmic Extractions**

Nuclear and cytoplasmic fractions were isolated using sequential centrifugation steps, in Hypotonic Buffer Solution (20mM Tris-HCl pH7.4, 10mM NaCl and 3mM MgCl<sub>2</sub>) and Cell Extraction Buffer (100mM Tris pH7.4, 2mM NaVO<sub>4</sub>, 100mM NaCl, 1% Triton-X-100, 1mM EDTA, 10% glycerol, 1mM EGTA, 0.1% SDS, 1mM NaF, 0.5% deoxycholate and 20mM Na<sub>4</sub>P<sub>2</sub>O<sub>7</sub>, 1mM PMSF, Protease Inhibitor). Cells seeded onto 100mm culture dishes were gently washed with PBS then scraped and centrifuged at 3000 x g at 4°C to collect the cell pellet. The supernatant was discarded and the cell pellet resuspended in 500µl hypotonic buffer and incubated on ice for 15 minutes. 25µl of 10% IGEPAL (Sigma Aldrich) was added to each sample and vortexed for 10 seconds. The samples were centrifuged at 3000 x g for 10 minutes at 4°C. The supernatant contained the cytoplasmic fraction. The nuclear pellet was then resuspended in 50µl Cell Extraction Buffer and incubated on ice for 30 minutes, vortexing at 10 minute intervals. The sample was then centrifuged at 10 000 x g for 30 minutes at 4°C. The supernatant contained the nuclear fraction. SDS sample buffer was added to both fractions and subjected to Western blotting analysis.

## **2.10 Immunoprecipitation: Cell Lysates, Purified Proteins and Nuclear Cell Fractions**

### ***2.10.1 Immunoprecipitation from Cell Lysates***

To analyse protein-protein interactions, immunoprecipitations (IP) were carried using cell lysates. 1ml IP lysis buffer (50mM Tris pH7.4, 150mM NaCl, 1mM EDTA, 1% Triton-X-100, 1x protease inhibitor tablet (Roche), phosphatase inhibitor (100µl in 10ml Sigma)) was added directly to cells grown on 100mm culture dishes and incubated on ice for 5 minutes. Cells were then scraped, transferred into Eppendorf tubes and sonicated. Cells were centrifuged at 4°C for 25 minutes at 20,000 x g to remove insoluble cell debris. 50µl was taken from each sample as an input sample. 20µl (per sample) of protein G dynabeads (Life Technologies) were washed in PBS and incubated with 1µg of primary antibody overnight at 4°C with rotation. An isotype immunoglobulin antibody was included to serve as a negative control. The following day, the samples were washed 3 times with 1ml FLAG wash buffer (50mM Tris pH7.4, 150mM NaCl, 1mM EDTA, 1% Triton-X-100, 1x protease inhibitor tablet (Roche) and phosphatase inhibitor (Sigma Aldrich)). After the final wash, samples were centrifuged to remove any excess wash buffer and re-suspended in 50ul SDS-sample buffer (10ml 3x stock: 2.4ml 1M Tris pH 6.8, 3ml 20% SDS, 3ml glycerol, 1.6ml β-merceptoethanol and few grains of bromophenol blue) and subjected to SDS-PAGE and Western blotting analysis.

### ***2.10.2 Immunoprecipitation with Nuclear Cell fractions***

Immunoprecipitations were also carried out on nuclear cell fractions, in which case nuclear fractions were extracted from cells (section 2.9) before being incubated with protein G dynabeads.

### ***2.10.3 Immunoprecipitation with Purified Proteins***

Recombinant human SET9 (Millipore) and either purified GST-SMAD3 C or GST-SMAD3 NL were mixed together and incubated on ice for 30mins before 500µl PBS containing protease inhibitors (Sigma) was added. Protein G sepharose beads (Life Technologies) were washed in PBS and blocked with 1ml 0.2% BSA in PBS for 1 hour on rotation. 25µl of blocked sepharose beads were added to 1ug SET9 primary antibody and 1ug control IgG antibody (Sigma). Samples of recombinant SET9 and GST-SMAD3 C and SET9 and GST-SMAD3 NL were then added to tubes of SET9 coupled sepharose beads and IgG control-coupled sepharose beads and incubated on rotation at 4°C overnight. After 3-5 washes in PBS buffer B (10ml containing 100mM Tris pH8.0, 500mM NaCl, 0.5% Tween 20, and 1x

protease inhibitor tablet) and elution in 50µl SDS sample buffer, samples were subjected to SDS-PAGE and Western blotting analysis.

### **2.11 Proliferation Assay**

Approximately 5000 cells/well were seeded into a 96-well plate, starved in BM and treated as required. 5µl WST-1 reagent (Roche) was then added directly to the medium in each well and incubated at 37°C for 30 minutes. The plate was then read at 450nm on Multiskan™ FC Microplate Reader (Thermo Scientific).

### **2.12 Protein Half-Life Assay**

10 000 cells/well were seeded onto a 96-well plate and left overnight to adhere. The following day cells were treated with 5ng/ml TGF β-1 for 24 hours. Subsequently, medium was replenished with fresh FM containing 5ng/ml TGF β-1 and 60µg/ml cycloheximide (CXH) was added to wells for set time-points 0-6 hours. At each time-point, the medium was removed and cells gently washed with PBS. SDS-sample buffer was added to the wells and the cells subjected to Western blotting analysis.

### **2.13 Ubiquitylation**

To examine ubiquitylation, cells were transfected overnight with the indicated plasmids, then treated with 10ng/ml TGF β-1 and a low-dose 1µM MG-132 then subjected to Ni-NTA chromatography. For immunoprecipitation of ubiquitylated proteins, 50 µl equilibrated nickel-agarose (Ni-NTA Qiagen) was added to each sample and incubated at 4°C for 8 h, followed by subsequent washes of the pelleted agarose in wash solutions 1 (8M urea, 0.1M Na<sub>2</sub>HPO<sub>4</sub>/NaH<sub>2</sub>PO<sub>4</sub>, 0.01M Tris-HCl, pH8, 10mM β-mercaptoethanol) and 2 (8M urea, 0.1M Na<sub>2</sub>HPO<sub>4</sub>/NaH<sub>2</sub>PO<sub>4</sub>, 0.01M Tris-HCl, pH 6.3, 10mM β-mercaptoethanol and 0.1% Triton-X-100). The proteins were then eluted from the agarose using 70 ul elution buffer (200 mM imidazole, 0.15M Tris-HCl, pH6.7, 30% glycerol, 0.72M β-mercaptoethanol and 5% SDS). The samples were mixed with SDS sample buffer then subject to Western blotting analysis probing with an anti-SMAD3 antibody.

### **2.14 Immunofluorescence**

Cells were seeded on 8-chamber tissue culture slides (Falcon). After treatment with TGF β-1 and/or SET9 inhibitor R-PFI, the cells in each chamber of the culture slide were washed with 200µl PBS (Sigma), fixed with 200µl ice-cold 100% methanol and blocked in 200µl PBS containing 5% goat serum (Sigma) for 1 hour at room temperature. Primary antibodies were

applied at a dilution of 1:100 in PBS overnight at 4°C. Secondary Alexa Fluor antibodies were then applied at 1:200 in PBS for 2 hours in the dark at RT. Lastly, DAPI nuclear stain (Sigma) was applied at 0.5µg/ml in PBS for 10 minutes in the dark at room temperature. The chambers were washed 3 times in PBS, chamber wells removed and a coverslip mounted with Fluorescent mounting medium (Dako). Control slides were treated with secondary only antibodies. The slides were imaged using a Zeiss Axioimager microscope and analysis completed with Image J software to determine fluorescence intensity.

## **2.15 Luciferase Reporter Assay**

### ***2.15.1 Cell Transfection***

pCAGA12-luc reporter stably-transfected HKC8 cells were seeded in 48-well plates, reverse transfected with either control or a library of pooled methyltransferase siRNAs, acquired from Dr. Luke Gaughan (Northern Institute of Cancer Research, Newcastle University) at a final concentration of 25nM. After 24 hours, cells were treated with 1ng/ml TGF β-1. Each siRNA was transfected in quadruplicate. After 24h, cells were washed in PBS and harvested in 55µl per well 1x Reporter Lysis Buffer (Promega) and one freeze-thaw cycle (-80°C for 10 minutes then 37°C for 10 minutes) was performed.

### ***2.15.2 Luciferase Assay***

Cells were scraped into microcentrifuge tubes and 30µl of each sample transferred into a 96-well white opaque microplate (Greiner Bio-one). 50µl of luciferase Assay Reagent (Promega) was then added to the samples in each well of the plate. The plate was inserted into a FilterMax plate-reader (Molecular Devices), shaken for 30 seconds and luminescence measured.

### ***2.15.3 BCA Assay***

A bicinchoninic acid assay (BCA) assay (Thermo Scientific) was performed on the remaining 25µl of each sample following the manufacturer's protocol, to correct for protein quantity. 25µl of each sample was transferred to a clear 96-well culture microplate (Greiner Bio-one), alongside a standard prepared from 0-2000µg/ml BSA. 200µl of working reagent (WR) – 1:50 Reagent A (sodium carbonate, sodium bicarbonate, bicinchoninic acid and sodium tartrate in 0.1M sodium hydroxide) and Reagent B (4% cupric sulfate), respectively, was added to each sample and standard and incubated for 30 minutes at 37°C and absorbance measured by a FilterMax plate-reader (Molecular Devices) at 450nm.

The luciferase readouts were corrected for BCA readouts and the data represented by bar graphs of the fold change in luciferase activity with error bars of standard deviation.

### **2.16 Wound Healing Assay**

Cells were seeded into a 2-well silicone cell culture insert (Ibidi) to create reproducible 500 $\mu$ m cell-free wounds in 12-well plates. The following day the cells were treated with or without 10ng/ml TGF  $\beta$ -1 and in subsequent experiments with or without SET9 inhibitor (Tocris) 5-30 $\mu$ M or transfected with SCR or SETDB1 siRNA. 24h after treatment, the inserts were carefully removed and the cells imaged at 4h intervals over 0-48h using a Zeiss Axiomager II microscope. Wound closure was measured by % cell surface coverage using NIS-Elements and Image J microscope imaging software.

### **2.17 Collagen Contractility Assay**

Adapted from (Grinnell *et al.*, 1999), 10ml of collagen gel solution was prepared (2ml 5X DMEM, 0.81ml rat tail Collagen I, 37 $\mu$ l NaOH and 7.15ml ddH<sub>2</sub>O). 6x10<sup>5</sup> cells treated with or without SET9 inhibitor for 24 hours were pelleted then re-suspended in the 5ml Collagen gel solution and aliquoted into a 24-well plate. Collagen gels were left to set for 30 minutes at 37°C before the addition of FM with or without 10ng/ml TGF  $\beta$ -1 to the top of the gel matrices. A stress period of 24 hours was allowed for the cells to develop  $\alpha$ -SMA stress fibers, after which the Collagen matrices were released with a needle to detach the matrices from the sides of the wells. The diameter of the Collagen matrices were measured 24-48 hours after release. In subsequent experiments the cells were transfected with siRNAs before being pelleted.

### **2.18 Chromatin Immunoprecipitation (ChIP)**

Chromatin from PRFs was prepared, after cross-linking cells in 1% formaldehyde for 10min at room temperature, using ChromaFlash High-Sensitivity ChIP Kit (Epigentek). 20 $\mu$ g of chromatin was used, with 1 $\mu$ g of respective antibody. Oligonucleotide sequences TTTTCAGCTTCCCTGAACACC and CGGGTAATTAAAAGAGCCACTG were used to amplify the human sequence corresponding to the Rat SBE2 SMAD binding element, identified by sequence alignment 55, with 19 cycles of PCR. GAPDH oligonucleotides were used as recommended.

## **2.19 *In Vitro* kinase reactions**

Recombinant SMAD3 (Sino 50991-M20B) and recombinant AURKA (Abcam ab42595) were incubated at 30°C in kinase buffer containing 50mM Hepes pH 7.4, 3mM MgCl<sub>2</sub>, 3mM MnCl<sub>2</sub>, 1mM DTT, 3µM Na orthovanadate and 0.5mM ATP. One unit of calf intestinal phosphatase (CIP) (Promega) was added where shown. Reactions were stopped by the addition of Laemmli buffer prior to either NuPAGE 4-12 % gradient gel electrophoresis (Thermofisher) in MOPS buffer (Thermofisher) to resolve band shifted proteins, or standard discontinuous NuPAGE 10 % polyacrylamide gel electrophoresis (Thermofisher) in MOPS buffer, followed by immunoblotting.

## **2.20 Flow Cytometry**

To measure apoptosis, FITC annexin V staining was used as per manufacturer's instructions (BD, 556547), on cells exposed to 10µM drug compounds or 1µM Staurosporine for the indicated times. For cell cycle analysis cells were treated overnight with 1µM drug compounds then fixed in 70% ethanol for 30 minutes prior to washing twice in PBS, treatment with 5µg/ml RNase then staining with 1µg/ml propidium iodide before analysis of cells gated to remove sub-G1 populations.

## **2.21 Unilateral Ureteral Obstruction (UUO) Model of Renal Fibrosis**

UUO surgery was performed on 14 female mice under isoflurane general anaesthesia in accordance with aseptic protocols approved by Comparative Biology Centre (CBC) and Animal Scientific guidelines implemented by the Home Office. The lower abdominal area was shaved and a subcutaneous injection of buprenorphine diluted in injectable saline was given as pain relief. A laparotomy was performed, cutting through the skin and muscle via the linea alba. A retractor was used to allow access to the internal viscera. The intestines were moved up and out of the abdominal incision and rested on gauze soaked in sterile saline. The intestines were then covered with more gauze and soaked in saline to prevent them drying out. The left ureter was then isolated and double ligated using non-degradable 5/0 mersilk suture. The ureter was then cut between the two sutures. The intestines were then replaced and the muscle layer sutured using normal interrupted sutures of round bodied 5/0 vicryl. The skin was sown shut using inverted interrupted sutures of cutting 5/0 vicryl in order to bury the knot to prevent the mice scratching them. The incision site was finally glued shut. Mice were then allowed to develop fibrosis. The contralateral, uninjured kidney served as an intraindividual

control. Animals were culled at days 10-post surgery. A minimum of 7 mice were used in each group. UUU surgery was performed by Dr Ana Moles.

## **2.22 Immunohistochemistry**

### ***2.22.1 Immunohistochemistry: $\alpha$ -SMA, Phospho-SMAD3, Phospho-Aurora A, Collagen I and III***

Immunohistochemistry (IHC) as performed on 5 $\mu$ m paraffin-embedded tissue sections that were cut by Newcastle Molecular Pathology Node Proximity Lab, Cellular Pathology, Newcastle upon Tyne Hospitals NHS Foundation Trust. Slides of tissue were placed into a glass rack and placed in glass jars of xylene (Cell Path), xylene, 100% ethanol (Fisher Chemicals), 70% ethanol, respectively, for 5 minutes each to de-wax and hydrate the sections. The sections were then quenched in 2% hydrogen peroxide (Sigma Aldrich) for 15 minutes to block endogenous peroxidase activity. The slides were washed in PBS before performing antigen retrieval, following the primary antibody manufacturer's recommendation. Antigen retrieval for  $\alpha$ -SMA, phospho-SMAD3, phospho-aurora A was heat-mediated using 40mM sodium citrate buffer boiled for 1 minute in a pressure cooker. Antigen retrieval for Collagen I and Collagen III was enzymatic using Collagenase (Sigma Aldrich) 8mg/ml in TBS preheated to 37°C and incubated on slides for 1 hour at 37°C. The slides were then blocked with ready-to-use (2.5%) normal horse blocking serum (ImmPRESS HRP Reagent Kit, Vector Laboratories) for 30 minutes at RT. Primary antibodies were applied overnight at 4°C at dilutions of 1:100-1:500. The following day, the slides were washed in PBS for 5 minutes before the application of secondary ImPRESS™ Reagent for 30 minutes at room temperature. The slides were washed again in PBS then incubated with DAB substrate solution (Buffer Stock solution, DAB stock solution, Hydrogen Peroxide solution, Vector Laboratories) for 1-2 minutes until the tissue just started to turn brown, then washed immediately with PBS for 5 minutes. The slides were then counterstained with haematoxylin (Weigert's Haematoxylin Solution Set, Sigma Aldrich) for 4 minutes and rinsed with water for 5 minutes to wash off excess stain. Finally, the sections underwent dehydration in 50% ethanol, 70% ethanol, 100% ethanol, 100% ethanol, xylene, xylene, respectively, for 5 minutes each then coverslips were mounted over the stained tissue using DPX mounting medium (Sigma Aldrich) and left to dry for 30 minutes.

### ***2.22.2 Picro-Sirius Red***

For Picro-Sirius red staining, slides were de-waxed and hydrated as described above then stained with haematoxylin for 8 minutes and washed in running tap water for 5 minutes. The slides were stained in Picro-Sirius Red for 1 hour (0.5g Sirius Red in 500ml (1.3% in water) saturated aqueous solution of picric acid, both from Sigma Aldrich). The slides then underwent 2 rapid (0.5 seconds) washes in acidified water (5ml glacial acetic acid (Sigma Aldrich) in 11ml distilled water) followed by dehydration in three rapid changes of ethanol 70%, 100%, 100%, respectively. The slides were finally cleared in xylene and mounted in DPX/pertex and left to dry for 30 minutes.

### ***2.22.3 Masson's Trichrome***

Masson's Trichrome staining was performed by Newcastle Molecular Pathology Node Proximity Lab, Cellular Pathology, Newcastle upon Tyne Hospitals NHS Foundation Trust.

Masson's Trichrome staining is used for the detection of collagen fibres in tissues. The collagen fibres are stained blue, the nuclei are stained black and the cytoplasm and muscle fibres are stained red. The slides were deparaffinised and rehydrated using 100% ethanol, 95% ethanol then 70% ethanol, respectively, then washed in distilled water. The slides were then placed in Weigert's iron hematoxylin working solution for 10 minutes to stain the nuclei then rinsed in running warm tap-water for 10 minutes to remove excess stain. The slides were then stained in Biebrich scarlet-acid fuchsin solution for 10-15 minutes, washed in distilled water then stained in phosphomolybdic-phosphotungstic acid solution for 10-15 minutes. Without rinsing, the slides were transferred to aniline blue solution and stained for 5-10 minutes, rinsed in distilled water and differentiated in 1% acetic acid solution for 2-5 minutes. The slides were washed in distilled water and dehydrated very quickly through 95% ethanol, 100% ethanol (to remove Biebrich scarlet-acid fuchsin staining) and then cleared in xylene. Lastly, the slides were mounted with resinous mounting medium (Vector Laboratories).

### ***2.22.4 Imaging and analysis***

Tissues were imaged on a Nikon Eclipse Upright Microscope at x20 and x40 magnifications. A threshold was set to determine positive staining. 10-15 images per slide were taken and scored for % positive staining. Outliers were removed and median % positive staining was plotted per slide with error bars of standard deviation.

### ***2.22.5 Acute CCl<sub>4</sub> Liver Injury Model***

6 mice were used per group. Mice received carbon tetrachloride at a dose of 2.0ml/kg of body weight (1:1 v/v in olive oil), as a single intraperitoneal injection. Control mice received a single intraperitoneal injection of olive oil at a dose of 2.0ml/kg of body weight. Mice were harvested 48 hours post-injection.

### ***2.22.6 $\alpha$ -SMA Immunohistochemistry***

IHC was performed on paraffin-embedded tissue sections of mouse liver. The sections were deparaffinised and hydrated in xylene and graded ethanol washes then endogenous peroxidase activity was blocked with 0.6% hydrogen peroxide solution for 10 minutes. Antigen retrieval was achieved using unmasking solution at 1:1000 dilution (F3777 Sigma Aldrich).

Avidin/Biotin Blocking Kit (Vector Laboratories) was used for 20 minutes to block endogenous avidin and biotin. Non-specific binding was blocked using 20% swine serum for 30 minutes followed by  $\alpha$ -SMA primary antibody applied at 1:100 overnight at 4°C. The following day, the slides were washed with PBS and incubated with biotinylated goat anti-fluorescein at 1:300 (BA-0601 Vector Laboratories) for 30 minutes at room temperature. The slides were then washed with PBS followed by a 30 minute incubation with Vectastain Elite ABC Reagent (Vector Laboratories). DAB peroxide substrate kit (Vector Laboratories) was used to visualise the staining, counterstaining with Mayer's haematoxylin (Sigma Aldrich) and then the slides were mounted. Stained slides were analysed at 10x magnification using a Nikon Eclipse Upright microscope and NIS-Elements BR analysis software. Ten random fields were analysed per mouse liver tissue section.

## **2.23 Isolation of Stellate Cells**

### ***2.23.1 Obtaining the Liver from the Mouse***

To harvest the liver from the mouse, the abdomen was cut open, the intestines were moved to the right hand side to expose the portal vein. The portal vein was then injected with Hanks Balanced Salt Solution + (HBSS+, Gibco) to blanch the liver. The vena cava was then cut and the liver removed and placed into a specimen tube with HBSS +.

### ***2.23.2 Processing the Liver to Isolate Hepatic Stellate Cells (HSC)***

Pronase 1 and Collagenase were added to the specimen tubes of 8 livers, the livers were cut into small pieces to aid digestion and placed into an incubated specimen shaker at 37°C at 180 rpm for 15-25 minutes. The liver mixture was then pushed through fine mesh into a beaker

containing DNase (Sigma Aldrich) in HBSS + and centrifuged for 7 minutes at 1800 x g. The supernatant was carefully removed and the cells resuspended in DNase and HBSS +. The resuspended cell mixture was then carefully added to a new falcon tube containing Optiprep (Sigma Aldrich) to create 2 layers then HBSS + was added on top, creating a tri-layered solution. The layered solution was centrifuged at 1500 x g for 23 minutes. After centrifugation, there should be a visible layer of stellate cells present just below the top layer of solution. The stellate cells were removed and added to a new falcon tube of DNase and HBSS + and centrifuged at 1800 x g for 7 minutes. The supernatant was removed and the resultant cell pellet was stellate cells which were then placed in culture flasks containing DMEM (Sigma Aldrich) supplemented with 10% FBS and 1% penicillin streptomycin.

## **2.24 Statistical Analyses**

T-test and ANOVA were performed using Statistical Software Prism 7.0 (Graph Pad). No normalisation test was performed due to the limited number of samples in each experiment. Unpaired t-test was performed to compare the means of two unmatched groups. One-way ANOVA was performed to determine statistically significant differences between means of more than two groups affected by one factor. Data are represented as the mean +/- standard deviation (SD). p Value <0.05 was considered statistically significant, the following classifications were used to represent significance: \* = p <0.05; \*\* = p<0.01; \*\*\* = p<0.001.

Z-score, a screening window coefficient was performed to identify hits from the methyltransferase high-throughput siRNA screen (Zhang *et al.*, 1999). Hits from the screens were identified as having a Z-score of above 3 or below -3.

## Chapter 3. SMAD3:SET9 Interaction in the TGF $\beta$ -1 Signalling Pathway

### 3.1 Introduction and Objectives

SET9 belongs to the evolutionarily conserved suppressor of variegation (Su(var)), enhancer of zeste (E(z)) and Trithorax (Trz); SET-domain family of lysine methyltransferases that are known to be involved in transcriptional regulation. SET9 is known to monomethylate lysine 4 of histone 3 (H3K4) to activate gene transcription (Wang *et al.*, 2001).

SET9 has also been shown to methylate several transcription factors including p53, estrogen receptor (ER), androgen receptor (AR) and Transcription initiation factor TFIID subunit 10 (TAF10) (Kouskouti *et al.*, 2004; Subramanian *et al.*, 2008; Gaughan *et al.*, 2011; Lehnertz *et al.*, 2011) as well as non-transcriptional proteins, such as p300/CBP-associated factor (PCAF) (Oudhoff *et al.*, 2016), (Masatsugu and Yamamoto, 2009) which demonstrates alternative, non-transcriptional roles for SET9.

With reference to fibrosis, it has been demonstrated that histone H3 monomethylation on lysine 9 is involved in the regulation of ECM gene expression and that silencing SET9 attenuates TGF  $\beta$ -1 mediated ECM gene expression (Sun *et al.*, 2010). Furthermore, RNAi-mediated SET9 knockdown significantly attenuated renal fibrosis in UUO mice (Sasaki *et al.*, 2016). In pulmonary fibrosis, studies show that SET9 is involved in the regulation of the TGF  $\beta$ -1 signalling pathway and subsequent ECM production through lysine methylation of an inhibitory downstream effector SMAD7. SET9 methylation of SMAD7 targets this inhibitory SMAD for ubiquitin-dependent degradation. Silencing or inhibiting SET9 therefore causes an increase in SMAD7 levels, resulting in reduced TGF  $\beta$ -1-mediated ECM protein expression (Elkouris *et al.*, 2016).

Together, these studies demonstrate an important role of SET9 in ECM production but the potential role of SET9 in key processes leading to myofibroblast differentiation, migration and contractility has yet to be explored. Additionally, the role of SET9 in the regulation of other SMADs has yet to be determined.

SMAD3 activation and translocation into the nucleus is a process that could be manipulated to reduce TGF  $\beta$ -1 signalling and therefore renal fibrosis. Identification of factors involved in SMAD3 nuclear import could be crucial in identifying novel therapeutic targets to down-

regulate TGF  $\beta$ -1 signalling in renal fibrosis and other diseases in which TGF  $\beta$ -1 is implicated.

Interestingly, a lysine-rich KKLKK (K denotes lysine) nuclear import signal between residues 40-44 has been identified in human SMAD3 (Xiao et al., 2000). Mutation of lysine residues 40 and 41 or 43 and 44 eradicates TGF  $\beta$ -1-induced SMAD3 nuclear import. Although, KKLKK motif alone does not function as a classical nuclear localization sequence (NLS) as fusion to a heterologous protein is not sufficient to allow nuclear import (Yao et al., 2008). Interestingly, this suggests that although KKLKK is required for SMAD3 nuclear import, there are additional unidentified factors that interact with this motif to facilitate SMAD3 nuclear import.

Similarity between the KKLKK nuclear import motif of SMAD3 and the lysine-rich sequences targeted by the lysine methyltransferase, SET9 in other SET9 substrates suggests a potential role for SET9 in the regulation of SMAD3 nuclear import via this KKLKK motif. Should this be true, SET9 would be an attractive, novel target in renal fibrosis. Figure 3.1 highlights SET9 methylation targets including possible methylation targets of SMAD3.

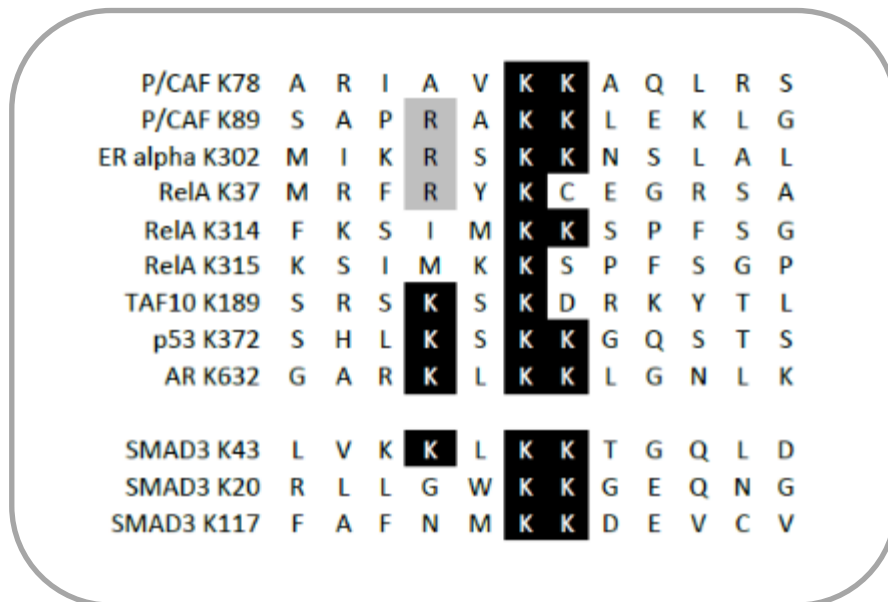


**Figure 3.1. Methylation Targets for SET9.** Sequence alignment of published methylation targets for SET9 and putative SMAD3 methylation sites (below). Conserved basic residues are highlighted including lysine (K) and arginine (R).

Here I present a novel interaction between SET9 and SMAD3, the most important downstream mediator of TGF  $\beta$ -1 signalling. SET9 regulates SMAD3 transcriptional activity and influences the subsequent expression of TGF  $\beta$ -1-regulated fibrotic genes such as  $\alpha$ -SMA, Collagen I and Collagen III in renal cell lines and human PRFs, isolated as part of this project. I go on to suggest that pharmacological inhibition of SET9 would be an attractive therapeutic target in the treatment of renal fibrosis and CKD.

## **3.2 Results**

### ***3.2.1 SMAD3 Interacts with SET9***

SET9 has previously been shown to interact with proteins by recognising 'KKLKK' motifs within partner proteins. Analysis of SMAD3 protein identifies a 'KKLKK' motif at amino acids 41-44, therefore the ability for SET9 to regulate the TGF  $\beta$ -1 signalling pathway through interacting with SMAD3 was examined.

Immunoprecipitation of endogenous SET9 from HK C-8 whole cell lysates resulted in co-immunoprecipitation of SMAD3, whereas immunoprecipitation with control immunoglobulins did not recover SMAD3. Upon treatment with exogenous TGF  $\beta$ -1, an enrichment of the SET9-SMAD3 interaction was observed (Figure 3.2A).

A reciprocal experiment was performed in which immunoprecipitation of endogenous SMAD3 from HK C-8 whole cell lysates resulted in co-immunoprecipitation of SET9 (Figure 3.2A). In order to test the strength of the SMAD3-SET9 interaction, this immunoprecipitation was also performed after adjustment of cell lysates by the addition of sodium chloride. Co-immunoprecipitation of SMAD3-SET9 was still observed in 600mM sodium chloride, demonstrating a strong interaction between SET9 and SMAD3. The inclusion of control immunoglobulins and lack of GAPDH immunoprecipitation demonstrate specificity in the SMAD3-SET9 interaction (Figure 3.2B).

Finally, to exclude antisera cross-reactivity, a third immunoprecipitation was performed. FLAG-tagged SET9 was overexpressed by transient transfection into HK C-8 cells and immunoprecipitated via the FLAG epitope. Co-immunoprecipitation of endogenous SMAD3 was observed, again with enrichment upon TGF  $\beta$ -1 treatment (Figure 3.2C). There was no detectable SMAD3 in immunoprecipitation from control cells transfected with an empty vector. Overall, the data suggested that SET9 interacts with SMAD3 and this interaction is enhanced in response to TGF  $\beta$ -1.

### ***3.2.2 SMAD3 Interacts with SET9 Through its NL Domain***

The SMAD3 protein contains two globular domains; one at either terminus. The SMAD3 C terminus contains the MH2 domain, responsible for protein-protein interactions with co-SMADs such as SMAD2 and SMAD4. The N terminus contains the DNA binding domain (DBD) and the cryptic nuclear localisation signal (NLS) (Xiao *et al.*, 2000). In order to identify the region of SMAD3 that interacts with SET9, vectors encoding GST-tagged SMAD3 residues 1-211 (NL domain) or residues 199-425 (C-terminal domain) were used to generate truncated, recombinant SMAD3 proteins from BL21 *E.coli* bacterial cells (Figure 3.2D). These proteins were purified over GST-sepharose columns, as described in Materials and Methods section 2.8 and individually tested for interaction with commercially sourced recombinant human SET9 protein, by immunoprecipitation. Following immunoprecipitation with SET9 antibody, Western blotting demonstrated that only the SMAD3 NL fragment protein was co-immunoprecipitated with SET9. The IgG control immunoglobulins showed only minor recovery of the SMAD3 NL protein, most likely due to low level, non-specific binding but not sufficient to account for the levels of SMAD3 NL co-immunoprecipitated by SET9 antibody (Figure 3.2E). These data suggest that SET9 interacts with N-terminus of SMAD3, but not the C-terminus of SMAD3.

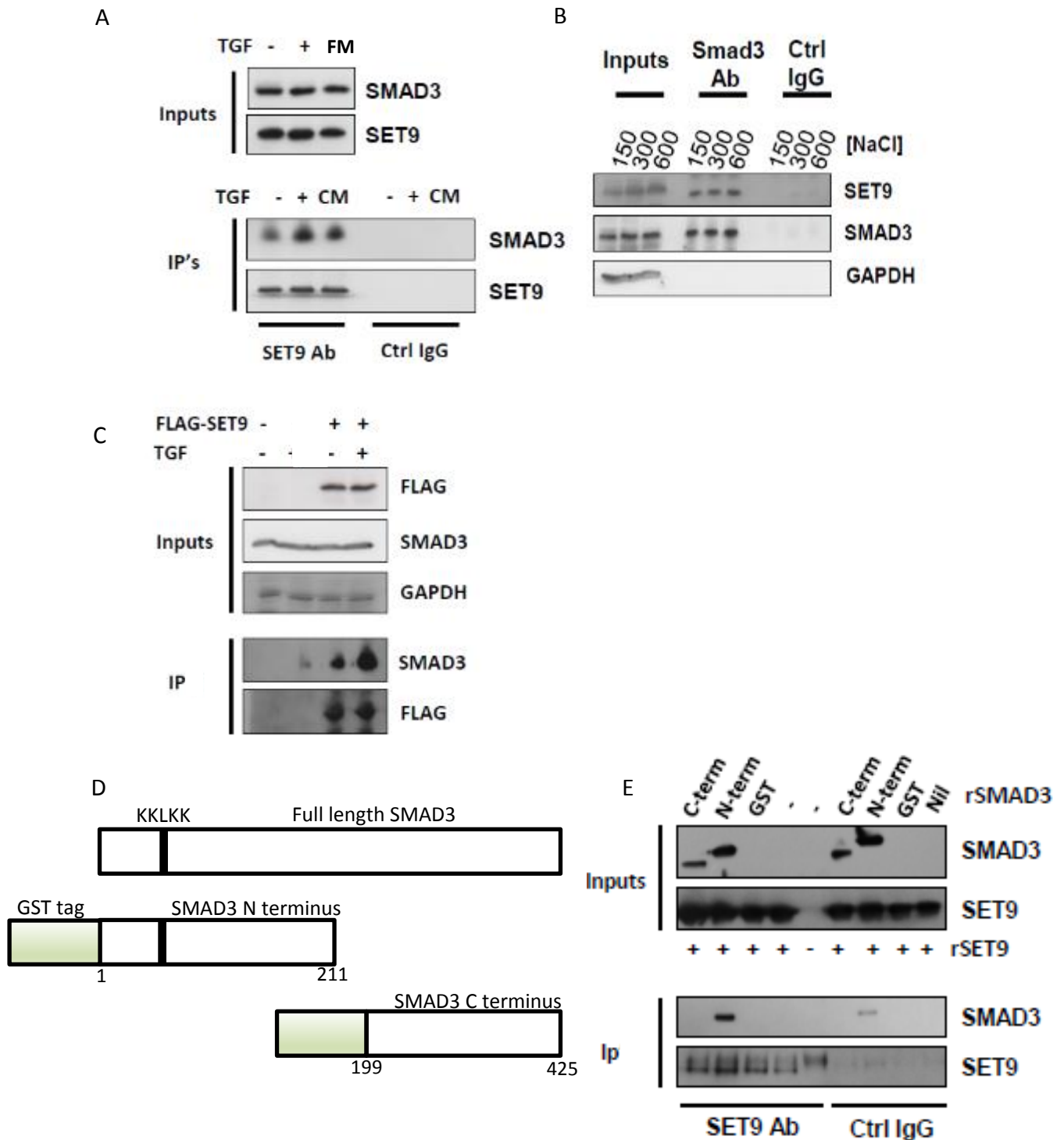


**Figure 3.2. SET9 Interacts with SMAD3.** (A) HK C-8 cells were cultured for 24 hours in basal medium (BM) or full medium (FM) then treated with DMSO vehicle (-) or 5ng/ml TGF  $\beta$ -1 (+) overnight. Immunoprecipitations (IPs) with either SET9 or control antibody (Ctrl IgG) were followed by immunoblotting as indicated. Representative experiments of 3 are shown. (B) HK C-8 cells treated as in (A) were used for immunoprecipitation with either SMAD3 or isotype control antisera (Ctrl IgG) as indicated. Cell lysates were adjusted by addition of sodium chloride (NaCl) in the case of 300mM and 600mM NaCl, prior to immunoprecipitation and immunoblotting as shown. IP washes contained the same NaCl concentration as that of the adjusted lysates. Representative experiment of 3 is shown. (C) HK C-8 cells were transfected with FLAG-SET9 or empty control vector overnight, starved for 24 hours in BM prior to treatment with DMSO vehicle or 5ng/ml TGF  $\beta$ -1 overnight. Immunoprecipitation was then performed using FLAG antibody prior to immunoblotting as indicated. (D) Vector maps of GST tagged SMAD3 residues used to generate SMAD3

recombinant proteins. (E) Purified recombinant full-length SET9 and SMAD3 C terminus or NL terminus proteins were mixed in PBS prior to immunoprecipitation with a SMAD3 antibody, then immunoblotting as shown.

### ***3.2.3 SET9 Regulates SMAD3 Nuclear Import and Protein Turnover***

To further delineate the role of SET9 in the TGF  $\beta$ -1/SMAD3 signalling pathway, the effect of SET9 on known key regulatory steps in the pathway was examined, including SMAD3 nuclear import and proteasomal turnover.

Firstly, to examine SMAD3 nuclear translocation, immunofluorescence was performed in HK C-8 cells transfected with SET9 siRNA or a control SCR siRNA. Upon SET9 knockdown, a marked redistribution of SMAD3 to the cytoplasm was observed, compared to cells transfected with control SCR siRNA that exhibited primarily nuclear staining (Figure 3.3A).

To support the immunofluorescence data, subcellular fractionation was performed in the presence of SET9 siRNA or a control SCR siRNA in HK C-8 cells. Upon transfection of the control SCR siRNA, SMAD3 was progressively translocated from the cytoplasm to the nucleus with increasing concentrations of exogenous TGF  $\beta$ -1. At 5ng/ml TGF  $\beta$ -1 SMAD3 was almost undetectable in the cytoplasmic fraction. However, transfection of SET9 siRNA resulted in two effects; firstly, the overall levels of SMAD3 protein were reduced compared to control transfectants. Secondly, SET9 knockdown resulted in a redistribution of SMAD3 between the nuclear and cytoplasmic compartments; SMAD3 exhibited persistent cytoplasmic presence despite the treatment of exogenous TGF  $\beta$ -1. Overall, the data suggest that SET9 is required for TGF  $\beta$ -1-driven SMAD3 nuclear translocation in addition to the ability for SET9 to modulate SMAD3 protein levels (Figure 3.3B).

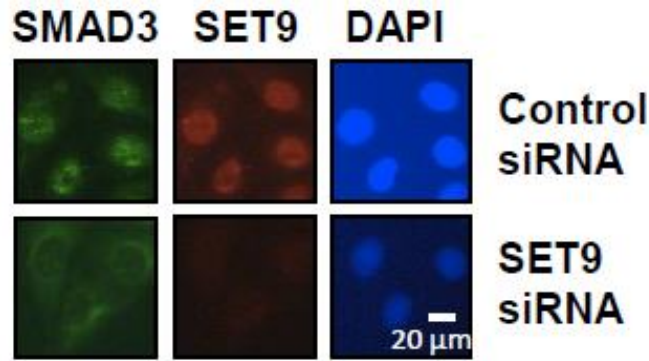
Given that SET9 silencing resulted in a reduction in SMAD3 levels, this was examined further by studying the half-life of SMAD3. Cycloheximide (CXH) was applied to HK C-8 cells to block *de novo* protein synthesis, then SMAD3 levels were examined by Western blotting, in the presence of exogenous TGF  $\beta$ -1 (Figure 3.3C). Densitometric analysis (not shown) demonstrated that the half-life of SMAD3 was approximately 118 minutes in cells transfected with a control siRNA (Figure 3.3). However, transfection of SET9 siRNA produced not only a lower steady-state level of SMAD3 but also an increase in SMAD3 turnover, reducing SMAD3 half-life to approximately 48 minutes (Figure 3.3D).

The half-life of SMAD3 was also examined in SET9  $+/+$  and SET9  $-/-$  MEF cells to exclude any confounding effects of siRNA transfection. Western blotting showed similar steady state

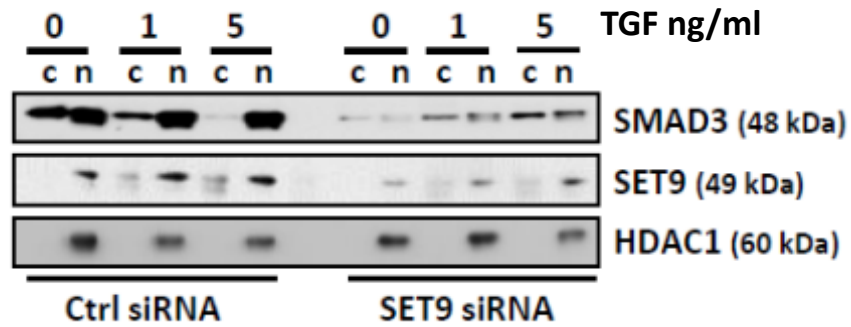
levels of SMAD3 in both cell types, but SMAD3 exhibited a shorter half-life in the SET9 <sup>-/-</sup> MEF cells compared to the wild type SET9 <sup>+/+</sup> MEF cells upon CXH treatment (Figure 3.3), suggesting that SMAD3 is destabilised upon loss of SET9.

Finally, to determine whether the methyltransferase activity of SET9 is involved in the regulation of SMAD3 protein turnover, the half-life of SMAD3 was examined in stably transfected cells expressing either wild type FLAG-SET9<sup>WT</sup> or the methyltransferase-deficient mutant SET9, FLAG-SET9<sup>H297A</sup> (Figure 3.3E). SMAD3 levels exhibited increased stability in the FLAG-SET9<sup>WT</sup> overexpressing cells compared to those cells expressing FLAG-SET9<sup>H297A</sup>, upon CXH treatment. This demonstrated that SET9 stabilises SMAD3 in a methyltransferase-dependent manner.

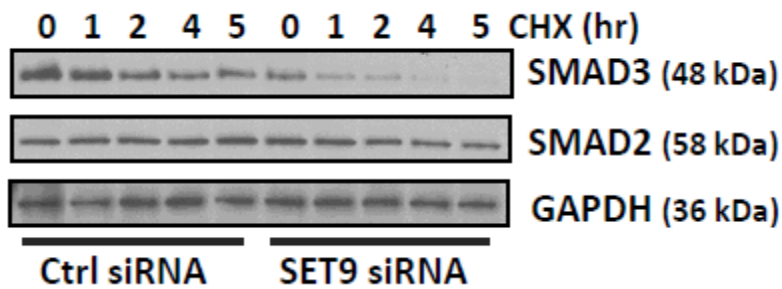
A



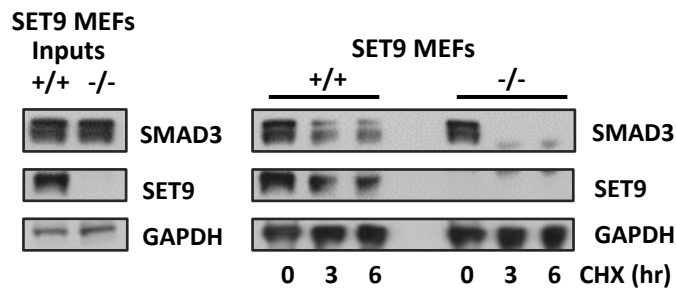
B



C



D



E



**Figure 3.3. SET9 Regulates SMAD3 Nuclear Import and Protein Turnover.** (A) HK C-8 cells were transfected with either control siRNA or SET9 siRNA for 12 hours, starved in BM for 24 hours prior to overnight treatment with 5ng/ml TGF  $\beta$ -1. Fixed cells were stained with the indicated antibodies and appropriate Alexa Fluor-labelled secondary antibodies. Control slides with secondary antibodies only did not exhibit fluorescence (Appendix). (B) HK C-8 cells were transfected and starved as in (A) then treated with vehicle (0) or TGF  $\beta$ -1 (1–5ng/ml) overnight. Nuclear (n) and cytoplasmic (c) fractions were subject to immunoblotting as indicated, using HDAC1 as a nuclear marker. (C) HK C-8 cells were transfected and starved as in (A) then treated with TGF  $\beta$ -1 (5ng/ml) overnight. 50 $\mu$ g/ml cycloheximide (CHX) was then applied for the indicated times prior to Western blotting as indicated. (D) SET9  $+/+$  and  $-/-$  MEFs were treated as in (C) and subject to Western Blotting. (E) HK C-8 cells stably expressing FLAG-SET9<sub>WT</sub> or methyltransferase-deficient FLAG-SET9<sub>H297A</sub> were treated and a half-life assay performed as in (C).

Ubiquitylation is known to target SMAD3 for proteasomal destruction, as a means of downregulating TGF  $\beta$ -1 signalling (Fukuchi *et al.*, 2001). Given the effects of SET9 methyltransferase activity upon SMAD3 protein turnover, SMAD3 ubiquitylation was examined in the presence of a selective SET9 inhibitor, R-PFI-2 (Figure 3.4), or upon overexpression of the FLAG-SET9<sub>H297A</sub> mutant (Figure 3.4). The proteasomal inhibitor MG-132 was also used to enrich for the presence of ubiquitylated SMAD3, which would otherwise be destroyed by the proteasome.

His-tagged ubiquitin was transfected into HK C-8 cells prior to nickel agarose (Ni-NTA) pull down to retrieve ubiquitylated SMAD3 species. Treatment with MG-132, produced an abundance of ubiquitylated SMAD3 (high molecular weight SMAD3). Addition of the SET9 inhibitor R-PFI-2 resulted in an increase in the levels of ubiquitylated SMAD3 compared to control cells treated with MG-132 only (Figure 3.4A). Finally, the ubiquitylation of SMAD3 was examined in the HK C-8 cells stably expressing FLAG-SET9<sub>WT</sub> or methyltransferase-deficient FLAG-SET9<sub>H297A</sub> mutant. Enrichment of ubiquitylated SMAD3 was observed in the cells expressing the FLAG-SET9<sub>H297A</sub> mutant compared to the cells expressing FLAG-SET9<sub>WT</sub> (Figure 3.4B). In conclusion, these data suggest that SET9 methyltransferase activity plays a role in the stabilising SMAD3 protein levels, through influencing SMAD3 ubiquitylation and subsequent proteasomal destruction.

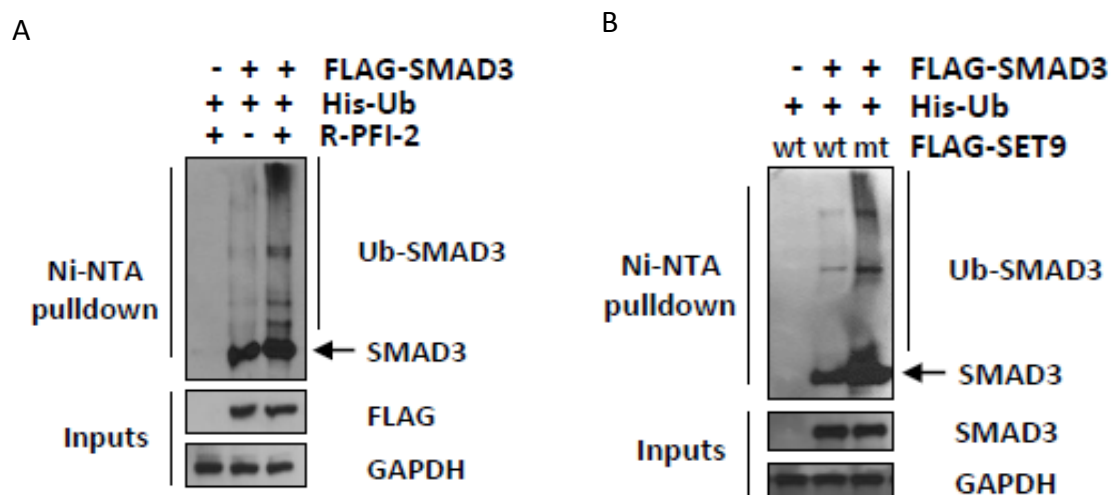


**Figure 3.4. SET9 Regulates SMAD3 Ubiquitylation.** (A) HK C-8 cells were transfected with His-tagged ubiquitin (His-Ub) and either empty vector or FLAG-SMAD3 prior to treatment with 5ng/ml TGF  $\beta$ -1 for 24 hours. Either DMSO vehicle or 30uM R-PFI-2 was then applied overnight along with 1 $\mu$ M MG-132 prior to Ni-NTA pulldowns followed by immunoblotting. All cells received MG-132 and TGF  $\beta$ -1. Ubiquitylated SMAD3 species are indicated (Ub-SMAD3). (B) HK C-8 cells stably expressing wild-type FLAG-SET9<sub>WT</sub> (wt) or methyltransferase-deficient FLAG-SET9<sub>H297A</sub> (mt) were transfected and treated with TGF  $\beta$ -1 and MG-132 as in (A), then subjected to Ni-NTA pulldowns and immunoblotting as indicated. Ubiquitylated SMAD3 species detected with SMAD3 antibody are indicated (Ub-SMAD3). All results are representative of  $n=3$  experiments.

### 3.2.4 Characterisation of Mouse Embryonic Cell Lines (MEFs)

Given the observed effects of SET9 on TGF  $\beta$ -1 signalling, cells from the SET9 knockout mouse were obtained for further characterisation. SET9 knockout MEFs are a useful model because fibroblastic cells respond to TGF  $\beta$ -1 and the permanent absence of SET9 expression provides a system which does not rely upon transient overexpression of SET9 or transient siRNA knockdown of SET9. To determine whether loss of SET9 might phenotypically mimic loss of SMAD3, cells from the SMAD3 knockout mouse were also studied. Wild-type (+/+) and matched knockout (-/-) SMAD3 mouse embryonic fibroblasts (MEFs) were obtained from Erwin Bottinger, Mount Sinai Hospital, New York and wild-type (+/+) and matched knock-out (-/-) SET9 MEFs from Giuseppe Testa, European Institute of Oncology, Milan.

Initially, the MEFs of different genotypes were treated with TGF  $\beta$ -1 for 24-72h and then imaged to examine cell phenotype (Figure 3.5). SMAD3 +/+ and -/- cells maintained in FM have a similar phenotype of an ordered monolayer of largely rounded cells. When treated with TGF  $\beta$ -1 the differences between +/+ and -/- emerge. Upon treatment with TGF  $\beta$ -1, the SMAD3 +/+ cells exhibit a spindle shaped morphology, typical of activated myofibroblasts, whereas SMAD3 -/- cells show a more unstructured morphology with gaps between cells. The

SET9  $+/+$  and  $-/-$  MEF cells treated in parallel showed the same phenotypic changes in response to TGF  $\beta$ -1 as the SMAD3 MEFs, respectively (Figure 3.5). This demonstrates that loss of SET9 results in the same phenotype as loss of SMAD3, evident upon treatment with exogenous TGF  $\beta$ -1 and might suggest that SET9 is required for the activation of fibroblasts to the myofibroblast phenotype.

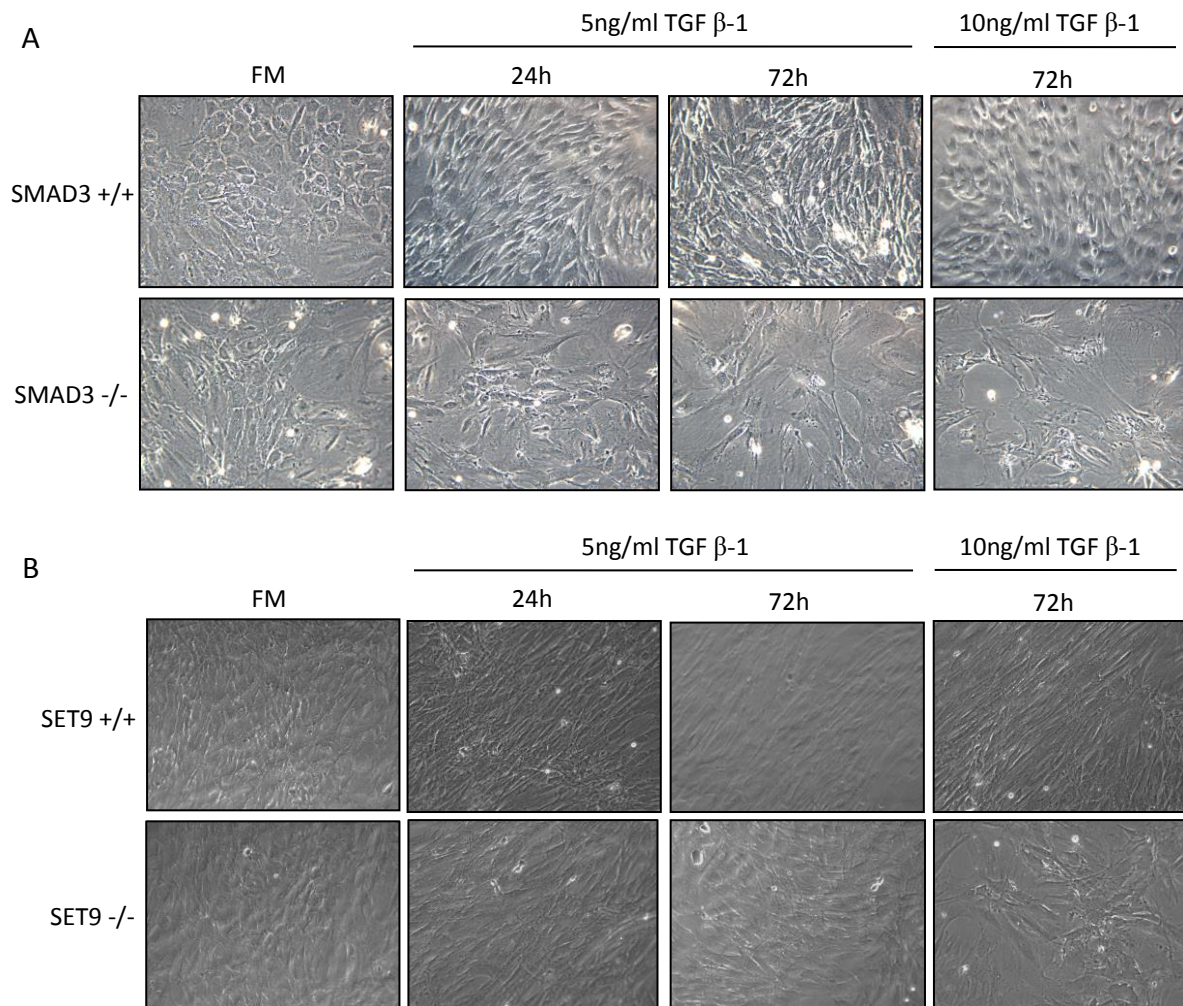


**Figure 3.5. Phenotypes of SMAD3 and SET9  $+/+$  and  $-/-$  MEF cells.** (A) SMAD3  $+/+$  and  $-/-$  MEFs and (B) SET9  $+/+$  and  $-/-$  MEFs were seeded into 24-well plates in FM and treated with or without 10ng/ml TGF  $\beta$ -1 for 24-72 hours then imaged in brightfield to observe differences in phenotypes between the cell lines.

To further characterise the transition to myofibroblasts, SET9 $-/-$  MEFs were subject to immunofluorescence for accepted pro-fibrotic markers Collagen I (COLI), Collagen III (COLIII), Fibronectin (FN1), Plasminogen Activator Inhibitor-1 (PAI-1) and Alpha-Smooth Muscle Actin ( $\alpha$ -SMA). Cells seeded in 6 well plates on glass coverslips were treated with or without 10ng/ml TGF  $\beta$ -1 for 120h before immunofluorescence staining as described in Materials and Methods section 2.14. The pro-fibrotic markers showed a reduction in

expression in the SET9  $-/-$  cells compared to SET9  $+/+$  cells, with both cell types showing a slight of induction of expression when treated with TGF  $\beta$ -1 (Figure 3.6).

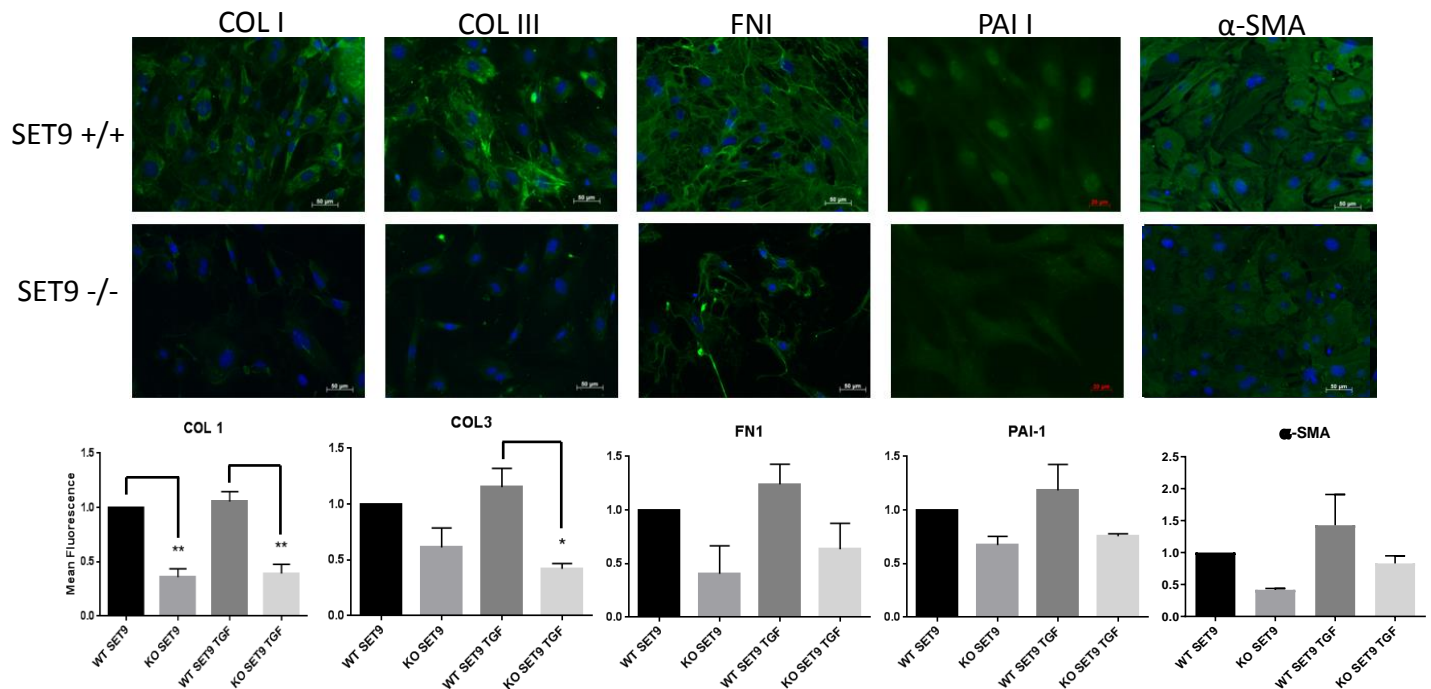


**Figure 3.6. Expression of Pro-Fibrotic Markers in SET9  $+/+$  and  $-/-$  MEF Cells.** SET9  $+/+$  and  $-/-$  MEFs were treated with or without TGF  $\beta$ -1 and subjected to immunofluorescence for expression of the pro-fibrotic markers COL1, COL3, FN1, PAI-1 and  $\alpha$ -SMA. Images of cells treated with 10ng/ml TGF  $\beta$ -1 shown. Top row images display the expression of the pro-fibrotic markers in SET9  $+/+$  cells with TGF  $\beta$ -1 treatment, bottom row of images shows expression of pro-fibrotic markers in SET9  $-/-$  cells with TGF  $\beta$ -1 treatment (untreated images not shown). Control slides with secondary antibodies only did not exhibit fluorescence (Appendix). The images were quantitatively analysed using Image J and are represented as bar graphs of fold change in mean fluorescence per cell. All results are representative of  $n=3$  experiments; values are mean $\pm$ s.d. P values: \*\* denotes  $P<0.01$  (t-test).

### 3.2.5 SET9 is Required for Fibroblast Migration in Wound Healing Assays

Fibrosis has been described as an aberrant wound healing response (Wynn, 2007), involving migration of activated myofibroblasts to the site of tissue injury, fibroblast migration was therefore studied, by performing wound healing assays on the SMAD3 and SET9 MEF cells. SMAD3 and SET9  $+/+$  and  $-/-$  MEFs were seeded into wound forming chambers as described in Materials and Methods section 2.16, treated with or without TGF  $\beta$ -1 and imaged at 4 hour intervals until the wound was completely closed (Figure 3.7A). Both SMAD3 and SET9  $+/+$  MEFs in FM closed the wound in less than 20 hours whereas both SMAD3 and SET9  $-/-$  MEFs only achieved 80% closure of the wound, even after 24 hours. This effect was further enhanced with the treatment of TGF  $\beta$ -1 (Figure 3.7B). The results from these assays demonstrate that the SET9 and SMAD3  $-/-$  MEF cell lines have reduced capacity to migrate to

close the wound compared to their respective WT. The finding that SET9  $-/-$  MEFs and SMAD3  $-/-$

MEFs have similar phenotypes implies that SET9 could have an important role in the wound healing response to tissue injury and might therefore be involved in fibrosis.

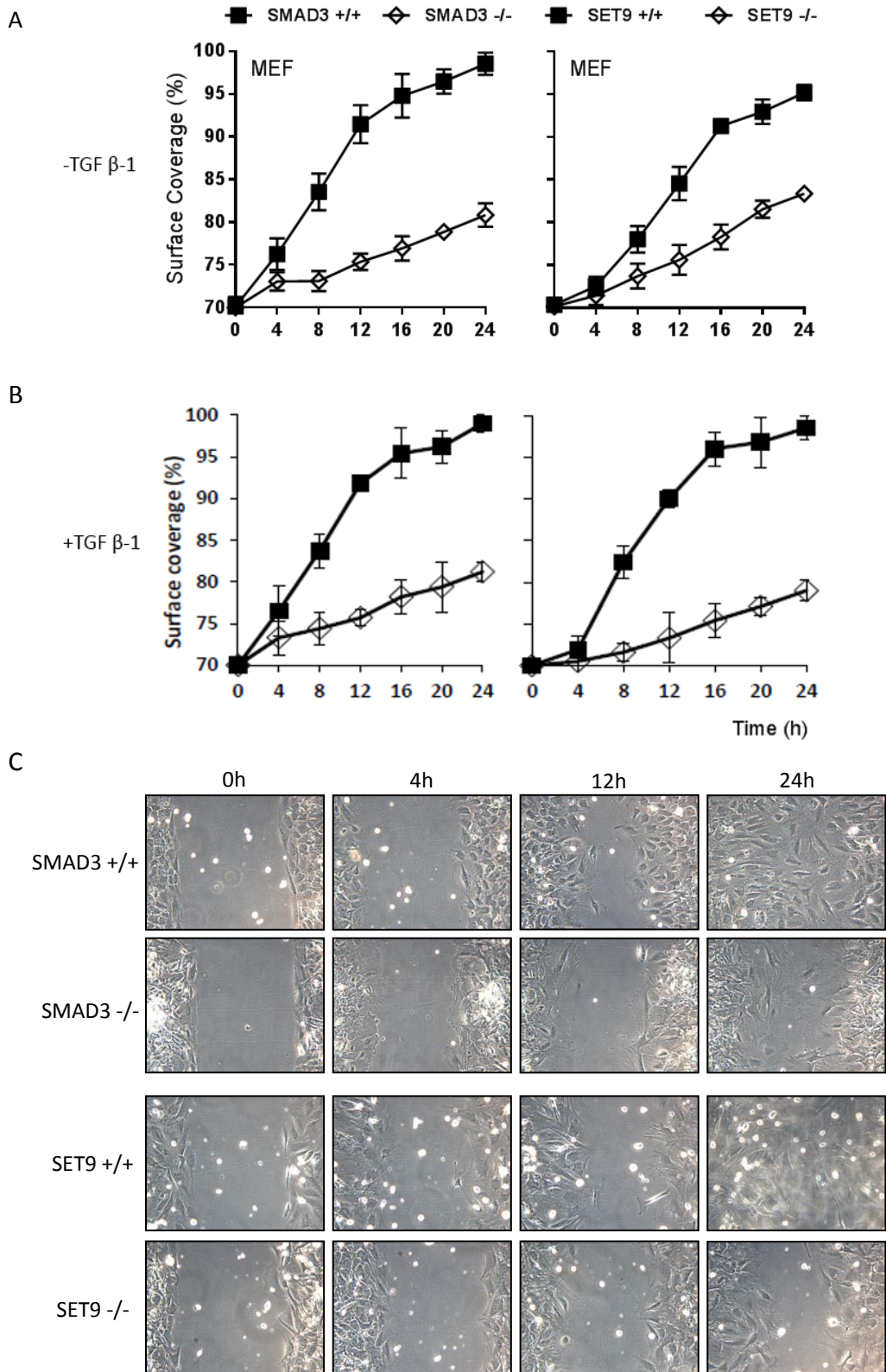


**Figure 3.7. SET9 Regulates TGF  $\beta$ -1-driven Transformation and Wound Healing.** (A) MEFs with the indicated genotypes were grown in cell culture inserts, in triplicate, overnight prior to wound formation by chamber removal. Wounds were photographed every 4 hours, then surface coverage was calculated. (B) Performed as in (A) with the addition of 5ng/ml TGF  $\beta$ -1 overnight. Representative data from one patient of three are shown. Values are mean $\pm$ s.d. (C) Representative images of the indicated genotypes at 0, 4, 12 and 24 hours during wound healing assay (A).

Further wound healing assays were performed with SET9  $+/+$  MEFs treated with a commercially available specific SET9 inhibitor, R-PFI-2. Initially, SET9  $+/+$  MEFs were seeded into chamber inserts and treated with a range of R-PFI-2 concentrations of 10-30 $\mu$ M or a DMSO vehicle control. Whilst DMSO had no effect on wound closure compared to no treatment control, a reduction in wound healing in response to R-PFI-2 treatment was observed (Figure 3.8A). To exclude off-target effects of the inhibitor, the effect of R-PFI-2 on both SET9  $+/+$  and  $-/-$  MEFs was examined (Figure 3.8B). The inhibitor had minimal effect on wound healing in the SET9  $-/-$  cells, suggesting that the inhibition in wound closure seen in the SET9  $+/+$  cells in response to R-PFI-2 is indeed mediated through SET9. Taken together, the data demonstrate that SET9 is involved in fibroblast migration into the site of the wound.

A cell line derived from human renal mesangial cells isolated from the glomerulus of normal kidneys (THMC) acts as an additional model of fibrosis as mesangial cell proliferation and matrix overproduction are predominant pathological features of glomerular sclerosis, for example in diabetic nephropathy (Sraer *et al.*, 1996). Therefore, wound healing assays were performed in THMC cells and demonstrated comparable results with the R-PFI-2 SET9 inhibitor reducing the cells capability to migrate (Figure 3.8).

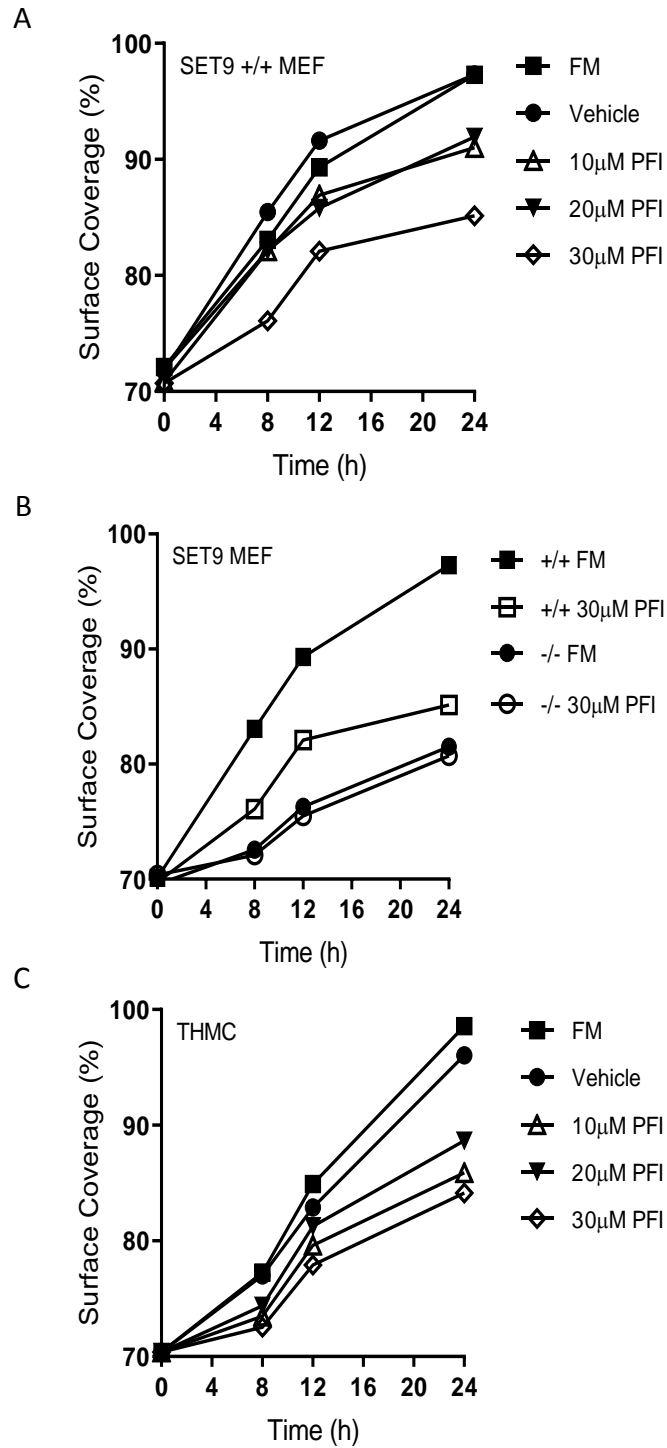


**Figure 3.8. The Effect of SMAD3 and SET9 on Wound Healing in MEFs and THMCs.** (A) SET9 +/+ MEF cells were seeded into chamber inserts and treated with a range of concentrations of R-PFI-2 as indicated, a DMSO vehicle control and untreated cells as a further control prior to wound healing assays. (B) SET9 +/+ and -/- MEF cells set up as in (A) with or without 30µM R-PFI-2 treatment. (C) THMCs set up as in (B). All graphs representative of n=3 experiments.

### ***3.2.6 SET9 is Required for Collagen Contractility Mediated by Fibroblasts***

A hallmark of renal fibrosis is the ability of activated fibroblasts to increase tissue contractility, which involves increased expression of intracellular  $\alpha$ -SMA and subsequent extracellular Collagen contraction. Fibroblasts migrate to the site of injury and attach to Collagen fibrils where they exert mechanical tension to cause contraction of the Collagen lattice. In the presence of TGF  $\beta$ -1, fibroblasts differentiate into myofibroblasts and exert greater contractile forces on the ECM, resulting in reorganisation of the actin cytoskeleton and wound contraction (Li and Wang, 2011). A Collagen gel contractility assay can assess wound contraction by cells. A polymerized Collagen matrix containing fibroblasts remains attached to the culture dish during contraction. Mechanical tension develops during contraction, and cellular stress fibers assemble. This leads to mechanical loading, followed by release of the matrices, resulting in mechanical unloading and further contraction as mechanical stress dissipates.

To analyse the effect of SET9 on the MEF cells' ability to contract Collagen gels were prepared in 24-well plates containing purified rat tail Collagen I into which SMAD3 or SET9 MEF cells were added. The Collagen matrices were treated with or without 5ng/ml TGF  $\beta$ -1 in FM for 24 hours, then released from the bottom and the edges of the wells with a needle and allowed to contract over 24 hours. The Collagen disc diameter was measured at 0, 6, 12 and 24 hour time-points after being released from the wells to give a measure of contraction of the gels. . Figure 3.9A represents the amount of contraction (mm) of the Collagen discs over a 24 hour period after being released. The graphs demonstrate that the Collagen discs embedded with SMAD3 and SET9 +/+ cells contracted up to 10mm in diameter over 24 hours compared to the discs embedded with SMAD3 and SET9 -/- cells which only showed contraction of 4mm and 3mm, respectively. SMAD3 and SET9 -/- cells have significantly reduced ability to contract the Collagen gels compared to the SMAD3 and SET9 +/+ cells in the presence of TGF  $\beta$ -1.

THMC mesangial cells were also examined using Collagen contractility assays to determine the effect of R-PFI-2 on contractility. The THMCs were treated with and without R-PFI-2 and with and without 5ng/ml TGF  $\beta$ -1. R-PFI-2 significantly reduced the ability of the THMC cells to contract Collagen gels compared to DMSO treated cells. TGF  $\beta$ -1 treatment enhanced contractility of the THMCs Collagen gels but R-PFI-2 maintained its suppressive effect on the contractility (Figure 3.9B).

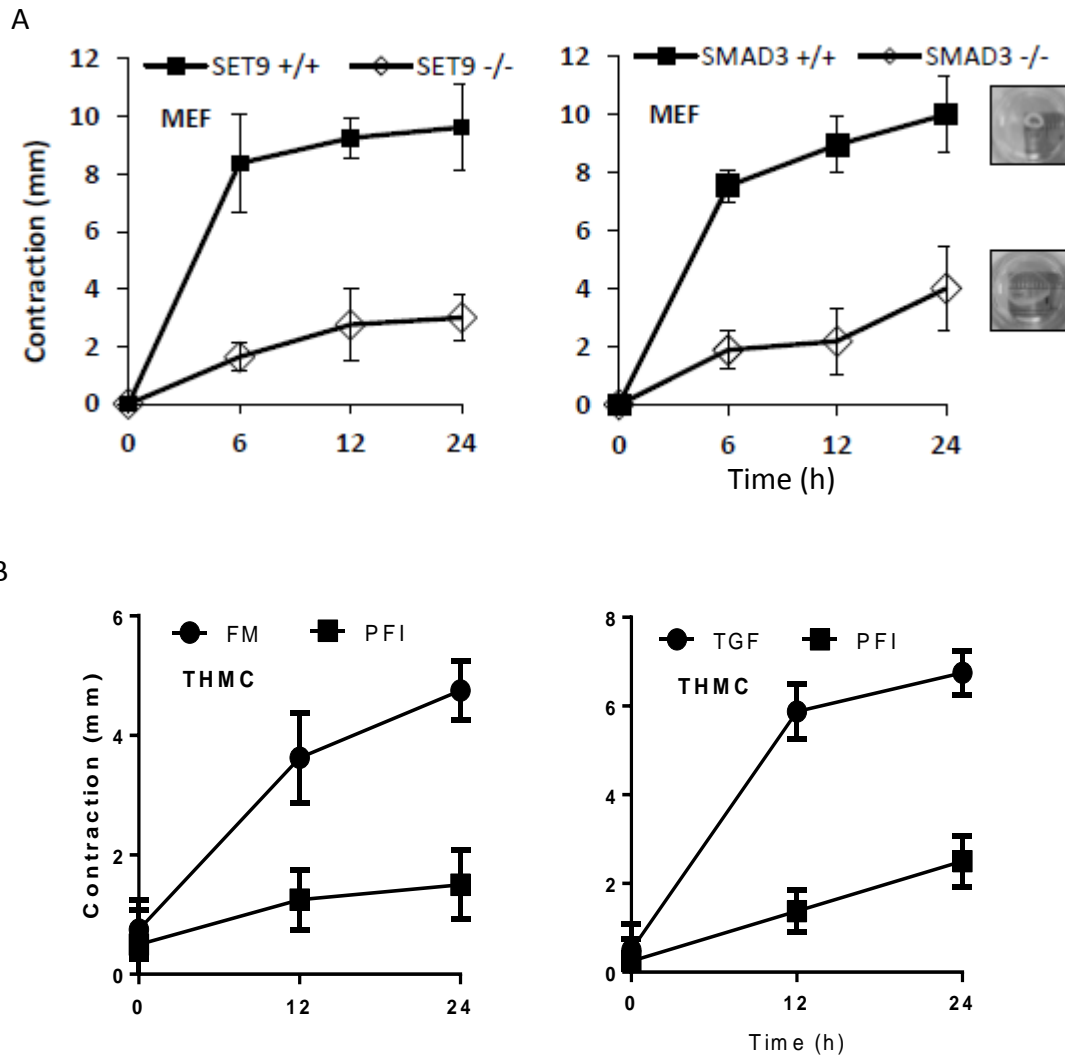


**Figure 3.9. SET9 Regulates TGF  $\beta$ -1-driven Collagen Contractility.** (A) MEFs with the indicated genotypes were used in Collagen contractility assays in triplicate, after treatment with 5ng/ml TGF  $\beta$ -1. The Collagen disc diameters were measured over the indicated time-points, representing the amount of contraction of the Collagen discs. Images show single representative Collagen discs overlying ruler measure. (B) THMCs were treated with either DMSO vehicle or 5 $\mu$ M R-PFI-2, with and without 5ng/ml TGF  $\beta$ -1 and examined in Collagen contractility assays, in triplicate. All graphs representative of n=3 experiments.

### 3.2.7 Isolation and Characterisation of Primary Human Renal Fibroblasts (PRFs)

As renal fibroblasts are responsible for ECM deposition in CKD, isolation of primary human renal fibroblasts was undertaken. These cells should mimic the behaviour of activated myofibroblasts upon exposure to TGF  $\beta$ -1 and serve as a more representative model of CKD than other cell types, such as immortalised cell lines. An outgrowth method was established, to isolate primary renal fibroblasts from human nephrectomised kidney segments or kidney sections from organs deemed unsuitable for transplantation (rejected due to donor reasons). This method involved finely dissecting renal cortical tissue then attaching this onto a pre-

scratched cell culture petri dish. The tissue was then maintained in high glucose enriched medium, for 14 days, during which time cells began to outgrow from the tissue (Figure 3.10A,B). The cells were trypsinised once they reached a monolayer of 75% confluency and sub-cultured in cell culture flasks until confluent. The resultant populations of cells were characterised to ensure fibroblasts had been isolated, as described in more detail below.

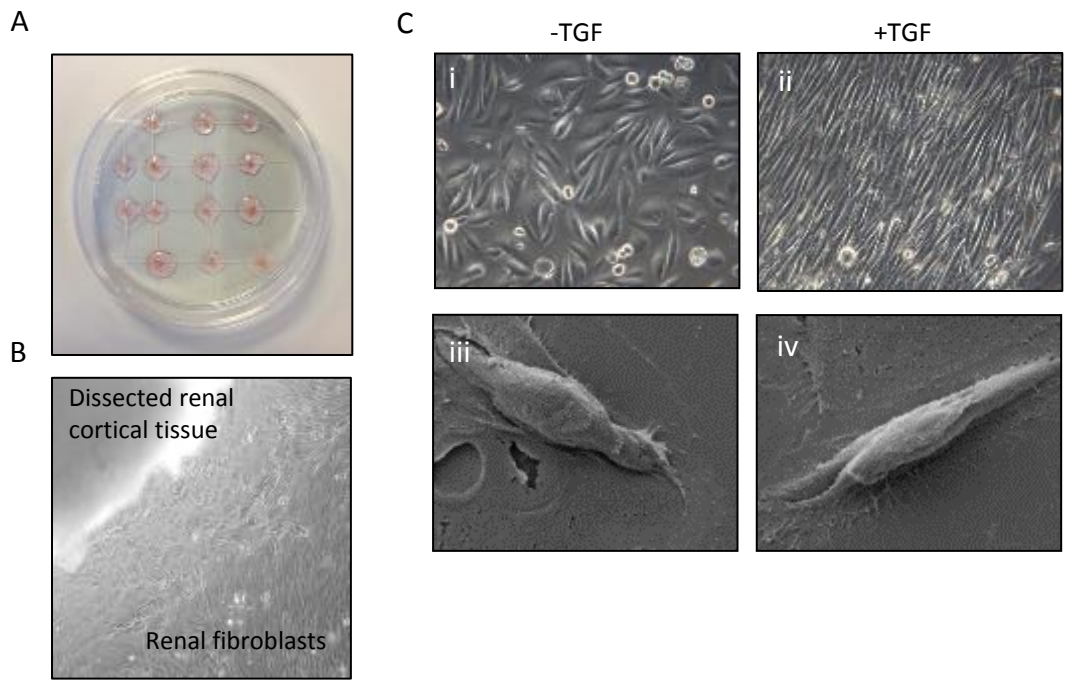
The primary cells were treated with or without 5ng/ml TGF  $\beta$ -1, then brightfield microscopy images obtained to examine their morphology. The primary cells took on an elongated, spindle morphology, typical of the appearance of fibroblasts when treated with TGF  $\beta$ -1 (Figure 3.10C). Electron microscopy images were also taken of the cells treated with TGF  $\beta$ -1. Elongated, spindle-shaped cells with rough membranes were observed, in keeping with fibroblastic appearance (Figure 3.10C).

The isolated cells were next characterised by immunofluorescence to examine the expression of characteristic fibroblast markers. Cells stained positively for the fibroblast markers  $\alpha$ -SMA, Collagen I, and Collagen III, all of which were more highly expressed upon TGF  $\beta$ -1 treatment. The mesenchymal marker Vimentin, and Zonula occludens-1 (ZO-1) were also expressed in the isolated cells. Importantly, the expression of E-cadherin and K-cadherin, known epithelial cell markers were completely absent in the cells (Figure 3.10D). This pattern of expression suggests that the isolated cells were fibroblasts.

Next, proliferation assays were performed to determine whether the cells would respond to growth factors that are known to stimulate fibroblast growth. Stimulation of the cells with TGF  $\beta$ -1 produced a significant increase in the proliferation of the isolated cells. Additionally, the cells showed significantly increased proliferation in response to PDGF, a known mitogen for fibroblasts (Figure 3.10F).

Finally, the cells were transiently transfected with siRNAs targeting either SMAD3 or SET9. Western blotting demonstrated effective knockdown of the respective targets, thereby allowing analysis of cells depleted of our proteins of interest, SMAD3 and SET9 (Figure 3.10G).

Altogether, the data suggest that the outgrowth method described can be used to isolate rather pure populations of primary renal fibroblasts. These cells were subsequently used to study profibrotic markers, wound healing and Collagen contractility assays upon treatment with the SET9 inhibitor.



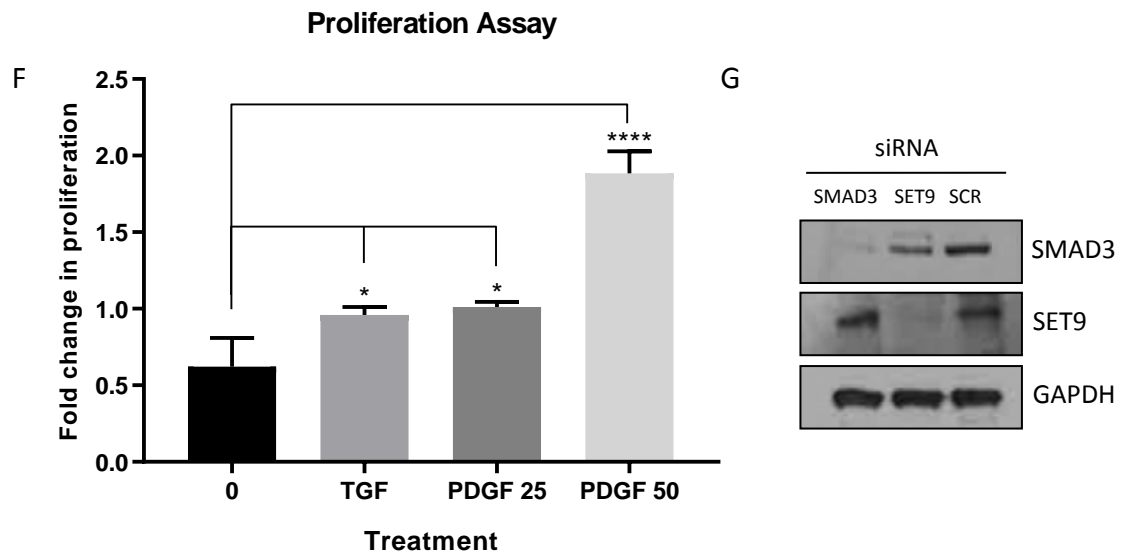


**Figure 3.10. Isolation and Characterisation Primary Renal Fibroblasts.** (A) Cortical kidney sections were dissected and inserted onto 90mm tissue culture dishes for the outgrowth method of renal fibroblasts. (B) Brightfield image of fibroblast cells outgrowing from cortical kidney section. (C) Brightfield images of isolated PRF cells in the absence (i) or presence (ii) of 10ng/ml TGF  $\beta$ -1 treatment. Scanning electron microscope images of isolated PRF cells (iii and iv). (D) Immunofluorescence images showing the expression of fibroblastic markers in PRF cells;  $\alpha$ -SMA, Collagen I, Collagen III treated with or without TGF  $\beta$ -1 as indicated. (E) Vimentin and ZO1 were also present, whereas E-cadherin and K-cadherin, both epithelial cell markers were absent in the PRFs. Control slides with secondary antibodies only did not exhibit fluorescence (Appendix). (F) WST-1 proliferation assay showing fold response to treatment with 10ng/ml TGF  $\beta$ -1 and 25-50ng/ml in 0.5% serum-starved PRF cells. (G) Knock downs in PRF cells using SMAD3 and SET9 specific siRNAs compared to a scrambled (SCR) control siRNA.

### 3.2.8 Treatment of PRFs with SET9 Inhibitor Reduces Expression of Pro-Fibrotic Markers

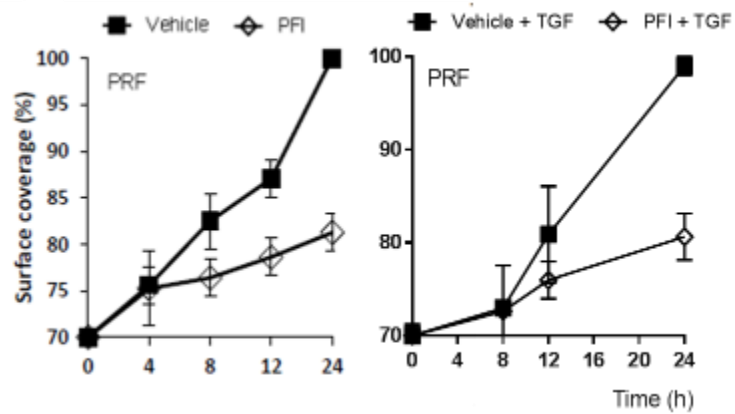
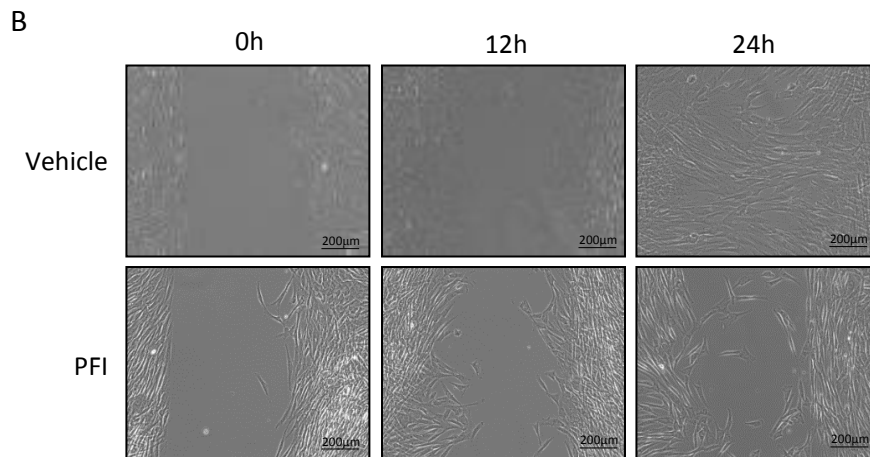
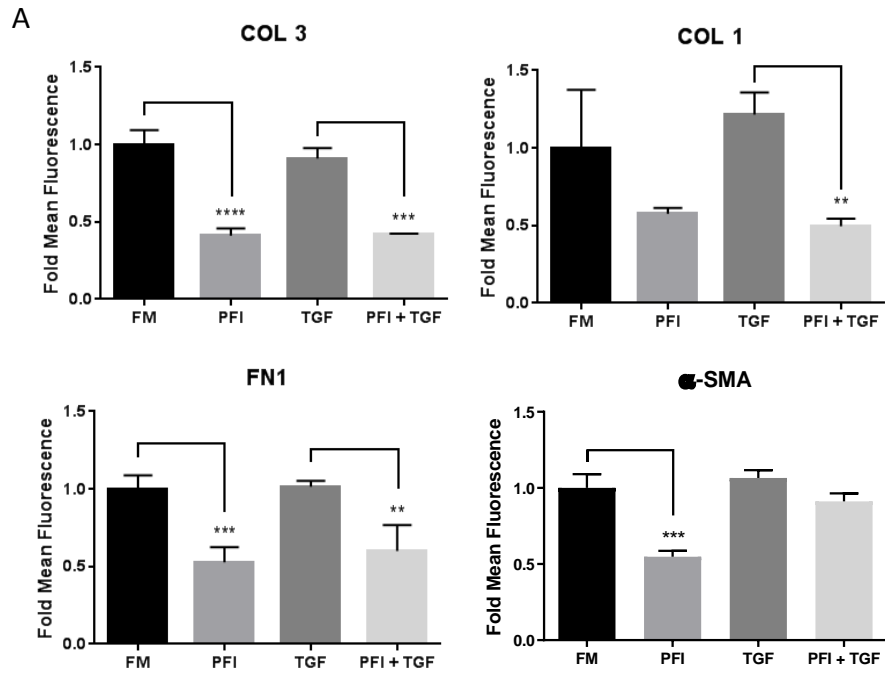
To determine whether PRFs respond in the same manner as the MEFs, PRF cells were subjected to SET9 inhibition with R-PFI-2 hydrochloride at a dose of 30 $\mu$ M. Upon SET9 inhibition, expression of pro-fibrotic markers Collagen I and III, Fibronectin and  $\alpha$ -SMA were all reduced in the absence and in the presence of TGF  $\beta$ -1 (Figure 3.11). This suggests that treatment of TGF  $\beta$ -1-activated fibroblasts with SET9 inhibitor might reduce the deposition of ECM in the context of CKD, if the PRFs treated with TGF  $\beta$ -1 are representative of the diseased state.

### 3.2.9 Treatment with SET9 Inhibitor Reduced Wound Healing and Collagen Contractility of PRFs

It is established that fibroblast migration to the site of tissue injury is critical for tissue contraction and ECM deposition in normal wound healing and fibrosis. In order to examine the role that SET9 might have in these processes, wound healing assays were performed to

examine fibroblast migration in the presence or absence of the SET9 inhibitor R-PFI-2 (Figure 3.11B). In the presence of TGF  $\beta$ -1, PRF cells treated with R-PFI-2 showed reduced wound healing compared with cells maintained in full medium (FM). Figure 3.11B shows brightfield images of PRFs at 0h, 12h and 24h with and without 30 $\mu$ M R-PFI-2 treatment (in the absence of TGF  $\beta$ -1) and quantitative analysis represented by line graphs as % of cell surface coverage (Figure 3.11C).

A key feature of activated fibroblasts (myofibroblasts) is their ability to contract extracellular Collagen. This is achieved through intracellular expression, and incorporation, of  $\alpha$ -SMA into the cell cytoskeleton which can communicate to the extracellular compartment, to facilitate matrix tension and traction against extracellular Collagen. The role of SET9 in Collagen contractility was examined using the contractility assay previously described. Treatment of PRFs with R-PFI-2 significantly reduced the PRF cells ability to contract Collagen discs (Figure 3.11C). Cells treated with 30 $\mu$ M R-PFI-2 and suspended in Collagen gel matrices presented a larger diameter than cells without treatment. The addition of 10ng/ml TGF  $\beta$ -1 resulted in significantly increased contractility of the gel matrices in the presence and absence of the inhibitor. Cells treated with the inhibitor and TGF  $\beta$ -1 still presented with larger diameters than TGF  $\beta$ -1 treatment only (Figure 3.11C).



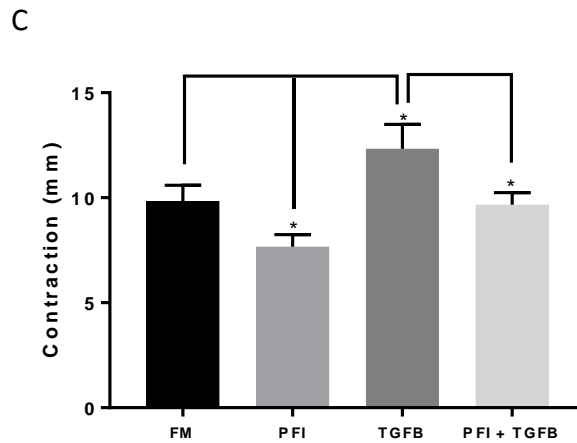


**Figure 3.11. Treatment of PRFs with a SET9 Inhibitor Significantly Reduces Expression of Pro-Fibrotic Markers.** (A) PRFs treated with or without 5ng/ml TGF  $\beta$ -1 and with and without 5 $\mu$ M R-PFI-2 then subjected to immunofluorescence for fibrotic markers Collagen III, Collagen I, Fibronectin and  $\alpha$ -SMA. All results are representative of n=3 experiments; values are mean $\pm$ s.d. \*\* denotes P<0.01 \*\*\* denotes P<0.001 \*\*\*\* denotes P<0.0001 (t-test). The images were analysed using Image J and represented as bar graphs. (B) PRFs treated with or without R-PFI-2 and imaged at 12 hour time-points during wound healing. Graph represents 3 images per time point plotted as a line graph. (C) PRFs were subject to Collagen contractility assays simultaneously treated with either DMSO vehicle or 5 $\mu$ M R-PFI-2, +/- TGF  $\beta$ -1.

### 3.2.10 SET9 Regulates TGF $\beta$ -1-driven $\alpha$ -SMA Expression

The expression of  $\alpha$ -SMA in response to TGF  $\beta$ -1 is considered a hallmark of myofibroblast transdifferentiation to the active, diseased state. Expression of  $\alpha$ -SMA not only marks these cells as active but plays a role in cytoskeletal reorganisation to produce the spindle-shaped morphology that was absent in the SET9  $-/-$  MEFs studied earlier. Additionally,  $\alpha$ -SMA expression facilitates Collagen contractility, critical to tissue retraction that occurs in normal wound healing and fibrosis, and that was shown to be reduced upon SET9 inhibition in the previous section.

Given that SET9 is known to be a transcriptional regulator, and SMAD3 interacts with SET9 in response to TGF  $\beta$ -1, I hypothesised that the mechanism by which SET9 can regulate  $\alpha$ -SMA expression and myofibroblast transdifferentiation is through the modulation of SMAD3 recruitment to *cis*-regulatory regions of the human  $\alpha$ -SMA gene. This was examined using chromatin immunoprecipitation assays.

The putative SMAD3 binding site within the human *ACTA2* gene was identified by sequence homology to the rat  $\alpha$ -SMA gene, which has previously shown to be directly regulated by SMAD3 (Hu *et al.*, 2003). Oligonucleotides were designed to flank this SMAD3 binding site and used in polymerase chain reaction.

Chromatin immunoprecipitation assays using antibodies to either SMAD3 or SET9 were performed to study their recruitment to the aforementioned putative SMAD3 binding site within the *ACTA2* gene in PRF cells. In response to TGF  $\beta$ -1, recruitment of SMAD3 to the  $\alpha$ -*SMA* gene was increased compared to vehicle treated cells indicating that in PRF cells SMAD3 is indeed recruited to the SMAD3 binding site of  $\alpha$ -*SMA*. No SMAD3 binding to the *GAPDH* control gene could be detected, demonstrating specificity of SMAD3 recruitment to the *ACTA2* gene (Figure 3.12A).

Treatment with TGF  $\beta$ -1 also resulted in recruitment of SET9 to the *ACTA2* gene, indicating that SET9 may regulate  $\alpha$ -*SMA* at the transcriptional level. The recruitment of SMAD3 and SET9 to the same *cis*-regulatory region is in keeping with a model whereby an interaction between SET9-SMAD3 may be required for regulation of  $\alpha$ -*SMA*. To test this hypothesis further, the effect of SET9 knockdown was also examined. Transfection of SET9 siRNA produced a significant reduction in SMAD3 recruitment (Figure 3.12B), an effect that could be partly rescued by the addition of the proteasomal inhibitor MG-132. These data argue against the model in which SET9 is passively recruited to the *ACTA2* gene but fit with the previously presented data in which SET9 facilitates SMAD3 nuclear import, in response to TGF  $\beta$ -1, to allow SMAD3 binding to the *ACTA2* gene regulatory sequence.

Upon R-PFI-2 treatment of PRFs, approximately a 60% reduction in  $\alpha$ -*SMA* protein expression is seen, suggesting that the inhibition of SET9 reduces the further activation and differentiation of myofibroblasts in response to TGF  $\beta$ -1 (Figure 3.12C).

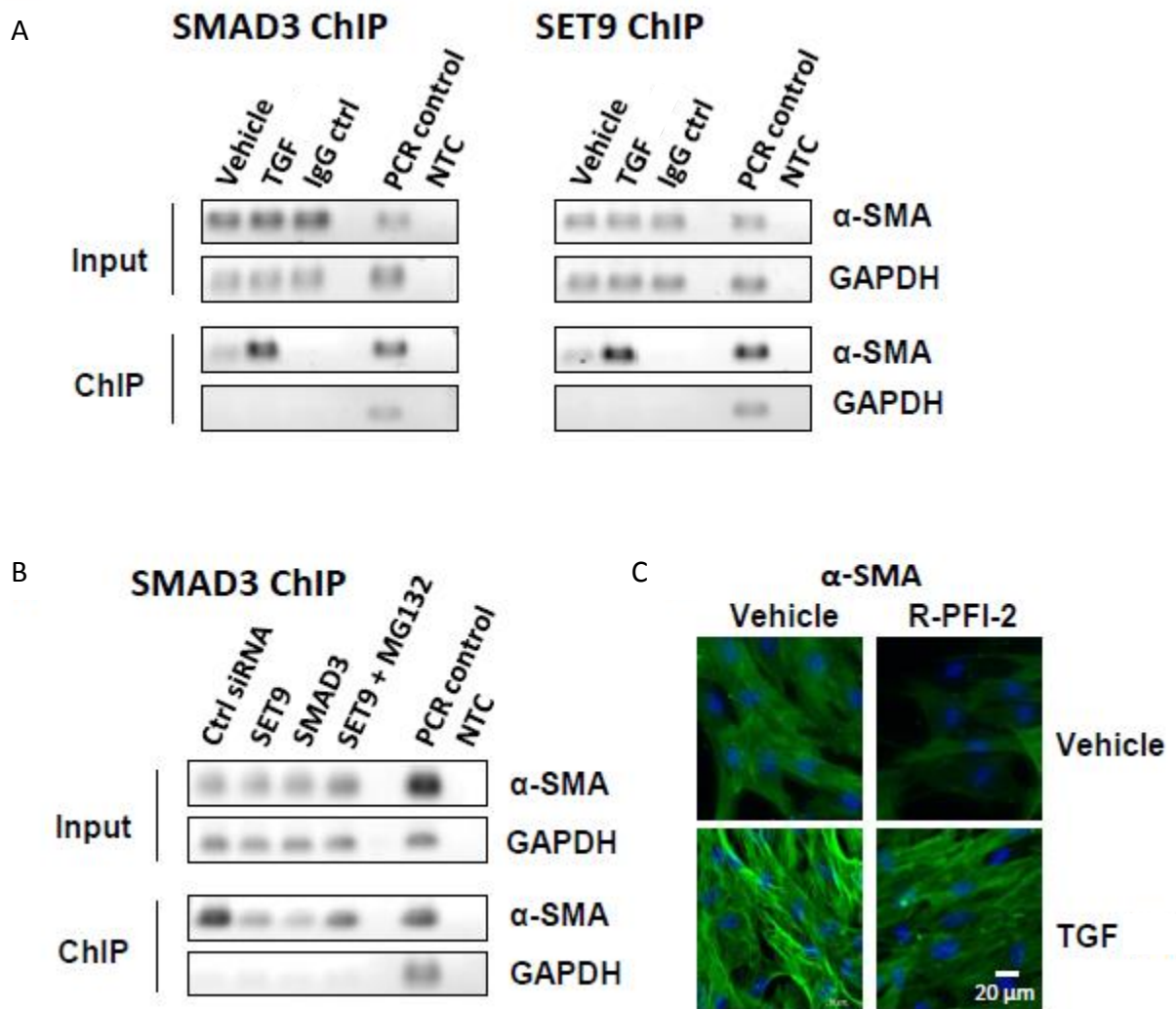


**Figure 3.12. SET9 Regulates TGF  $\beta$ -1-driven  $\alpha$ -SMA Expression.** (A) PRFs were treated with either vehicle or 5ng/ml TGF  $\beta$ -1 for 24 hours prior to chromatin immunoprecipitation with either SMAD3 (left) or SET9 (right) antibodies. Control slides with secondary antibodies only did not exhibit fluorescence (Appendix). ChIP material was subject to PCR for either  $\alpha$ -SMA or GAPDH to demonstrate selective recruitment. Purified human genomic DNA was used as a positive control in PCR (PCR control); NTC, no template control reaction. (B) PRFs were transfected with siRNA targeting either SET9, SMAD3 or control siRNA (Ctrl siRNA). 24 hours later, all cells were treated with 5ng/ml TGF  $\beta$ -1 and 5 $\mu$ M MG-132 where indicated. A further 24 hours later, cells were used in chromatin immunoprecipitation assays with SMAD3 Ab28379, as described in (A). (C) PRFs were treated simultaneously with either DMSO vehicle or 5 $\mu$ M R-PFI-2 along with 5ng/ml TGF  $\beta$ -1 as in (B) and immunostained to detect  $\alpha$ -SMA; nuclei are stained blue with DAPI. All results are representative of  $n=3$  experiments.

### 3.3 Discussion

Fibrosis is the main characteristic of almost all forms of CKD. Recent studies in animal models of kidney disease have suggested that fibrosis and fibrogenesis are major contributors to CKD progression (Duffield, 2014) and fibrosis predicts a poorer clinical outcome in CKD (Menn-Josephy et al., 2016). With the increasing prevalence of ESRD, research has been

focused on identifying anti-fibrotic therapies however to-date no specific treatments have been developed to reduce fibrosis (Tampe and Zeisberg, 2014).

With TGF  $\beta$ -1/SMAD3 signalling cascade being a key signalling pathway in the pathogenesis of renal fibrosis, there has been focus on using blocking antibodies and inhibitors of TGF  $\beta$ -1 as a treatment in fibrotic diseases. Although there has been success in animal models (Sharma *et al.*, 1996; Ziyadeh *et al.*, 2000), in clinical trials metelimumab, a TGF  $\beta$ -1 neutralizing antibody, did not demonstrate efficacy in patients and resulted in serious adverse effects (Denton *et al.*, 2007). These studies indicate that targeting downstream signalling mediators of the TGF  $\beta$ -1 pathway such as SMADs may be more effective than targeting upstream signalling.

SMAD3 in particular has been a focus of research as the literature has shown SMAD3 has an important role in renal fibrosis, demonstrated by SMAD3 knockout mice that are resistant to renal fibrosis (Sato *et al.*, 2003; Inazaki *et al.*, 2004). Similarly, SMAD3 inhibitors have been developed but none are used clinically therefore an alternative approach to interfere with TGF  $\beta$ -1 signalling is required. A lysine methyltransferase SET9 has already been shown to be involved in TGF  $\beta$ -1 signalling and ECM production in fibrosis (Elkouris *et al.*, 2016) and siRNA knockdown of SET9 significantly reduced renal fibrosis in mice. SET9 has been shown to already have a role in the TGF  $\beta$ -1/SMAD pathway; SET9 inhibition increased the expression of SMAD7, an inhibitory downstream effector of the TGF  $\beta$ -1 pathway (Elkouris *et al.*, 2016). This further supports the suggestion that SMAD3 and SET9 could provide desirable therapeutic targets in the treatment of CKD and other fibrotic diseases. SET9's role and interaction with other transcription factors to regulate TGF  $\beta$ -1 signalling is still to be explored.

SMAD proteins are known to be subject to phosphorylation and ubiquitylation to regulate TGF  $\beta$ -1 signalling (Ebisawa *et al.*, 2001; Massague, 2012) but can also be regulated by other modifications such as acetylation and methylation. For example, SMAD6, a BMP-signalling effector protein, has been found to interact and be methylated by arginine methyltransferase PRMT, facilitating the BMP-signalling pathway (Elkouris *et al.*, 2016). Methylation can regulate transcription factor function by several mechanisms including regulating protein stability, interaction with other proteins and genomic targets (Sarris *et al.*, 2014).

SET9 has been shown to methylate non-histone proteins such as TAF10 (Kouskouti *et al.*, 2004), p53 (Chuikov *et al.*, 2004) and the ER (Subramanian *et al.*, 2008) to regulate their transcription. The methylation of p53 and ER by SET9 results in their stabilisation and

subsequent transcriptional activation, supporting the theory that SET9 can also control non-histone transcriptional regulators.

A nuclear localisation signal (NLS)-like motif KKLKK has been identified in SMAD3 and is thought to be conserved across all TGF  $\beta$  pathway-specific SMADs. This motif is located within the N terminus of SMAD3 and has been shown to be responsible for its nuclear import (Xiao *et al.*, 2000). Given the presence of the KKLKK motif in SMAD3 and previous findings that have shown SET9 to interact with similar motifs in other non-histone proteins such as TAF10 (Kouskouti *et al.*, 2004), p53 (Chuikov *et al.*, 2004) and AR (Gaughan *et al.*, 2011), I sought to interrogate the role of SET9 on SMAD3 function. Immunoprecipitation experiments demonstrated an interaction between the two proteins. Interestingly, this interaction is shown to be mediated through the N-terminal domain of SMAD3 which harbours the KKLKK motif indicating that like other non-histone proteins the interaction between SET9 and SMAD3 may be mediated through this motif.

In response to TGF  $\beta$ -1, the type I and type II receptors positioned at the cell membrane form an active heterotetrameric complex which then phosphorylates an intracellular modulator, SMAD3. The phosphorylated SMAD3 then forms a heterodimer with SMAD4 and the active complex is translocated to the nucleus where it binds to *cis*-regulatory elements of target genes promoting the recruitment of additional transcriptional co-factors to mediate target gene transcription (Kretzschmar and Massague, 1998). I hypothesised that SET9 could also have a role in this signalling pathway by interacting with and regulating SMAD3 to modulate the expression of fibrotic genes and therefore could present as a novel therapeutic target for the treatment of renal fibrosis.

Immunofluorescence and cellular fractionation of HK C-8 cells demonstrated that following siRNA-mediated depletion of SET9, SMAD3 nuclear import was markedly reduced following addition of TGF  $\beta$ -1. The failure of SMAD3 to translocate to the nucleus following SET9 depletion may indicate that the interaction with SET9 occurs in the cytoplasm and is required for activation and translocation of SMAD3. SET9 is known to methylate histone 3 lysine 4 which is a marker of transcriptional activity but the data presented here shows that SET9 interacts with the SMAD3 protein rather than mediating activation of SMAD3 genes, illustrating a new role for SET9.

SET9 depletion negatively impacts the stability of SMAD3, reducing its half-life upon knockdown compared to control. SET9 has been shown to positively regulate the stability of another transcription factor, p53 by methylating one residue within the carboxyl-terminus

regulatory region (Chuikov *et al.*, 2004). When the methyltransferase activity of SET9 is disrupted, this reduces the stability of SMAD3 suggesting the methyltransferase activity of SET9 could play a role in the stability of SMAD3, perhaps by regulating SMAD3 ubiquitylation and subsequent proteosomal destruction. Conversely, SET9 interacts with and methylates SMAD7 promoting interaction with the E3 ligase Arkadia and subsequent ubiquitylation-dependent degradation (Elkouris *et al.*, 2016). However, SMAD7 is an inhibitory SMAD, the inhibition of SET9 results in elevated SMAD7 levels and inhibition of TGF  $\beta$ -1/SMAD signalling and subsequent expression of fibrotic genes. This demonstrates that SET9 can dictate different outcomes depending on the substrate and type of interaction. We were unable to determine whether SET9's interaction with SMAD3 was enough to regulate its transcriptional activity or whether SET9 directly methylated SMAD3, as it has been shown to do with other non-histone substrates. The data we have collected strongly indicates that SET9 methylates SMAD3 but this must be further explored to determine the exact mechanism of SET9.

It has been demonstrated that SET9 H3 monomethylation is involved in the regulation of ECM gene expression and silencing of SET9 attenuates TGF  $\beta$ -1 ECM gene expression (Sun *et al.*, 2010). Furthermore, knockdown of SET9 expression significantly attenuated renal fibrosis in UUO mice (Sasaki *et al.*, 2016). Additionally, we found that SET9  $-/-$  MEFs exhibited significantly reduced expression of fibrotic markers Collagen I, Collagen III, Fibronectin, PAI-1 and  $\alpha$ -SMA in the presence of TGF  $\beta$ -1 compared to SET9  $+/+$  MEFs, this mimics the phenotype of SMAD3  $-/-$  MEFs suggesting that SET9 could also have an important role in TGF  $\beta$ -1 signalling and the development of renal fibrosis.

For the first time, the data presented here shows that SET9 regulates several TGF  $\beta$ -1-driven myofibroblast functions and that SET9 is required for SMAD3 to be recruited to the *ACTA2* gene.  $\alpha$ -SMA is known to be a marker of myofibroblasts in the kidney, in a transgenic reporter mouse model under the regulation of the Collagen Type I, Alpha 1 (*Col1 $\alpha$ 1*) promoter, all cells in UUO mouse kidney interstitium that produce Collagen I also express  $\alpha$ -SMA, whereas very few cells expressed  $\alpha$ -SMA that did not produce Collagen (Lin *et al.*, 2008), therefore  $\alpha$ -SMA can be used as an imperfect marker of myofibroblasts in the kidney. The results demonstrated that SET9 is required for SMAD3 recruitment to the *ACTA2* gene in PRFs. Taken together, the data show that SET9 is required for and regulates SMAD3 stabilisation, nuclear import and then recruitment to the *ACTA2* gene. These activities lead on to myofibroblast differentiation, increased  $\alpha$ -SMA expression and Collagen contractility. With myofibroblast differentiation, the increased expression of  $\alpha$ -SMA and consequent

Collagen contractility being the main characteristics of fibrosis, inhibition of SET9 could be exploited as a therapeutic target in the treatment of CKD (Liu *et al.*, 2003; Duscher *et al.*, 2014).

A key feature of fibrosis is the increased migration and contractility of activated fibroblasts. SMAD3 knockdown has been shown to significantly reduce migration of fibroblasts and their ability to contract Collagen (Flanders, 2004; Dobaczewski *et al.*, 2010; Branski *et al.*, 2016) I have also replicated these findings in SMAD3 *-/-* MEFs. However, the role of SET9 in regulating fibroblast migration and contractility has not been examined until now. SET9 *-/-* MEFs exhibited significantly retarded migration and reduced ability to contract Collagen gels in response to TGF  $\beta$ -1 compared to SET9 *+/+* MEFs. These results are also in keeping with studies in SMAD3-null mouse models. SMAD3-null mice have been reported to exhibit reduced migratory ability of myofibroblasts and reduced Collagen gel contraction (Dobaczewski *et al.*, 2010), suggesting that SET9 could have an equally important role in regulating these key mechanisms.

In fibrosis, myofibroblast migration results in their accumulation at the site of injury and subsequent ECM deposition. Previous work has shown SET9 to be required for ECM deposition (Sun *et al.*, 2010), therefore, targeting and inhibiting SET9 to retard the migration and accumulation of myofibroblasts at the site of injury will further reduce ECM deposition and provide an additional option to treat CKD. Additionally, a study showed SET9-null mice exhibited a strong protective effect against the development of pulmonary fibrosis but showed no major phenotypic changes (Elkouris *et al.*, 2016). This suggested that SET9 inhibitors could be potential therapeutics for fibrosis.

Furthermore, a potent and selective SET9 inhibitor, R-PFI-2 applied to human primary renal fibroblasts in the presence of TGF  $\beta$ -1 also retarded the cells' ability to migrate and contract collagen. The SET9 inhibitor also reduced expression of fibrotic markers in PRFs in the presence of TGF  $\beta$ -1, mimicking the effects we demonstrated in the SET9 *-/-* MEFs. This further supports the hypothesis that SET9 has an important role in the development of renal fibrosis and can be targeted as a therapeutic with the use of selective inhibitors.

R-PFI-2 occupies part of the peptide-binding groove that is usually occupied by the target lysine residue and the peptide backbone of the preceding two residues of the substrate peptide. These two residues have been shown to be the most important residues for substrate binding by SET9 (Dhayalan *et al.*, 2011), suggesting that R-PFI-2 will be effective at inhibiting the wide variety of SET9 substrates. R-PFI-2, has been shown to exhibit over 1000-fold

selectivity to SET9 over other methyltransferases. Although very selective, negligible activity of the inhibitor can be seen on other methyltransferases G9a, EZH2, EHMT1 which could possibly result in some off-target effects on biological processes these methyltransferases are involved in such as embryogenesis and regulation of the cell cycle. This inhibitor would need to be tested further to exclude any off-target effects.

In summary, SET9 inhibition significantly reduces the activity of SMAD3 by impeding its nuclear import, protein turnover and recruitment to the *ACTA2* gene consequently reducing expression of fibrotic genes. SET9 knockdown also reduces myofibroblast migration and Collagen contraction; key mechanisms of fibrosis. Our findings present SET9 as a novel target for the treatment of renal fibrosis. The use of R-PFI-2 could provide an effective treatment for renal fibrosis but more research will need to be carried out to determine any off-target effects of the drug and its clinical relevance in the treatment of renal fibrosis.

## Chapter 4. The Role of Methyltransferase SETDB1 in TGF $\beta$ -1/SMAD3 Signalling in Renal Fibroblasts

### 4.1 Introduction and Objectives

Epigenetic post-translational modifications have been a hot topic in human disease research in recent years. Chromatin consists of tightly packed double-stranded DNA, wrapped around core histone proteins. Histones have long tails that undergo post-translational modifications to alter the structure of chromatin, thereby regulating the ability of transcription factors to access DNA binding sites in order to modulate gene expression. Acetylation, deacetylation and methylation of DNA and histones are examples of these modifications that regulate gene expression. Methylation of lysine residues within histones has received particular interest because of its critical role in the transcriptional regulation of gene expression in disease (Sun *et al.*, 2010).

Histone modifications cause transcriptional activation or repression depending upon the precise nature of the modification. For example, mono-methylation of histone 3 lysine 4 (H3K4) generally results in upregulation of gene expression whereas di- and tri- methylation of histone 3 lysine 9 (H3K9) often results in gene repression. Trimethylated H3K9 is frequently found in constitutive regions of transcriptionally silent heterochromatin, where it seems to prevent inappropriate transcription (Ruthenburg *et al.*, 2007). SETDB1 is a histone lysine methyltransferase (HKMT) known to methylate H3K9, causing transcriptional repression. SETDB1-mediated transcriptional repression is important in the context of embryogenesis and postnatal development (Matsui *et al.*, 2010), X-chromosome inactivation (Minkovsky *et al.*, 2014) and myogenesis (Song *et al.*, 2015).

On a molecular level, SETDB1 is involved in several signalling pathways such as Wnt and non-canonical Wnt signalling and TGF  $\beta$  signalling (Takada *et al.*, 2007; Sun *et al.*, 2015; Du *et al.*, 2018). In the non-canonical WNT signalling pathway, SETDB1 forms a co-repressor complex with NLK, a kinase and CHD7, a transcription factor resulting in H3K9 methylation. In turn, this attenuates recruitment of co-activators to the peroxisome proliferator-activated receptor-gamma (PPAR-gamma) gene, suppressing transcription from the PPAR-gamma locus. As a consequence, this event drives differentiation of mesenchymal stem cells to an osteoblastic cell lineage (Takada *et al.*, 2007).

SETDB1 is upregulated in Huntington's Disease and several cancer types in which SETDB1-mediated transcriptional repression is likely to contribute to disease pathogenesis (Ryu *et al.*, 2006). These cancers include breast cancer, ovarian cancer, lung cancer, hepatocellular cancer and melanoma (Ceol *et al.*, 2011; Rodriguez-Paredes *et al.*, 2014; Liu *et al.*, 2015; Wong *et al.*, 2016). In this context, SETDB1 overexpression is thought to cause transcriptional repression of tumour suppressor genes, leading to both tumourgenesis and metastasis.

Aside from histones, methyltransferases have been shown to methylate non-histone proteins. SETDB1 has been found to regulate non-histone proteins involved in transcription. For example, SETDB1 can directly methylate p53, resulting in increased p53 stability in cancer cells (Fei *et al.*, 2015). Additionally, SMAD3 can recruit SETDB1 to the IL-2 promoter in response to TGF  $\beta$ -1 to induce trimethylation of H3K9, resulting in transcriptional repression of the *IL-2* gene in immunoregulatory T cells (Wakabayashi *et al.*, 2011).

This opens up the possibility that SETDB1 could also regulate other genes downstream in TGF  $\beta$ -1/SMAD3 signalling. Together with our findings that SET9 directly interacts with SMAD3 to regulate its transcriptional activity, protein turnover and nuclear translocation, I sought to identify other methyltransferases that could be involved in the TGF  $\beta$ -1 signalling pathway in renal fibrosis.

## **4.2 Results**

### ***4.2.1 Methyltransferase siRNA Library Screen***

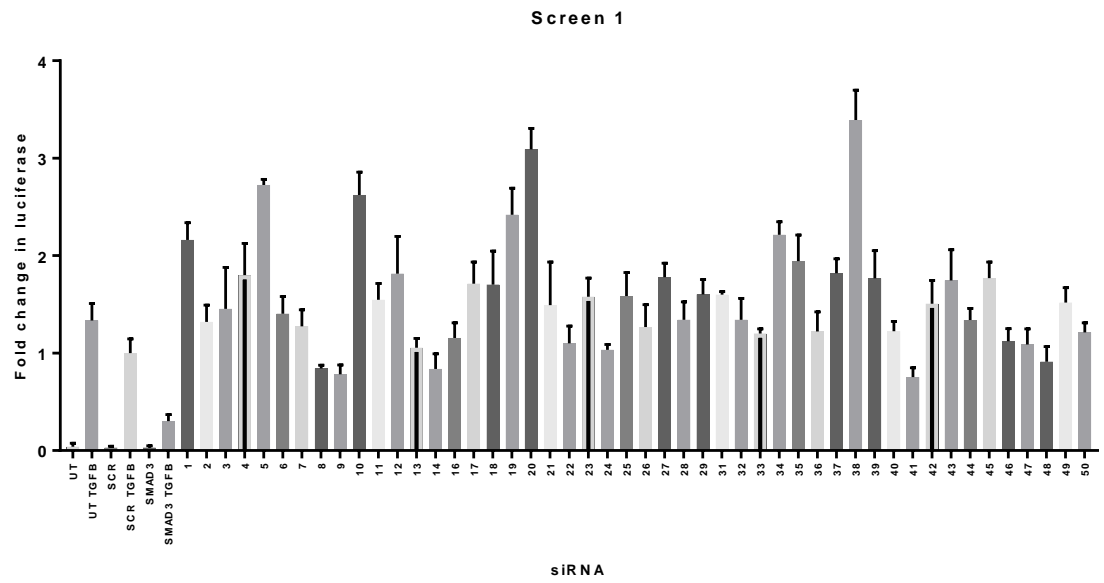
In order to identify methyltransferase enzymes that could be involved in the TGF  $\beta$ -1/SMAD3 signalling pathway, a library containing siRNA designed to target 50 methyltransferases was screened. The commercially available siRNA library contained three pooled specific siRNAs to each of the 50 methyltransferases. This library was introduced into HK C-8 cells that were stably transfected with a TGF  $\beta$ -1 responsive luciferase reporter construct termed pCAGA12-luc that contains multiple copies of the CAGA box. The stably transfected HK C-8 cells were reverse transfected with the siRNA library or SCR negative control siRNA and some cells were left untransfected as an additional control. The cells were then treated with 1ng/ml TGF  $\beta$ -1 for 24 hours and a luciferase assay was subsequently performed on cell lysates. The screen was performed twice with the siRNA added into different wells in each screen, in case the processing order within the luciferase assay introduced any bias into the results (Figure 4.1A,B). Z-scores were calculated from Screen 1 and 2 and potential hits were identified as having a Z-score of above 3 or below -3 (Figure 4.1C,D) (Zhang *et al.*, 1999).

Methyltransferases identified as potential hits in both Screen 1 and Screen 2 were then retested on an independent third assay for verification (Figure 4.1E). T-test analysis was applied and confirmed SETDB1 as a significant hit; SETDB1 siRNA knock-down resulted in a significant increase in SMAD3 luciferase activity confirming an inhibitory role for SETDB1 in TGF  $\beta$ -1/SMAD3 signalling.

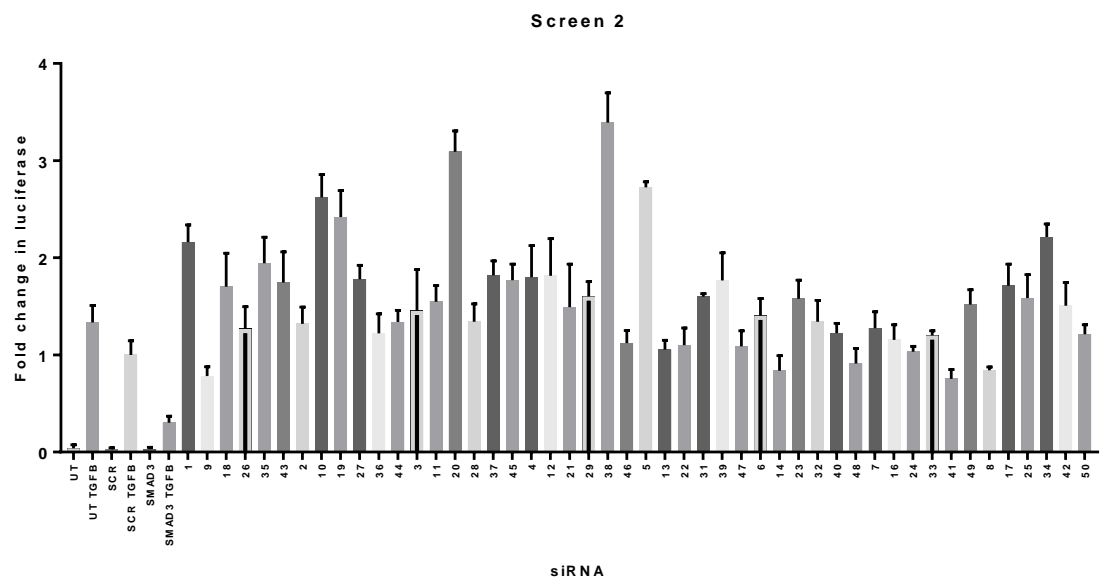
Number	Methyltransferase		Number	Methyltransferase
1	ASH1L		26	PRMT5
2	ASH2L		27	PRMT6
3	CARM1		28	PRMT7
4	DOT1L		29	PRMT8
5	EHMT1		30	SET7/9
6	EHMT2		31	SET8
7	EZH1		32	SETD1A
8	EZH2		33	SETD2
9	LCMT1		34	SETD3
10	LCMT2		35	SETD4
11	METT10D		36	SETD5
12	METT11D1		37	SETD6
13	METT5D1		38	SETDB1
14	MLL		39	SETDB2
15	MLL2		40	SETMAR
16	MLL3		41	SMYD2
17	MLL4		42	SMYD3
18	MLL5		43	SMYD5
19	NSD1		44	SUV39H1
20	PRDM1		45	SUV39H2
21	PRDM2		46	SUV420H1
22	PRDM5		47	SUV420H2
23	PRMT1		48	SUZ12
24	PRMT2		49	WHSC1
25	PRMT3		50	WHSC1L1

**Table 4.1 Methyltransferase siRNA Library.** Library of methyltransferase siRNAs with their designated number used in proliferation screens to identify potential targets of the TGF  $\beta$ -1/SMAD3 pathway in renal fibrosis.

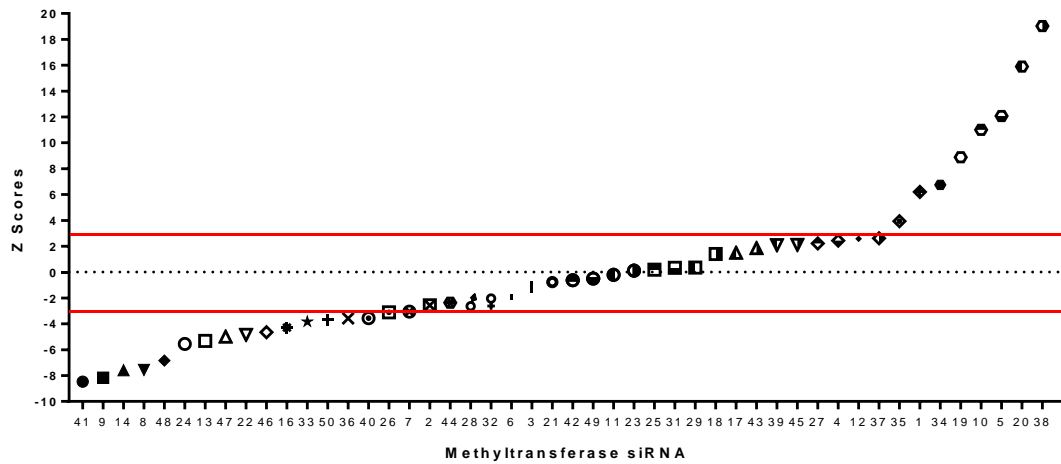
A



B



C



D

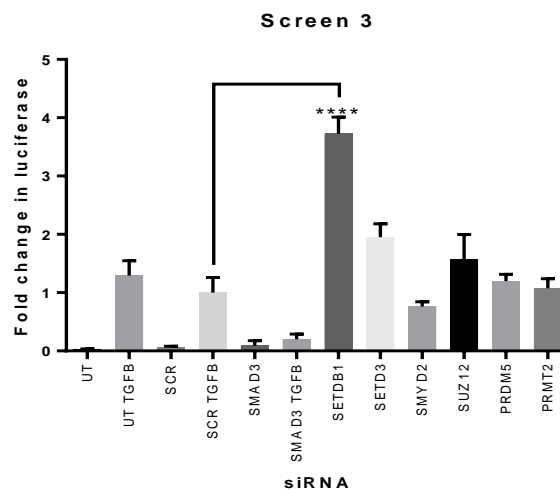


**Figure 4.1. Methyltransferase siRNA Library Screen.** (A) HK C-8 cells were stably transfected with the TGF  $\beta$ -1 responsive CAGA-luc reporter plasmid then reverse transfected with either control SCR siRNA or a library of 50 pools of methyltransferase siRNAs at a final concentration of 25nM. An untransfected control  $-/+$  TGF  $\beta$ -1 was also included. Each pool of siRNA was performed in quadruplicate. The cells were treated with 1ng/ml TGF  $\beta$ -1 for 24 hours, a luciferase assay was subsequently performed, correcting for protein quantity using a BCA assay. Luciferase readouts are presented as fold change in luciferase activity over SCR control siRNA transfectants. (B) The screen was repeated as in (A) but with the siRNAs transfected in the plates in a different order to avoid bias. (C) Z-scores were calculated from the results of Screen 1 and 2 (A and B) and plotted in ascending order. Potential hits were identified as having a Z-score above 3 or below -3. (D) A validation siRNA test was performed on methyltransferases which identified as top hits in screen 1 and 2 and presented with the greatest Z-scores. Values are mean $\pm$ s.d. P values: \*\* denotes  $P < 0.01$  \*\*\* denotes  $P < 0.001$  \*\*\*\* denotes  $P < 0.0001$  (t-test).

Gene Name	Z-Score	Effect	Gene N <sup>o</sup>	Function
SMYD2	-8.5	Negative	41	Lysine Methyltransferase *
LCMT1	-8.2	Negative	9	Leucine Carboxyl Methyltransferase
MLL	-7.6	Negative	14	Lysine Methyltransferase
EZH2	-7.6	Negative	8	Lysine Methyltransferase
SUZ12	-6.8	Negative	48	Component of Lysine Methyltransferase complex PRC2/EED-EZH2
PRMT2	-5.5	Negative	24	Protein Arginine Methyltransferase
METT5D1	-5.3	Negative	13	Probable Methyltransferase-Like Protein
SUV420H2	-5	Negative	47	Lysine Methyltransferase
PRDM5	-4.8	Negative	22	Sequence-specific DNA-binding Transcription Factor *
SUV420H1	-4.6	Negative	46	Lysine Methyltransferase *
MLL3	-4.3	Negative	16	Lysine Methyltransferase *
SETD2	-3.8	Negative	33	Lysine Methyltransferase *
WHSC1L1	-3.7	Negative	50	Lysine Methyltransferase
SETD5	-3.6	Negative	36	Function yet to be determined but like to function as a Lysine Methyltransferase *
SETMAR	-3.6	Negative	40	Lysine Methyltransferase *
SETD4	6.2	Positive	35	Lysine Methyltransferase *
ASH1L	6.2	Positive	1	Lysine Methyltransferase *
SETD3	6.7	Positive	34	Lysine Methyltransferase *
NSD1	8.9	Positive	19	Lysine Methyltransferase *
LCMT2	11	Positive	10	Probable S-adenosyl-L-methionine-dependent Methyltransferase
EHMT1	12	Positive	5	Lysine Methyltransferase
PRDM1	15.9	Positive	20	Repressor of beta-interferon gene expression
SETDB1	19	Positive	38	Lysine Methyltransferase *

**Table 4.2. Methyltransferase siRNA Screen Z-Score hits.** Positive and negative Z-score 'hits' from Screen 1 and 2. \* denotes methyltransferases containing a SET domain.

#### 4.2.2 SETDB1 Co-localises and Interacts with SMAD3

Although the luciferase assay used to identify SETDB1 is useful for a medium throughput screen, the non-physiological nature of the system may lead to false positive results.

Therefore, the role of SETDB1 in TGF  $\beta$ -1/SMAD3 signalling was examined in more detail to determine whether SETDB1 is a *bona fide* regulator of this pathway.

Firstly, to establish where SETDB1 was expressed in renal tubular epithelial cells with respect to SMAD3, dual-immunofluorescence was performed in HK C-8 cells treated with or without 10ng/ml TGF  $\beta$ -1 and stained for SMAD3 (red) and SETDB1 (green) (Figure 4.2A).

Quantitative analysis demonstrated that under basal conditions SMAD3 and SETDB1 were primarily localised to the cytoplasm (94% and 93% of total protein, respectively). Upon stimulation with TGF  $\beta$ -1, 83% of SMAD3 translocated from the cytoplasm to the nucleus. Interestingly, 30% of total SETDB1 also translocated to the nucleus upon TGF  $\beta$ -1 stimulation, demonstrating that SMAD3 and SETDB1 co-localised under basal conditions and translocate in a similar manner, in the presence of TGF  $\beta$ -1 (Figure 4.2B).

SETDB1 has previously been shown to interact with SMAD3 in human embryonic kidney cells, in response to TGF  $\beta$ -1 (Du *et al.*, 2018). To confirm this finding in the system used here, immunoprecipitation of endogenous SETDB1 from HK C-8 cell lysates was performed. Co-immunoprecipitation of SMAD3 could not be identified, even in the presence of TGF  $\beta$ -1 treatment. This could be a result of very low levels of endogenous SETDB1 within the cells, or that the interaction may take place in the nucleus which could therefore be difficult to detect from whole cell lysates. Immunoprecipitation of SETDB1 was therefore performed on nuclear fractions from HK C-8 cells which resulted in co-immunoprecipitation of SMAD3 in the presence of TGF  $\beta$ -1 (Figure 4.2C). Interestingly, no co-immunoprecipitation of SMAD3 was detected in the absence of exogenous TGF  $\beta$ -1 treatment. Additionally, SMAD3 could not be detected upon immunoprecipitation with control immunoglobulins, demonstrating specificity. The reason why the SETDB1-SMAD3 interaction could be detected only in nuclear lysates presumably reflects SMAD3 being present at higher levels in the nucleus upon TGF  $\beta$ -1 stimulation. Other studies have confirmed these findings, identifying a strong association of SETDB1 and SMAD3 in the nucleus compared with only very weak interaction in the cytoplasm, suggesting an enhanced affinity for the interaction with TGF  $\beta$ -1 activated SMAD3 (Du *et al.*, 2018).

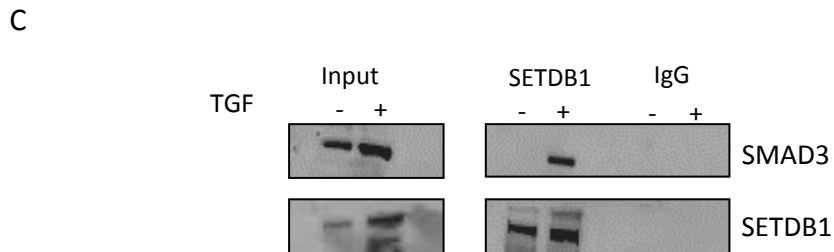
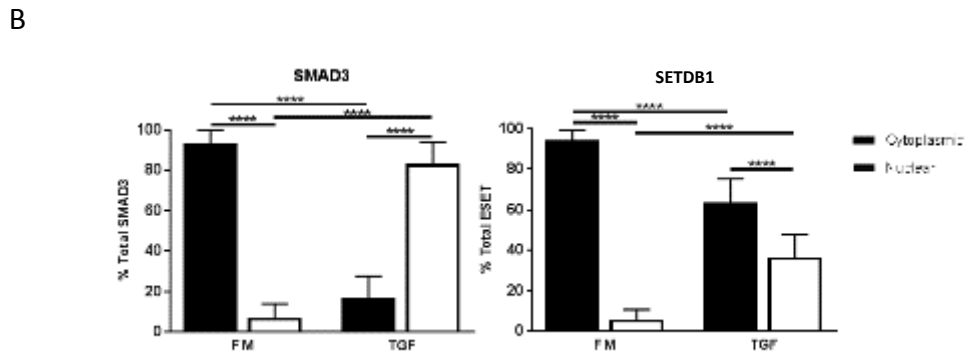
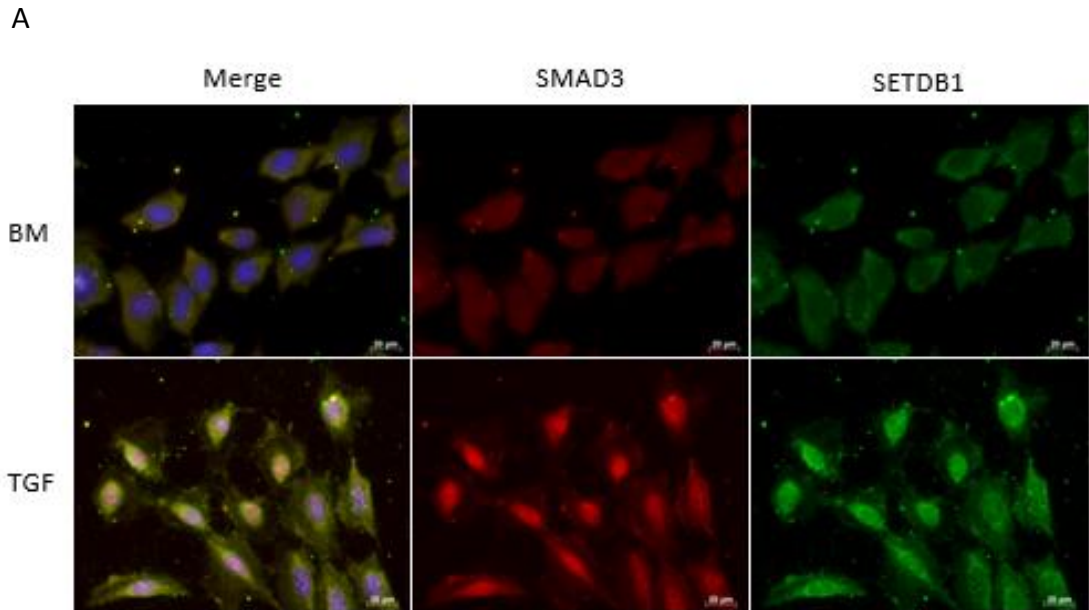
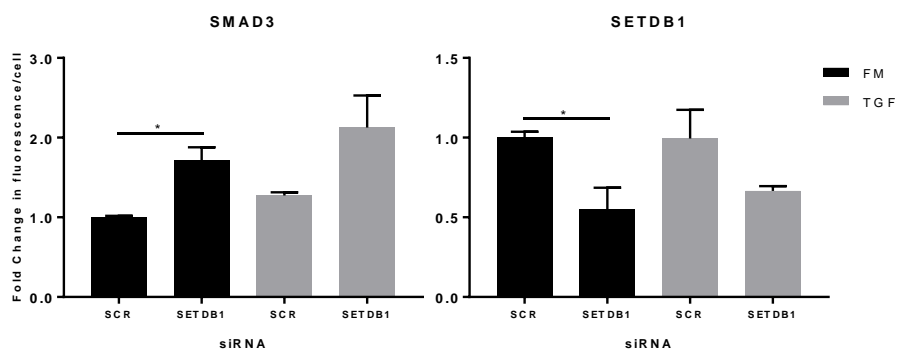
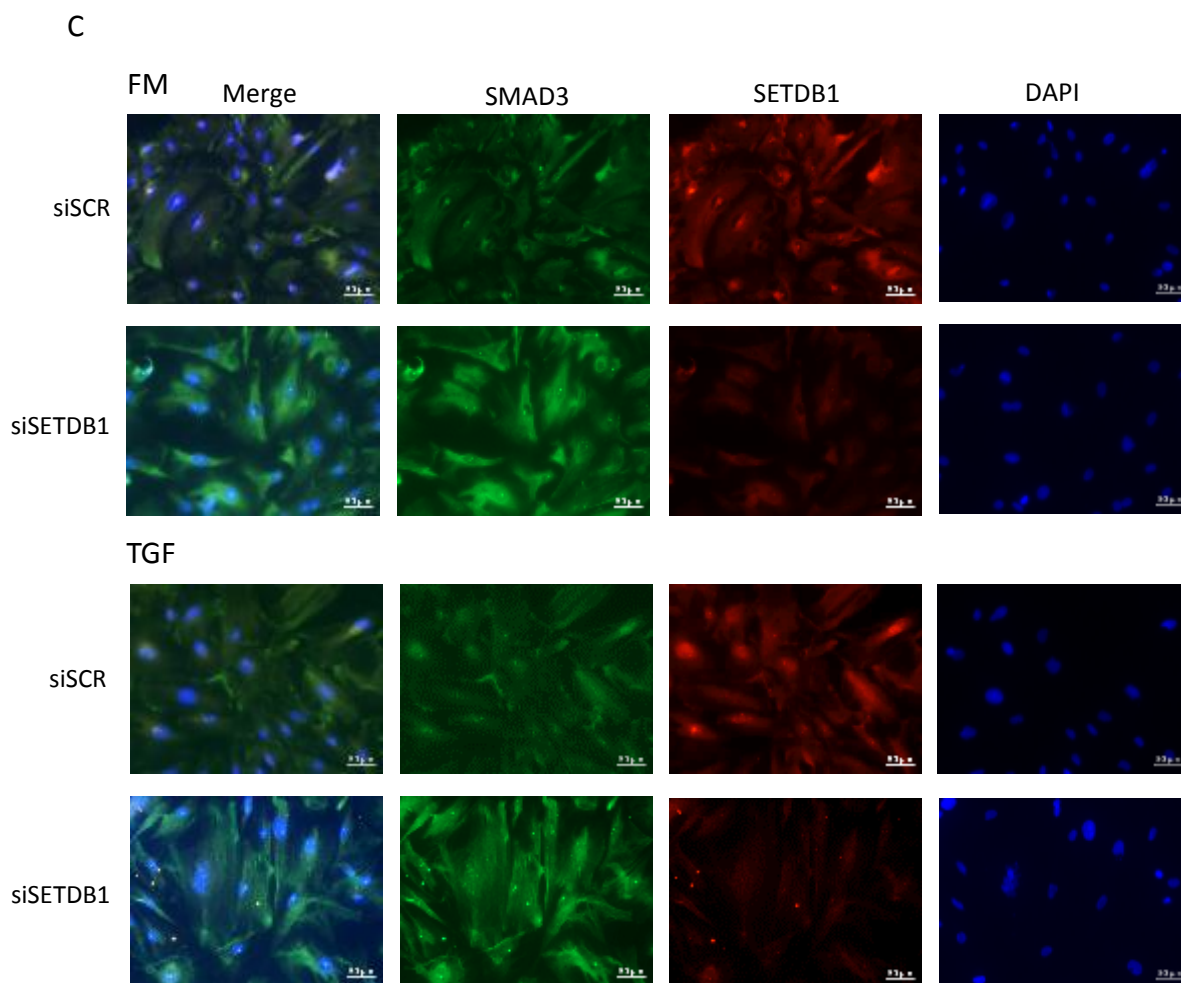
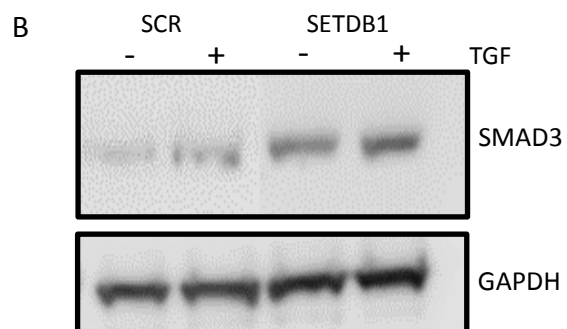
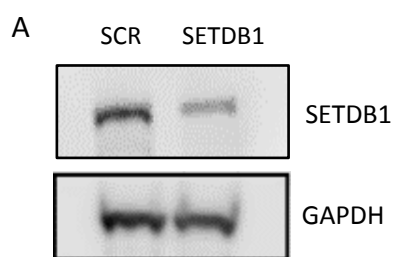


**Figure 4.2. SETDB1 Co-localises and Interacts with SMAD3.** (A) PRF cells were starved in BM for 24 hours prior to +/- 10ng/ml TGF  $\beta$ -1 treatment for 48 hours. Fixed cells were stained with the indicated antibodies for dual immunofluorescence with the appropriate Alexa Fluor-labelled secondary antibodies. Control slides with secondary antibodies only did not exhibit fluorescence (Appendix). (B) The immunofluorescence images were quantitatively analysed using Image J and are represented as bar graphs of % of total protein. (C) Immunoprecipitation was performed on HK C-8 nuclear fractions +/- 10ng/ml TGF  $\beta$ -1 with either SETDB1 antibody or control (IgG) antibody, followed by immunoblotting as indicated. All results are representative of n=3 experiments; values are mean $\pm$ s.d. P values: \*\* denotes P<0.01 \*\*\* denotes P<0.001 \*\*\*\* denotes P<0.0001 (t-test).

### ***4.2.3 SETDB1 Silencing Results in Increased Expression of SMAD3 and Pro-Fibrotic Markers***

To investigate the role of SETDB1 in the TGF  $\beta$ -1/SMAD3 signalling pathway, the effect of SETDB1 knockdown was examined. HK C-8 cells were transfected with SETDB1 siRNA or SCR control siRNA. Immunoblotting, performed on nuclear fractions, demonstrated a 52% reduction in expression of SETDB1 by densitometric analysis compared to SCR control (Figure 4.3A). Silencing SETDB1 in HK C-8 cells resulted in increased SMAD3 expression under basal conditions or upon exogenous TGF  $\beta$ -1 treatment, indicating that SETDB1 can regulate the expression of SMAD3 (Figure 4.3B). This result was subsequently confirmed by immunofluorescence of PRF cells transfected with SETDB1 siRNA or SCR siRNA control, treated with or without TGF  $\beta$ -1, then dual-stained with SMAD3 (green) and SETDB1 (red) antibodies (Figure 4.3). Analysis of immunofluorescence images demonstrated a 45% decrease in SETDB1 expression upon knockdown, which resulted in a 70% increase in SMAD3 expression under basal conditions. Comparable results were also seen with TGF  $\beta$ -1 treatment (Figure 4.3).

Because SMAD3 is a key regulator of TGF  $\beta$ -1 signalling in fibrosis, the effect of SETDB1 knock-down on the expression of the pro-fibrotic markers was then examined. Upon SETDB1 siRNA knock-down in PRF cells, the expression of  $\alpha$ -SMA, Collagen I and Collagen III proteins were all increased compared to SCR control siRNA transfectants, with or without TGF  $\beta$ -1 treatment, particularly  $\alpha$ -SMA which was significantly increased upon SETDB1 knock-down (Figure 4.3). This suggests that SETDB1 inhibits pro-fibrotic gene expression possibly through the regulation of SMAD3 protein levels.



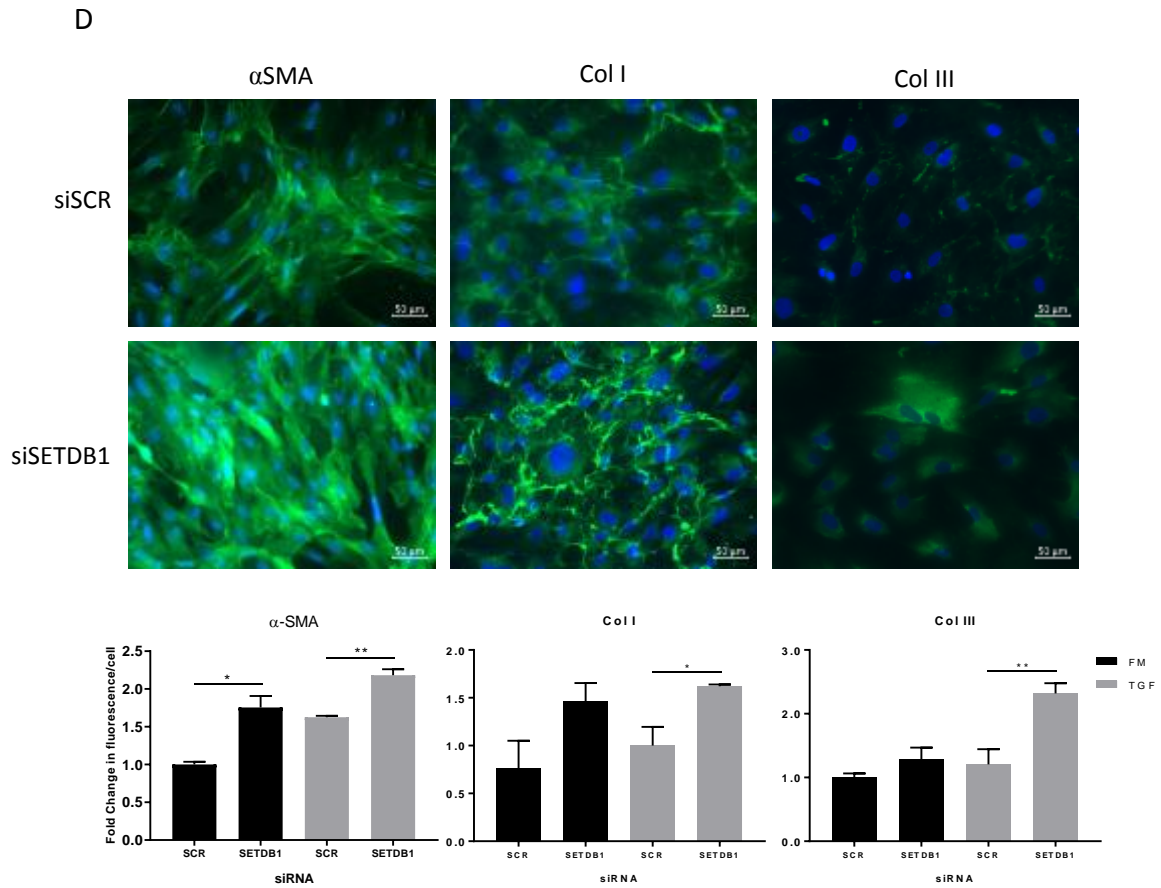


**Figure 4.3. SETDB1 Silencing Results in Increased Expression of SMAD3 and Pro-Fibrotic Markers.** (A) HK C-8 cells were transfected with SETDB1 siRNA or a control siRNA at a final concentration of 40nM, followed by 10ng/ml TGF  $\beta$ -1 treatment for 24 hours. Immunoblotting was then performed on nuclear fractions with antibodies as indicated. (B) HK C-8 cells were transfected as in (A) +/- 10ng/ml TGF  $\beta$ -1 with subsequent immunoblotting performed on whole cell lysates with antibodies indicated. (C) PRF cells were transfected with SETDB1 siRNA or control SCR siRNA at a final concentration of 40nM and treated +/- 10ng/ml TGF  $\beta$ -1 for 48 hours. Fixed cells were stained with the indicated antibodies and appropriate Alexa Fluor-labelled secondary antibodies. Control slides with secondary antibodies only did not exhibit fluorescence (Appendix). The images were quantitatively analysed using Image J and are represented as bar graphs of fold change in fluorescence per cell. (D) Immunofluorescence in PRFs was performed as in (C) but stained with antibodies as indicated. Images were quantitatively analysed as in (C). (TGF  $\beta$ -1 images not shown in D). All results are representative of n=3 experiments; values are mean $\pm$ s.d. P values: \* denotes P<0.05 \*\* denotes P<0.01 \*\*\* denotes P<0.001 \*\*\*\* denotes P<0.0001 (t-test).

#### 4.2.4 SETDB1 Silencing Enhances Wound Healing and Collagen Contractility of PRFs

As previously described, fibroblast migration to the site of tissue injury results in ECM deposition and extracellular Collagen contractility, which are essential processes in both normal wound healing and fibrosis. Because these are known to be regulated by TGF  $\beta$ -1, we examined the role of SETDB1 in these processes.

Firstly, wound healing assays were performed in PRFs transfected with either SETDB1 siRNA or SCR control siRNA. The assays were performed on glass coverslips which were then subjected to immunofluorescence for SETDB1, to ensure effective SETDB1 knock-down. SETDB1 knock-down increased the rate of migration of the cells which demonstrated 95% surface coverage at 12 hours compared to 83% cell surface coverage by SCR control (Figure 4.4A). This represents an approximate 50% increase in migration upon SETDB1 knock-down. This effect was also observed upon TGF  $\beta$ -1 treatment, albeit to a lesser extent (93% and 88% cell surface coverage at 12 hours, respectively, representing an approximately a 25% increase in migration) (Figure 4.4B). Immunofluorescence images confirmed knock-down of SETDB1 upon siRNA transfection compared to SCR control (Figure 4.4C).

Collagen contractility assays were next performed with PRFs transfected with SETDB1 or SCR control siRNA and resuspended in Collagen gel matrices. SETDB1 knock-down lead to an increase in the ability of the PRF cells to contract the Collagen matrices, resulting in appearance of smaller diameter Collagen gels compared to SCR control siRNA transfectants. This effect was seen under basal conditions or in the presence of exogenous TGF  $\beta$ -1 treatment (Figure 4.4D). The migration and Collagen contractility results in PRF cells suggest a role for SETDB1 in the regulation of renal fibroblasts, the cell type responsible for renal fibrosis.

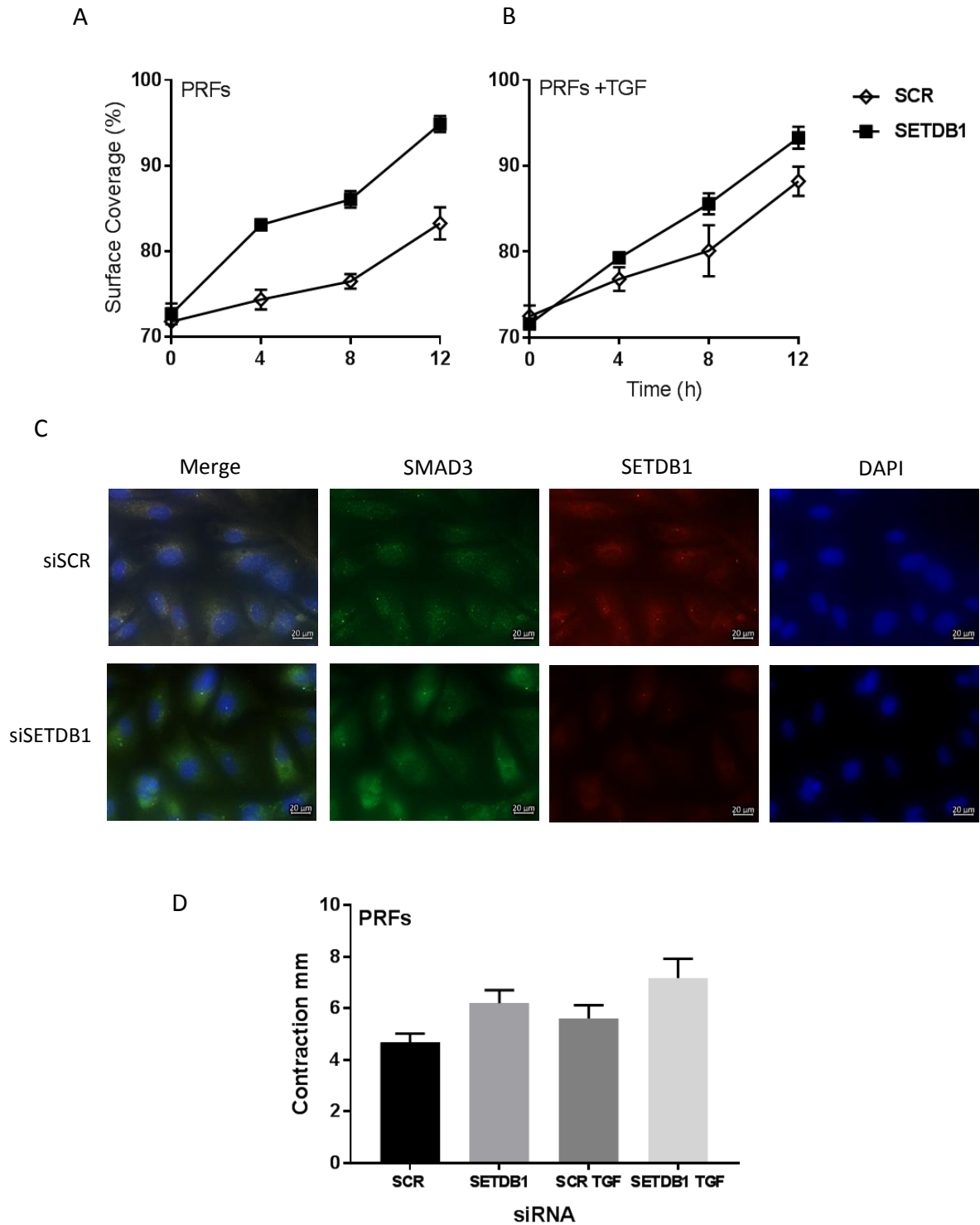


**Figure 4.4. SETDB1 Silencing Enhanced Wound Healing and Collagen Contractility of PRFs.** (A) PRF cells were transfected with SETDB1 siRNA or control SCR siRNA at a final concentration of 40nM on glass coverslips then subject to wound healing assays over a 24 hour period followed by immunofluorescence (C) stained with the indicated antibodies and appropriate Alexa Fluor-labelled secondary antibodies. (B) Performed as in (A) with the addition of 10ng/ml TGF  $\beta$ -1 treatment after transfection which was maintained throughout the 24 hours wound healing assay. Brightfield images of the wound healing assays were taken at 4 hour intervals, quantitatively analysed using Image J and represented as line graphs of % cell surface coverage over time. (D) PRF cells were transfected as in (A) for 24 hours followed by resuspension in Collagen matrix gels that were seeded into 24-well plates and allowed to set for 24 hours in FM +/- 10ng/ml TGF  $\beta$ -1. The Collagen matrices were then released from the edges of the wells and their diameters measured after a further 24 hours and

represented as a bar graph of contraction (mm). All results are representative of n=3 experiments, each point/bar is representative of a triplicate.

### 4.3 Discussion

Methyltransferase enzymes have been shown to modulate the activity of numerous transcription factors through multiple mechanisms including methylation of histone proteins that alter the chromatin landscape and by modifying non-histone proteins, thereby directly effecting their function.

As previously discussed, this work identified the lysine methyltransferase SET9 as having an important role in TGF  $\beta$ -1/SMAD3 signalling in renal fibrosis. This led to a screen for other methyltransferases involved in TGF  $\beta$ -1/SMAD3 signalling. From 2 screens of 50 human methyltransferase target genes in HK C-8 cells, 23 enzymes were identified as potential regulators of TGF  $\beta$ -1/SMAD3 signalling. Calculation of statistical Z-score analysis identified 15 enzymes with a Z-score cut-off of below -3 and 8 enzymes with a Z-score of above 3. A further validation screen was performed which identified the methyltransferase SETDB1 as having the greatest effect on TGF  $\beta$ -1 signalling, with SETDB1 knockdown resulting in a significant increase in SMAD3 transcriptional activity. Additionally, SETDB1 has previously been shown to be involved in TGF  $\beta$ -1 signalling and regulation of the ECM; suggesting SETDB1 as an attractive hit to further validate (Wakabayashi *et al.*, 2011).

Interestingly, the 3 methyltransferases SETDB1, SMYD2 and SETD3 that were identified as top hits in both screen 1 and 2 and validation screen 3 are all SET-domain lysine methyltransferases. Moreover, 15 of the 23 hits identified by Z-score analysis were lysine methyltransferases, 10 of which contain a SET-domain. This work has already identified SET9, another SET-domain lysine methyltransferase as playing an important role in TGF  $\beta$ -1 signalling, additionally the hits identified from this work suggesting that other SET-domain lysine methyltransferases play an important role in TGF  $\beta$ -1 signalling. Their mechanism of action may include i) direct interaction with SMAD3 ii) direct methylation of SMAD3 or iii) methylation of histone proteins present at SMAD3 target genes.

Silencing SMYD2, a lysine methyltransferase identified here, significantly reduced SMAD3 luciferase activity. This suggests that SMYD2 can upregulate TGF  $\beta$ -1 signalling, perhaps by acting as a co-activator for SMAD3. SMYD2 was previously shown to be activate the BMP signalling pathway by methylation of the kinase domain of the BMP receptor II (Gao *et al.*, 2017). BMP is also a member of the TGF  $\beta$  superfamily, thereby raising the possibility that

SMYD2 could also play a stimulatory role in TGF  $\beta$ -1/SMAD3 signalling. Further validation of SMYD2 as a potential co-factor in TGF  $\beta$ -1/SMAD3 signalling in renal fibrosis should also be determined.

Here a direct interaction was identified between SMAD3 and SETDB1 by immunoprecipitation from nuclear fractions, but not whole cell lysates, suggesting the SMAD3-SETDB1 interaction might occur in the nucleus rather than the cytoplasm. Additionally, the interaction was only detectable in the presence of exogenous TGF  $\beta$ -1; this could either be a result of significantly higher levels of SMAD3 present in the nucleus after TGF  $\beta$ -1 stimulation or because SETDB1 has a preference to interact only with activated phosphorylated SMAD3 which could explain why there was no interaction detected in whole cell lysates even though SMAD3 and SETDB1 are expressed in the cytoplasm under basal conditions. SETDB1 might additionally have a cytoplasmic role which would explain its expression in the cytoplasm or it may be sequestered there until its function is required in the nucleus, upon TGF  $\beta$ -1 exposure. SETDB1 has been shown to be localised in the nucleus but is exported to the cytosol after undergoing proteosomal degradation (Tachibana *et al.*, 2015). This could also explain why SETDB1 expression was observed in the cytosol in the work presented here.

SETDB1 knock-down resulted in increased SMAD3 protein expression in HK C-8 and PRF cells. It would be interesting to further examine whether regulation of SMAD3 involves post-translational modifications to SMAD3 such as lysine methylation, or whether SETDB1 could somehow regulate SMAD3 gene expression at a transcriptional level. Methylation assays and qPCR for SMAD3 upon SETDB1 knockdown could help answer these questions.

Immuofluorescence data showed an increase in expression of pro-fibrotic markers  $\alpha$ -SMA, Collagen I and Collagen III upon SETDB1 siRNA knock-down compared to SCR control. Immunofluorescence images showed a 70% increase in SMAD3, 75% increase in  $\alpha$ -SMA, 46% increase in Collagen I and 28% increase in Collagen III expression, with comparable results obtained in TGF  $\beta$ -1 treated cells. Analysis of SETDB1 following siRNA transfection demonstrated approximately 50% loss of SETDB1 protein. Achieving a more efficient knock-down would most likely further exaggerate the increased expression of these fibrotic markers. Additionally, the results should be confirmed using alternative siRNA sequences that target SETDB1.

SETDB1 is a lysine methyltransferase that specifically catalyses trimethylation of H3K9. Trimethylation of H3K9 produces a specific tag for epigenetic transcriptional repression

through recruitment of HP1 (CBX1, CBX3 and/or CBX5) proteins to methylated histones (Bannister *et al.*, 2001; Lomberk *et al.*, 2006). It is therefore possible that increases in  $\alpha$ -SMA, Collagen I and Collagen III are due to loss of this trimethylation of H3K9 at their *cis*-regulatory regions or it could be the direct result of increased SMAD3 protein levels.

SET9 has been shown to promote migration of PRFs in the development of renal fibrosis (Shuttleworth *et al.*, 2018) and protein arginine methyltransferase 1 (PRMT1) has been found to drive migration of human lung fibroblasts in the development of pulmonary fibrosis (Zakrzewicz *et al.*, 2015). SETDB1 demonstrates a negative effect on PRF cell migration and collagen contractility. These recent findings indicate that methyltransferases play different roles in the regulation of migration and Collagen contractility in fibrotic diseases.

Together, these data suggest that SETDB1 negatively regulates TGF  $\beta$ -1 signalling via its interaction SMAD3, although the mechanism is yet to be fully described. By acting as a brake on TGF  $\beta$ -1 signalling, SETDB1 may help avoid inappropriate or excessive TGF  $\beta$ -1 signalling.

SETDB1 promotes transcriptional repression by trimethylation of H3K9 and has previously been shown to be recruited to the IL-2 promoter by SMAD3 in T cells (Wakabayashi *et al.*, 2011). SETDB1 has also been shown to directly methylate non-histone protein p53, regulating its stability in cancer cells (Chuikov *et al.*, 2004). These two findings support the hypothesis that SMAD3 might recruit SETDB1 to the  $\alpha$ -SMA promoter to repress its transcription via trimethylation of H3K9. Or, SETDB1 might directly methylate SMAD3, leading to repression of transcriptional activity at the *ACTA2* gene and the other pro-fibrotic genes. Additionally, it has been shown that in response to TGF  $\beta$ -1, SMAD3 recruits SETDB1 to the *Snail* gene leading to H3K9 methylation which subsequently inhibits H3K9 acetylation resulting in *Snail* gene transcriptional repression. This raises a third possibility in that SETDB1 methylation might repress acetylation at the *ACTA2* gene, thereby resulting in transcriptional repression.

SETDB1 has also been shown to associate with histone deacetylase 1 (HDAC1) and HDAC2 as well as interact with co-repressors mSin3A and mSin3B; when recruited and bound to a promoter SETDB1 was shown to repress transcription independently of its histone methyltransferase activity but dependent on its interaction with co-repressors mSin3A/B (Yang *et al.*, 2003). This raises yet another potential mechanism by which SETDB1 could inhibit the TGF  $\beta$ -1/SMAD3 signalling pathway.

As SETDB1 is upregulated in many cancers, causing aberrant silencing of tumour suppressor genes, it is an attractive therapeutic target in cancer. However, the work presented here suggests that SETDB1 may act as a brake on TGF  $\beta$ -1/SMAD3 signalling. SETDB1 therefore does not lend itself to being a therapeutic target in CKD. Nevertheless, the research presented here offers an insight into how lysine methyltransferases may have different roles in the regulation of the TGF  $\beta$ -1/SMAD3 signalling pathway in renal fibrosis. Alternatively, if the mechanism of action of SETDB1 is determined to be methylation of SMAD3, its opposing demethylase enzyme could present a more suitable target for CKD.

## Chapter 5. Aurora Kinase A Promotes Renal Fibrosis through TGF $\beta$ -1 Signalling in Myofibroblasts

### 5.1 Introduction

The Aurora Kinase (AURK) family are a group of three serine/threonine kinases that have a critical role in the regulation of the cell cycle, particularly mitosis and maintenance of genome stability (Vader and Lens, 2008). Disruption of AURK signalling can result in mitotic errors such as chromosomal aneuploidy. Overexpression of both AURKA and AURKB has been linked to human malignancies and also correlates with a poor prognosis in several tumour types (Naruganahalli *et al.*, 2006).

In order to carry out its function, AURKA interacts with several co-factors during cell division that determine its localisation, activation and substrate preference (Vader and Lens, 2008). AURKA binds to and phosphorylates co-factor Ajuba, a protein that is required for AURKA initial centrosomal activation and autophosphorylation on threonine 288 within the AURKA activation loop (Hirota *et al.*, 2003). Mitotic spindle assembly requires the co-factor of AURKA, microtubule-associated protein TPX2, which interacts with and tethers AURKA to the mitotic spindle and along with the GTPase Ran; both are required for activation of AURKA (Kufer *et al.*, 2002). AURKA has also been found to bind to co-factors Bora and Enhancer of Filament 1 (HEF1), both of which enhance its kinase activity (Pugacheva and Golemis, 2005; Hutterer *et al.*, 2006).

Overexpression of AURKA increases chromosome instability and has been shown to lead to oncogenic transformation and tetraploidy (Bischoff *et al.*, 1998; Zhou *et al.*, 1998; Meraldi *et al.*, 2002). AURKA overexpression is therefore thought to promote tumourigenesis and so aneuploidy caused by chromosomal instability is now recognised as a marker of tumour progression as it is the most frequent form of genomic damage identified in cancer (Zhou *et al.*, 1998).

AURKA has also been shown to have non-mitotic roles such as regulation of Golgi apparatus architecture (Kimura *et al.*, 2018), regulation of ciliary disassembly (Pugacheva *et al.*, 2007) and cell migration and polarity (Wu *et al.*, 2005). These findings highlight alternative roles and substrates for AURKA.

The strong links with cancer make AURKA an attractive therapeutic target in the treatment of cancer. Many AUKA inhibitors have been developed and are being evaluated as anti-cancer

drugs, several of which are currently in clinical trials (Dar *et al.*, 2010). One of the most promising AURKA inhibitors, MK-5108, is a potent adenosine triphosphate competitive inhibitor which is 200-fold more selective for AURKA than AURKB (Amin *et al.*, 2016; Damodaran *et al.*, 2017). MK-5108 has been trialled in Phase I studies, both as a monotherapy and in combination with cytotoxic chemotherapy in solid tumours (Amin *et al.*, 2016) and has been found to be the least toxic AURKA inhibitor to-date. MK-5108 has been shown to induce apoptosis in cancer cells resulting in cell death.

Here, a novel role for AURKA is described, in the regulation of TGF  $\beta$ -1 signalling. AURKA phosphorylates SMAD3, an important downstream mediator of TGF  $\beta$ -1 signalling. Pharmacological inhibition of AURKA with MK-5108 leads to inhibition of myofibroblast activity in injured kidney and liver tissues.

## **5.2 Results**

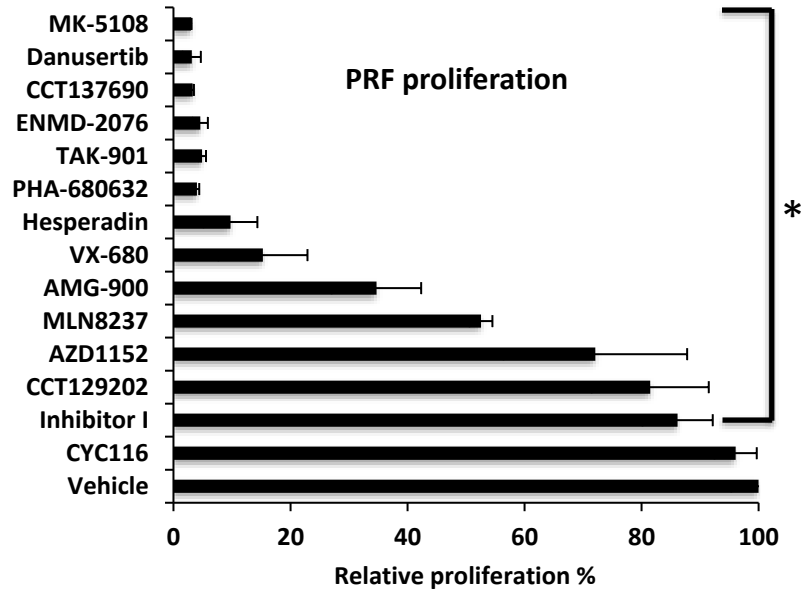
### ***5.2.1 Aurora Kinase Inhibitors Selectively Reduce Proliferation, Induce Apoptosis and Prevent Myofibroblasts Differentiation of Human Primary Renal Fibroblasts***

In an attempt to identify compounds that might inhibit PRF cell proliferation, a library of 283 small molecule inhibitors was screened in PRF cells stimulated with TGF  $\beta$ -1. Fourteen AURK inhibitors were screened, ten of which significantly reduced proliferation of PRFs by more than 50% at a concentration of 10 $\mu$ M, compared to control PRF treated with DMSO vehicle (Figure 5.1A). Seven out of the ten of these AURK inhibitors demonstrated highly potent activity in PRFs, reducing proliferation by more than 90% (Figure 5.1A). These seven AURK inhibitors demonstrated consistently potent activity in PRFs isolated from three different kidneys but exhibited very little effect on primary renal proximal tubular cells (PTC) which were isolated from the same three kidneys. Additionally, these 7 compounds were tested in the proximal renal tubular epithelial HK C-8 cell line, which demonstrated on average a 12-fold relative resistance compared to PRFs (Figure 5.1B). Other compounds targeting enzymes such as Janus Kinase 2 (JAK2) had little effect in PRFs but significantly reduced proliferation of tubular cells. This suggests that AURK inhibitors selectively reduced proliferation of PRFs in the presence of TGF  $\beta$ -1.

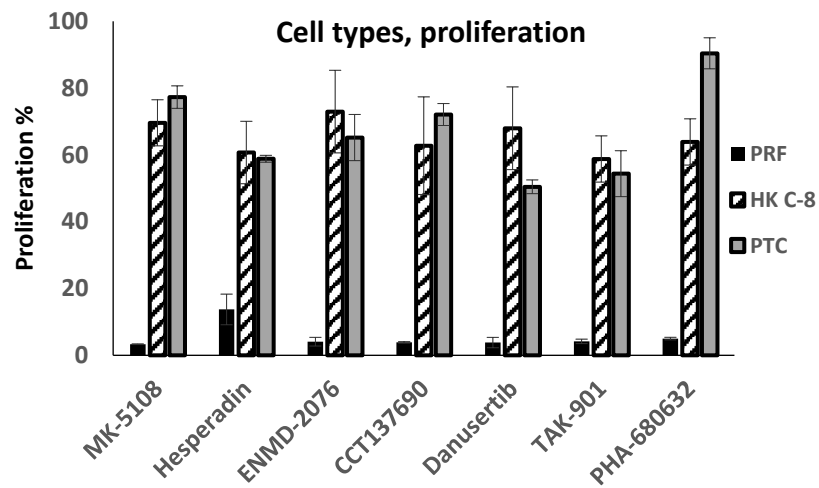
Cell cycle arrest and apoptosis have been previously shown to occur upon AURK inhibition (Scharer *et al.*, 2008; Shimomura *et al.*, 2010), so were therefore examined in PRFs with three selected AURK inhibitors. Upon treatment with these three compounds, an enrichment of Annexin V was observed from approximately 5% in control cells, to between 49-80 % after

72 hours drug exposure (Figure 5.1). This apoptotic effect was not observed in HK C-8 cells, which showed resistance to these AURK inhibitors, but were sensitive to the Staurosporine positive control. Further to this, a more detailed time course was performed in which cells progressed from being Annexin V positive and Propidium Iodide negative to becoming Annexin V and Propidium Iodide positive, demonstrating they were going through apoptosis subsequently resulting in cell death (Figure 5.1E).

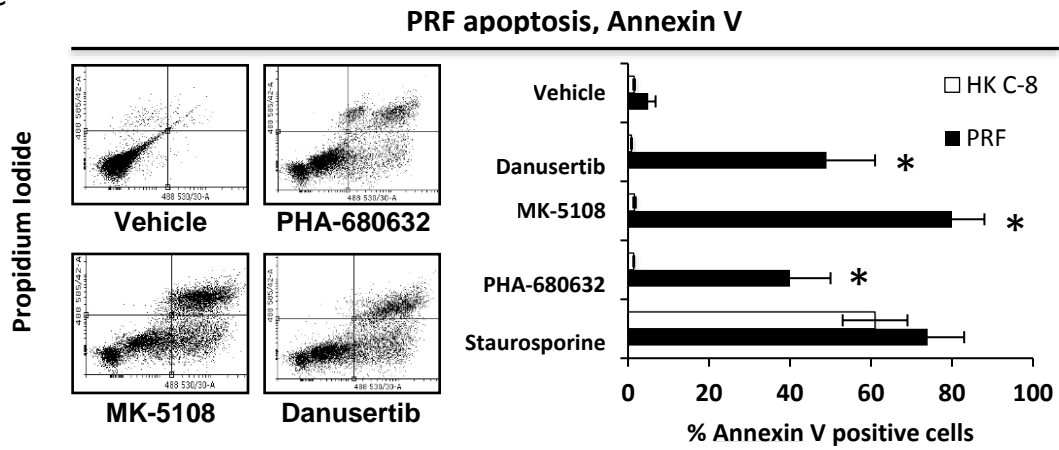
A



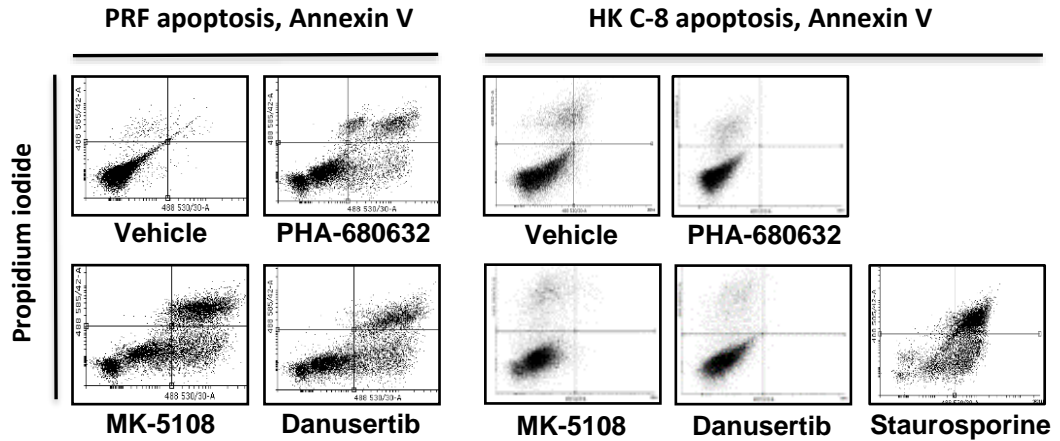
B



C



D



E

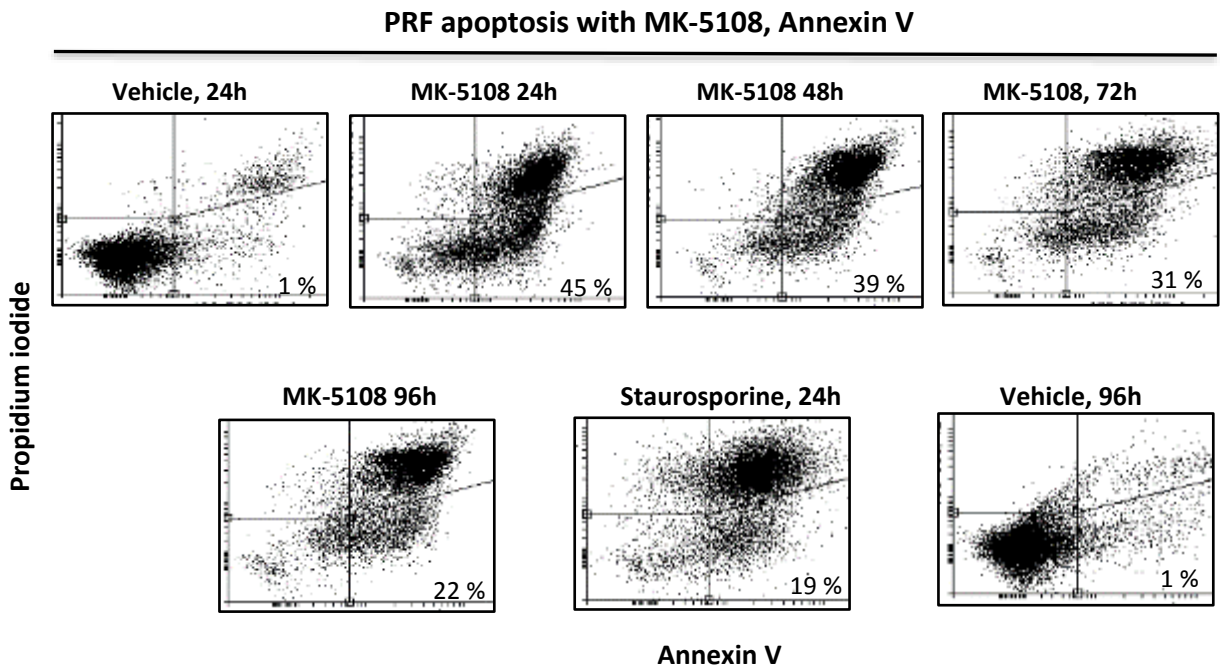
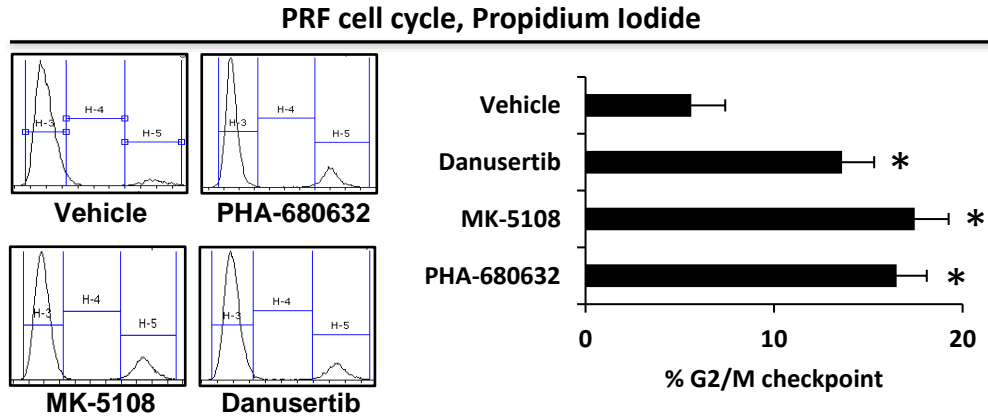


**Figure 5.1. Aurora Kinase Inhibitors Cause Selective Apoptosis in Primary Renal Fibroblasts.** (A) PRF cells were treated with 10 $\mu$ M of the indicated compounds, or DMSO vehicle control for 72 hours, in the presence of 5ng/ml TGF  $\beta$ -1, prior to WST-1 proliferation assay. Each condition was performed in quintuplet. Representative data from cells from one of three patients is shown. Error bars represent SD. \*  $p < 0.05$ ,  $t$ -test. (B) PRF or PTC isolated from the same patient, or HK C-8 cells, were exposed to 10 $\mu$ M of selected AURKA inhibitors for 72 hours prior to WST-1 proliferation assay. Absorbance values were calculated as a percentage of each respective cell type treated with DMSO vehicle control. \*  $p < 0.05$ ,  $t$ -test. (C) PRF or HK C-8 cells were exposed to 10 $\mu$ M of AURKA inhibitors indicated for 72 hours, or 1 $\mu$ M Staurosporine for 24 hours, then stained with Annexin V and Propidium Iodide prior to flow cytometry. Plots shown are representative PRF data with Annexin V staining on X axis. Graph indicates percentage positive Annexin V cells \*  $p < 0.05$ ,  $t$ -test. (D) PRF or HK C-8 cells were treated with 10 $\mu$ M of the indicated compounds for 72 hours prior to Annexin V apoptosis assays as previously described. Plots shown are representative data, from the same PRF patient as in Figure (C), with Annexin V staining on X axis. \*  $p < 0.05$ ,  $t$ -test. (E) PRF cells were treated with 10 $\mu$ M MK-5108 or 1 $\mu$ M Staurosporine for the indicated time periods prior to Annexin V apoptosis assays as previously described. Plots shown are representative PRF data with Annexin V staining on X axis.

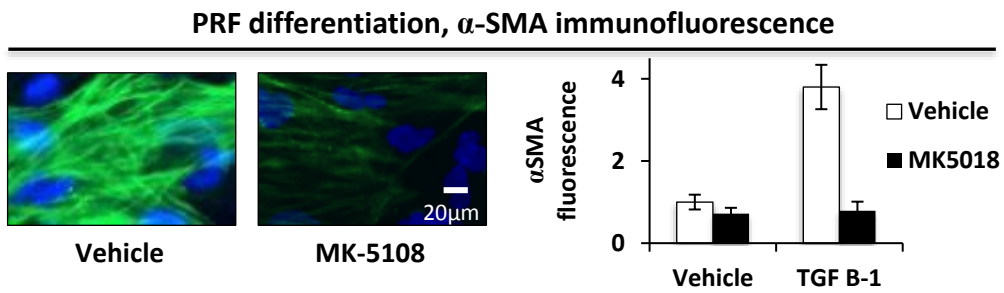
Cell cycle analysis was performed at a lower, sub-apoptotic dose of 1 $\mu$ M so that sufficient cell numbers could be analysed. The three AURK inhibitors showed a more than 2-fold increase in PRF cells in the G2/M checkpoint (Figure 5.2A). AURK inhibitors demonstrate a selective potency in PRFs, reducing proliferation in these cells primarily by apoptosis and cell death.

Transdifferentiation of PRFs was also examined in the presence of AURK inhibitor, MK-5108. TGF  $\beta$ -1-induced transdifferentiation of PRFs to an activated myofibroblast state, as shown by significantly increased expression of  $\alpha$ -SMA, a key marker of myofibroblast transdifferentiation (Figure 5.2B). TGF  $\beta$ -1 treatment also resulted in increased expression of Collagen I and III in PRF cells. Treatment with MK-5108 at a sub-lethal dose of 1 $\mu$ M caused a significant 75% reduction in  $\alpha$ -SMA expression in PRF. Reductions in Collagen I and III expression were also observed (Figure 5.2C). These results suggest that the AURK inhibitor MK-5108 causes apoptosis in PRFs as seen in cancer cells, but also prevents TGF  $\beta$ -1-mediated myofibroblast transdifferentiation of PRF.

A



B



C

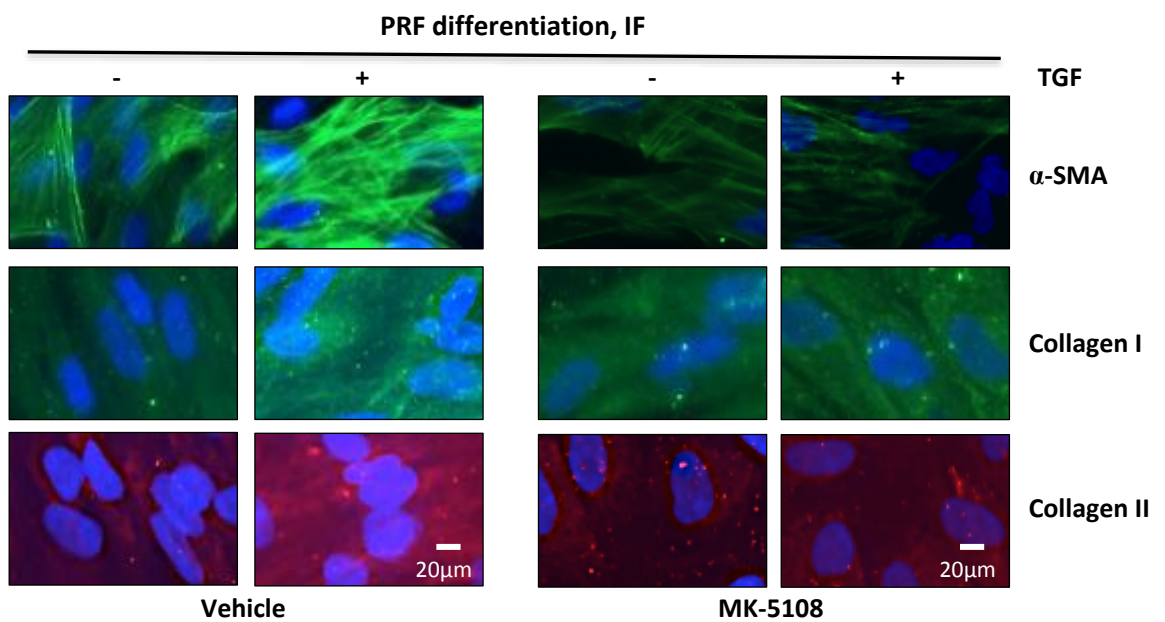


**Figure 5.2. Aurora Kinase Inhibitors Inhibit Proliferation and Transdifferentiation in Primary Renal Fibroblasts.** (A) PRF cultured in the presence of 5ng/ml TGF  $\beta$ -1 were subject to 1 $\mu$ M of the indicated AURKA inhibitors for 48 hours, then stained with Propidium Iodide prior to flow cytometry. Histograms shown are representative PRF data. Graph indicates percentage of cells in G2/M checkpoint. \*  $p < 0.05$ ,  $t$ -test. (B) PRF cultured in glass chamber slides were exposed to 5ng/ml TGF  $\beta$ -1 and 1 $\mu$ M MK-5108 or DMSO vehicle for 72 hours prior to indirect immunofluorescence for  $\alpha$ -SMA. Bar graph represents fold change in fluorescence over DMSO vehicle control-treated cells. \*  $p < 0.05$ , ANOVA. (C) PRF cultured in glass chamber slides were exposed to TGF  $\beta$ -1 and 1 $\mu$ M MK-5108 or DMSO vehicle for 72 hours prior to indirect immunofluorescence for the indicated markers. Control slides with secondary antibodies only did not exhibit fluorescence (Appendix).

### 5.2.2 AURKA Phosphorylates SMAD3 in Response to TGF $\beta$ -1

As MK-5108 had an impact on PRF transdifferentiation, in response to TGF  $\beta$ -1, a role for AURKA in the TGF  $\beta$ -1 signalling pathway was investigated. Firstly, SMAD3 protein turnover was examined to determine whether AURKA could regulate SMAD3 protein levels, a critical downstream mediator of TGF  $\beta$ -1 signalling in fibrosis. SMAD3 protein turnover is regulated by proteasomal destruction (Fukuchi *et al.*, 2001) and can be measured by immunoblotting and densitometry after the addition of cycloheximide, to inhibit *de novo* protein synthesis. In control PRF cells, the SMAD3 half-life was approximately 4 hours. Upon AURKA siRNA transfection the half-life of SMAD3 remained unchanged, suggesting AURKA has no involvement in the SMAD3 protein turnover (Figure 5.3A).

TGF  $\beta$ -1 stimulation leads to activation and autophosphorylation of TGF  $\beta$ RI and II which subsequently phosphorylate SMAD3 which is then translocated to the nucleus resulting in transcription of SMAD3 target genes. The effect of AURKA on the phosphorylation of SMAD3 was examined as an indication of its potential role in TGF  $\beta$ -1 signalling.

Immunoprecipitation of SMAD3 was performed followed by immunoblotting for SMAD3 C-terminal phosphorylation with C25A9 antibody. In the presence of TGF  $\beta$ -1, an enrichment of 423/5 phosphorylation of SMAD3 was observed. As expected, phosphorylation of SMAD3 was partially inhibited by inhibitor ALK5 inhibitor, a potent selective inhibitor of TGF  $\beta$ RI kinase. Addition of MK-5108 virtually abolished SMAD3 phosphorylation (Figure 5.3B), suggesting AURKA is involved in SMAD3 phosphorylation in TGF  $\beta$ -1 signalling. To confirm that this was not an off-target effect of MK-5108, immunoprecipitation of SMAD3 was performed after transfection of AURKA or AURKB siRNA, in the presence of TGF  $\beta$ -1. AURKA siRNA transfection resulted in a significant reduction in SMAD3 423/5 phosphorylation compared to AURKB siRNA which had no effect (Figure 5.3C).

Immunoblotting with an alternative phospho-SMAD2/3 antibody produced the same effect suggesting that AURKA is required for SMAD3 phosphorylation in PRFs. These data confirm that AURKA but not AURKB is involved in TGF  $\beta$ -1 signalling, via SMAD3 phosphorylation in PRFs.

To determine whether AURKA directly phosphorylates SMAD3, *in vitro* kinase reactions were performed using purified recombinant SMAD3 and AURKA proteins. Immunoblotting with total SMAD3 antibody demonstrated a higher molecular weight, band-shifted SMAD3 protein in the presence of AURKA suggestive of a phosphorylation event (Figure 5.3D). A time-course experiment with a fixed quantity of SMAD3 and AURKA demonstrated

accumulation of the band-shifted SMAD3 in a time-dependent manner (Figure 5.3E). These band-shifted SMAD3 species are likely to represent SMAD3 phosphorylation by AURKA given that they are present only in the presence of AURKA. Additional kinase reactions were performed and immunoblotted with a phospho-serine antibody which demonstrated a strong band at the correct molecular weight for SMAD3, only in the presence of AURKA, suggesting that AURKA phosphorylates SMAD3 on serine residues. This band was much weaker after the addition of calf intestinal phosphatase (CIP). Blotting with a phospho-threonine antibody did not reveal any bands of the correct molecular weight for SMAD3, suggesting that AURKA may phosphorylate SMAD3 specifically on serine, but not threonine residues. Finally, the kinase reactions were blotted with a specific SMAD3 phospho-serine 423/5 antibody. This demonstrated a strong band, of the correct molecular weight for SMAD3 that was only detectable in the presence of AURKA. This band became undetectable after the addition of CIP (Figure 5.3F). In conclusion, AURKA directly phosphorylates SMAD3 specifically on serine residues 423/5. This may account for the effects observed on TGF  $\beta$ -1-induced  $\alpha$ -SMA expression in PRFs by MK-5108.



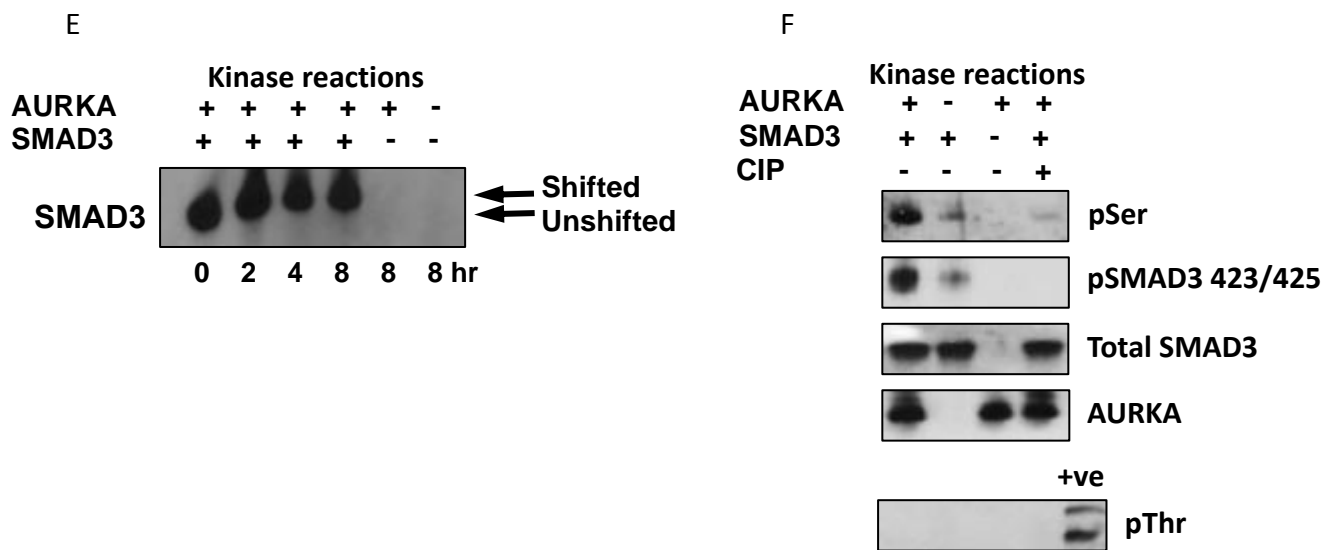


**Figure 5.3. AURKA Phosphorylates SMAD3.** (A) PRF cells were reverse transfected with 20nM of the indicated siRNA overnight, in the presence of 5ng/ml TGF  $\beta$ -1. Cycloheximide was then applied in fresh complete medium at 50 $\mu$ g/ml for the indicated time periods prior to immunoblotting whole cell lysates as shown. SMAD3 protein turnover, calculated by densitometry (not shown), was approximately 4 hours. (B) PRF cells were treated overnight with DMSO vehicle, 1 $\mu$ M MK-5108 or 5 $\mu$ M SB505124 in the presence of 5ng/ml TGF  $\beta$ -1 or vehicle prior to immunoprecipitation with SMAD3 antibody or control IgG then immunoblotting cell lysates (Inputs) and immunoprecipitated material (IPs) with the indicated antibodies including C25A9 to detect pSMAD3 423/5. \* indicates non-specific immunoglobulin light chain. (C) PRF cells were reverse transfected overnight with siRNA targeting AURKA (AurA) or AURKB (AurB), both targets combined (AurA+B) or control siRNA (SCR), treated with 5ng/ml TGF  $\beta$ -1 for a further 24 hours, then subject to immunoprecipitation as in (A). Immunoblotting was then performed using the indicated antibodies including C25A9 and sc-11769, both of which detect phospho-SMAD3. (D) Increasing quantities of SMAD3 (1-3 $\mu$ g) and a fixed quantity of 0.1 $\mu$ g AURKA proteins were incubated in kinase reactions for 4 hours, prior to gradient gel electrophoresis and immunoblotting for SMAD3. Upper arrow indicates band-shifted SMAD3. (E) Fixed quantities of 1 $\mu$ g SMAD3 and 1 $\mu$ g AURKA proteins were incubated for increasing times between 0-8 hours in kinase reactions, prior to gradient gel electrophoresis and immunoblotting for SMAD3. Upper arrow indicates time-dependent appearance of band-shifted SMAD3. (F) Fixed quantities of 1 $\mu$ g SMAD3 and 0.1 $\mu$ g AURKA proteins, were incubated for 4 hours in kinase reactions prior to standard electrophoresis and immunoblotting with the phospho-specific antibodies shown, including C25A9. Where shown, one reaction was treated with CIP at 37 $^{\circ}$ C for the final 20 minute period, resulting in disappearance of the phospho-specific bands.

### 5.2.3 MK-5108 Inhibits Renal Fibrosis in Mice

Aberrant TGF  $\beta$ -1 signalling is known play a critical role in fibrosis and SMAD3 is required for the development of renal fibrosis in mice (Flanders, 2004). The data presented here link AURKA to SMAD3 in TGF  $\beta$ -1 signalling in PRFs. The effect of MK-5108 in a UUO mouse model of renal fibrosis was therefore examined.

UUO surgery was performed on the left kidneys of 15 female mice, causing them to develop renal fibrosis. MK-5108 was administered to 7 mice at 45mg/kg by daily oral gavage, leaving

8 mice in the control group which received methylcellulose by daily gavage. After 12 days, the mice were culled and both left and right kidneys harvested for histology. Paraffin-embedded kidney tissues were cut and mounted onto slides for immunohistochemical staining. Staining with specific antibodies demonstrated a significant increase in  $\alpha$ -SMA, Collagen I and III and Masson's Trichrome staining (total Collagen) in obstructed left kidneys compared to uninjured control right kidneys (Figure 5.4). Mice treated with MK-5108 showed a significant reduction in expression of these pro-fibrotic markers, particularly  $\alpha$ -SMA, suggesting that AURKA has a role in driving renal fibrosis in vivo. No toxicity from MK-5108 was observed in the mice.

Total SMAD3 and phospho-serine 423/5 expression were also examined using immunohistochemistry. Expression of phospho-serine 423/5 was increase in UUO kidneys compared to control kidneys but total SMAD3 expression remained unchanged (Figure 5.4). Upon MK-5108 treatment, phospho-serine 423/5 expression was significantly reduced, whereas total SMAD3 expression remained unchanged, suggesting that AURKA reduces phosphorylation of SMAD3, in vivo. Finally, AURKA expression was examined but no significant difference between any groups was observed (Figure 5.4).

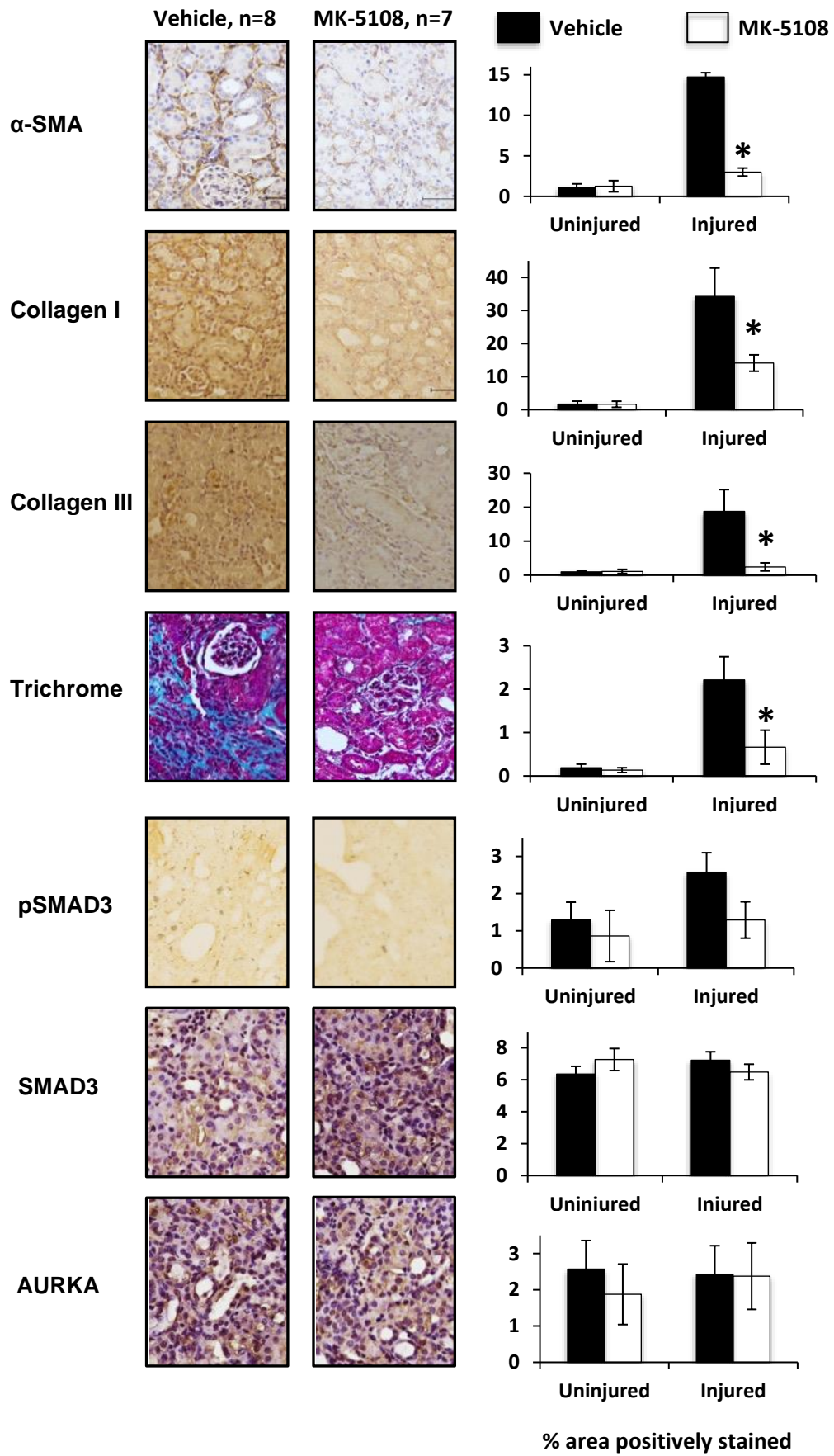


**Figure 5.4. MK-5108 Attenuates Renal Fibrosis after Ureteric Obstruction.** Mice that had undergone unilateral left ureteric ligation were treated with daily oral MK-5108 or methylcellulose vehicle then sacrificed after 12 days. Tissues from obstructed (injured) and control kidneys were stained with the antibodies indicated, or Trichrome, prior to automated analysis of staining with the exception of phospho-SMAD3 C25A9. Graphs show median percentage area positively stained for all kidneys, across 15 images per kidney, or mean visual score in the case of phospho-SMAD3. Error bars represent SD, \*  $p < 0.05$ , t-test.

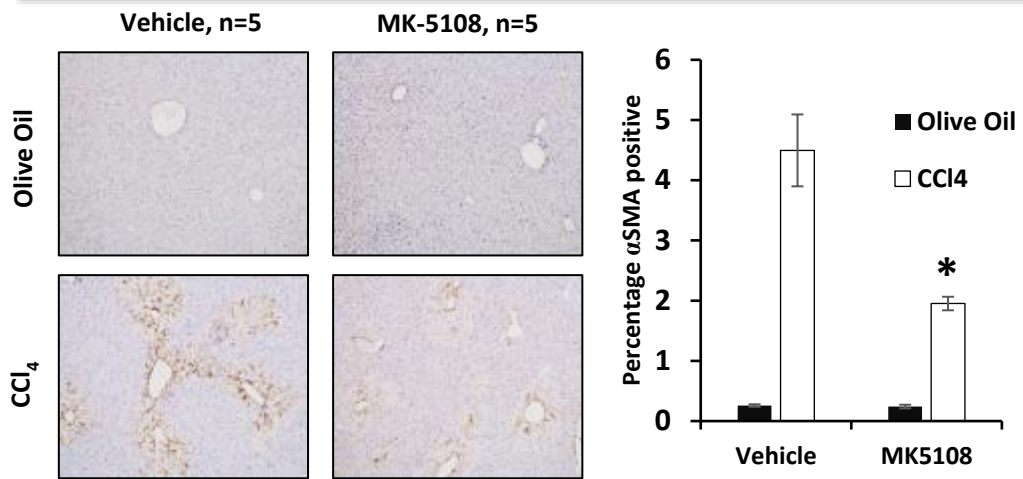
#### ***5.2.4 MK-5108 Reduces $\alpha$ -SMA Accumulation in Liver Injury in Mice***

After demonstrating MK-5108 has a significant effect in reducing  $\alpha$ -SMA expression in the UUO model, the effect of MK-5108 in a carbon tetrachloride-induced model of acute liver injury was examined, to determine whether MK-5108 could reduce the number of  $\alpha$ -SMA positive myofibroblasts in the early stages of wound healing, prior to the process of fibrotic Collagen deposition. Immunohistochemistry revealed a significant accumulation of  $\alpha$ -SMA in the livers of mice 3 days after a single injection of carbon tetrachloride, compared to control mice that received the olive oil vehicle (Figure 5.5A). Mice treated with a daily dose of MK-5108 at 45mg/kg demonstrated a significant 60% reduction in  $\alpha$ -SMA expression compared to carbon tetrachloride treated mice given olive oil vehicle (Figure 5.5A). This result suggests that MK-5108 is involved in the early stages of the wound healing response by either inhibiting accumulation of myofibroblasts or inhibiting their differentiation.

To examine this further, MK-5108 was tested in isolated mouse hepatic stellate cells (HSC), the myofibroblast precursor cells thought to be responsible for liver fibrosis. Culturing HSCs on plastic causes transdifferentiation, characterised by  $\alpha$ -SMA expression. After 7 days in culture, treatment of HSC with 1 $\mu$ M MK-5108 resulted in a significant reduction in  $\alpha$ -SMA expression compared to untreated cells (Figure 5.5B), similar to the data from PRFs. A reduction in Collagen I and III was also observed in HSCs treated with MK-5108 (Figure 5.5C). Furthermore, MK-5108 treatment resulted in inhibition of TGF  $\beta$ -1-induced proliferation of HSCs (Figure 5.5D). These data indicate that the AURKA inhibitor, MK-5108 is capable of inhibiting both transdifferentiation and proliferation of HSCs, which is likely to account for the reduction in  $\alpha$ -SMA expression observed in the carbon-tetrachloride mice treated with MK-5108.

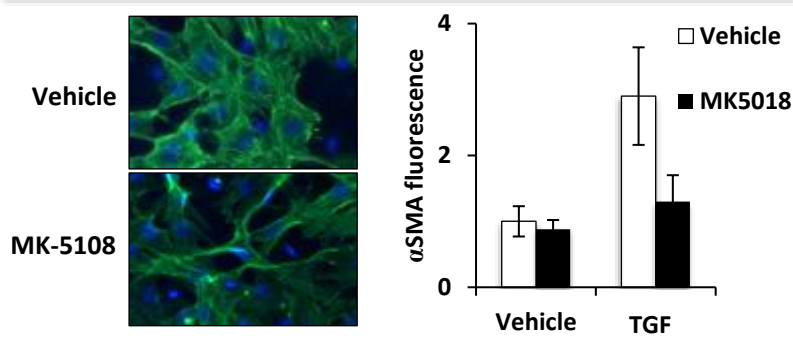
A

CCL<sub>4</sub> mice,  $\alpha$ -SMA IHC



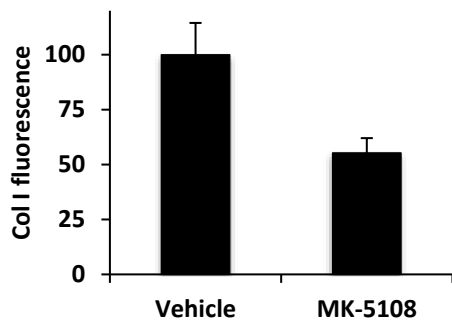
B

HSC differentiation,  $\alpha$ -SMA IF

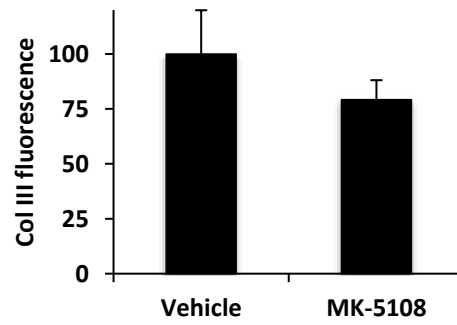


C

HSC differentiation, Collagen I, IF



HSC differentiation, Collagen III, IF



D

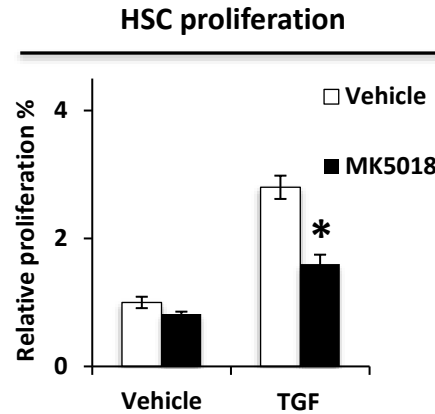


**Figure 5.5. MK-5108 Prevents  $\alpha$ -SMA Accumulation and HSC Proliferation in CCl<sub>4</sub> Mice.** (A) Mice received a single injection of carbon tetrachloride (CCl<sub>4</sub>) or olive oil vehicle, on day 1, in an acute model of liver injury to stimulate  $\alpha$ -SMA expression. They then received daily oral doses of MK-5108 or methylcellulose vehicle, starting on day 1, and were sacrificed on day 3. Liver tissues were stained for  $\alpha$ -SMA by IHC prior to automated analysis of staining as described previously. Graph represents percentage positive staining. (B) HSC isolated from 3 mouse livers were allowed to adhere to glass chamber slides prior to addition of 1 $\mu$ M MK-5108, 5ng/ml TGF  $\beta$ -1, or DMSO vehicle for 72 hours then indirect immunofluorescence for  $\alpha$ -SMA. Graph represents fold-change in fluorescence over DMSO vehicle treated cells. Representative data from one of three animals is shown. \*  $p < 0.05$ , ANOVA. (C) HSC cultured in glass chamber slides were exposed to TGF  $\beta$ -1 and 1 $\mu$ M MK-5108 or DMSO vehicle for 72 hours prior to indirect immunofluorescence for Collagen I and Collagen III as shown. Representative data, from one mouse are shown. Values are represented as fluorescence as percentage of TGF  $\beta$ -1-treated cells. \*  $p < 0.05$ , ANOVA. (D) HSCs isolated from mouse livers were allowed to adhere to 96-well plates prior to the addition of 10 $\mu$ M MK-5108, 5ng/ml TGF  $\beta$ -1, or DMSO vehicle for 72 hours then WST-1 proliferation assays performed. Representative data from one of three animals is shown. \*  $p < 0.05$ , t-test. Error bars represent SD, throughout Figure 4. \*  $p < 0.05$ , t-test.

### 5.3 Discussion

AURKs are essential for the regulation of mitosis and are known to be overexpressed in several cancers (Vader and Lens, 2008). AURKA overexpression is a result of gene amplification, transcriptional induction or post-translational stabilisation (Farruggio *et al.*, 1999). AURK inhibitors have been developed as anti-cancer drugs and have been shown to disrupt the cell cycle, inhibit proliferation and induce apoptosis in rapidly dividing tumour cells but comparatively, AURK inhibitors have little effect on normal cells (Harrington *et al.*, 2004). Similarly, AURK inhibitors selectively reduce proliferation of activated PRF cells and induce apoptosis but have little effect on PTCs. AURKA has been shown to interact with and phosphorylate p53 regulating its functional activity by two mechanisms; phosphorylation of serine-315 of p53 facilitating its degradation in cancer cells (Katayama *et al.*, 2004) and phosphorylation of serine-215 inactivating its transcriptional activity (Liu *et al.*, 2004). AURKA over-expression results in increased phosphorylation of p53 leading to suppression of apoptosis in cancer cells. Additionally, AURKA enhances phosphorylation of AKT, a pro-

proliferative kinase that promotes cell survival and inhibits apoptosis (Khwaja, 1999).

Therefore, it seems that cells undergoing aberrant proliferation become dependent on the cell cycle regulator AURKA for survival and so over-expression of AURKA has made it an attractive focus for drug discovery. The anti-proliferative activity of AURK inhibitors make them an attractive therapeutic in the treatment of diseases that are characterised by aberrant cell proliferation such as cancer and fibrosis (Harrington *et al.*, 2004; Tang *et al.*, 2017). It remains to be seen whether AURKA targets p53 or AKT in renal fibroblasts.

AURKA has been shown to induce EMT *in vitro* and *in vivo* in cancer cells (Wan *et al.*, 2008; Beltran *et al.*, 2011), promoting a mesenchymal phenotype, resulting in a reduction in E-cadherin expression and an increase in Vimentin expression (D'Assoro *et al.*, 2014). It is possible AURKA inhibitors might therefore inhibit EMT. Here, MK-5108 was shown to inhibit transdifferentiation of PRFs and HSCs. Inhibition of transdifferentiation of PRFs and HSCs by MK-5108 could be explained through the model in which AURKA phosphorylates SMAD3 resulting in transdifferentiation. Both the anti-proliferative activity and inhibition of transdifferentiation by AURKA inhibitors, particularly MK-5108, make AURKA a potential anti-fibrotic target for the treatment of CKD.

SMAD3 is phosphorylated at the C-terminus at serine 423/425 by ALK in response to TGF  $\beta$ -1, leading to direct interaction with SMAD4, and translocation of SMAD3 to the nucleus to promote gene transcription favouring transdifferentiation. Here, AURKA silencing by siRNA or MK-5108 also reduced SMAD3 phosphorylation in PRF cells. This is supported by the *in vitro* kinase assay which showed that AURKA is able to directly phosphorylate SMAD3 in response to TGF  $\beta$ -1. SMAD3 can be phosphorylated independently of TGF  $\beta$ -1 by kinases other than ALK5, suggesting that there is a role for other kinases such as AURKA in the phosphorylation of SMAD3 and regulation of TGF  $\beta$ -1 signalling (Li *et al.*, 2004; Wang *et al.*, 2009). For example, PAK4 is a kinase that has been shown to phosphorylate serine 423 of SMAD3 (Wang *et al.*, 2014). The exact mechanism by which ALK5 and AURKA can both phosphorylate SMAD3 in response to TGF  $\beta$ -1 remains to be established.

Whether AURKA is capable of phosphorylating additional residues of SMAD3 and whether AURKA can phosphorylate SMAD3 in other cell types remains to be established. The liver injury data indicates that AURKA could be involved in the early stages of wound healing, during myofibroblast activation and proliferation, preceding Collagen deposition. Due to time restraints, Collagen deposition in a longer-term liver fibrosis model was not examined but it is likely that treatment with MK-5108 would reduce Collagen deposition and inhibit fibrosis, as

shown in the UUO model. It remains unclear whether MK-5108 may affect normal wound healing, which should be tested.

In renal fibrosis, the source of myofibroblasts has been widely debated with suggestions that they can be derived from a number of precursor cell types including resident renal fibroblasts, BMDC, pericytes and epithelial cells (Sun *et al.*, 2016). It is therefore unknown whether AURKA inhibition has the same effects in these myofibroblast precursor cells. In all, the data presented indicates that AURKA is an attractive therapeutic target in the treatment of CKD.

## Chapter 6. Final Discussion

### 6.1 Overall Discussion

CKD is a worldwide socioeconomic health problem with very limited therapeutic options. There is a vital need for greater understanding of the molecular mechanisms driving CKD in order to rectify this unmet clinical need. Renal fibrosis, characterised by the aberrant expression of ECM proteins, forming scar tissue is the histological endpoint of almost all forms of CKD. Anti-fibrotic drugs should therefore find clinical utility in the future treatment of CKD.

TGF  $\beta$ -1/SMAD3 is the major signalling pathway in renal fibrosis. Much research has focussed on targeting TGF  $\beta$ -1, for example with the development of blocking antibodies. Several clinical studies using anti-TGF  $\beta$ -1 antibodies have been undertaken in patients with kidney disease. Although some early promising results were seen, a Phase II study was prematurely terminated due to lack of efficacy (Trachtman *et al.*, 2011; Science, 2015). Another alternative approach to TGF  $\beta$ -1 inhibition using ALK5 inhibitors has shown to be effective in liver and kidney mouse models of fibrosis (de Gouville *et al.*, 2005; Moon *et al.*, 2006). Clinical studies of these drugs are ongoing in patients with advanced cancer but they have not yet been tested in patients with kidney disease (Rodon *et al.*, 2015). In summary, targeting TGF  $\beta$ -1 directly has not demonstrated any clinical patient benefit to-date (Klinkhammer *et al.*, 2017). Because TGF  $\beta$ -1 is involved in so many essential biological processes such as immune regulation, cancer surveillance and glomerular defence against inflammation during injury (Kitamura and Fine, 1999) the development of clinically useful anti-TGF  $\beta$ -1 therapies that do not have detrimental effect on homeostasis is a major challenge.

Several SMAD3 inhibitors have been developed and have demonstrated some success in mouse models; the SMAD3 inhibitor SIS3 was shown to reduce renal fibrosis in a diabetic nephropathy mouse model and an inhibitor of SMAD3 phosphorylation, GQ5, reduced fibrosis in a UUO mouse model (Li *et al.*, 2010; Ai *et al.*, 2015). SMAD3 deficiency is not lethal to mice, unlike TGF  $\beta$ -1 deficient mice that die within 3-4 weeks after birth from uncontrolled inflammation (Bommireddy *et al.*, 2003). SMAD3 might therefore represent a more viable target to inhibit renal fibrosis in CKD without the undesirable side-effects of complete TGF  $\beta$ -1 inhibition (Goumans and Mummery, 2000). To-date however, no inhibitory SMAD3 compounds have been used clinically. One approach to inhibit the

function of SMAD3 has been to target SMAD3 indirectly, through SMAD3 co-factors which have a role in the regulation of TGF  $\beta$ -1 signalling. The research presented here has focussed on the identification and validation of such co-regulatory proteins in CKD.

Previous studies have identified a role for lysine methyltransferase dysregulation in human disease. For example, the lysine methyltransferase, SET9, has been shown to be overexpressed in prostate cancer and is important in activating the androgen receptor (AR), a key transcription factor in prostate cancer development (Gaughan *et al.*, 2011). SET9 has also been shown to have a role in renal fibrosis; silencing SET9 significantly attenuated renal fibrosis in UUO mice (Sasaki *et al.*, 2016). Given these previous findings the role of SET9 and other methyltransferases in the regulation of TGF  $\beta$ -1 signalling in renal fibrosis was examined.

SET9 has been previously found to interact with transcription factors AR and ER at the N terminus and has been shown to directly methylate lysines within a conserved KKLKK motif (Subramanian *et al.*, 2008; Gaughan *et al.*, 2011). This work demonstrated an interaction with SMAD3 at the N terminus which harbours a KKLKK motif, suggesting that SET9 might also methylate SMAD3 at this conserved motif to regulate SMAD3. Mass spectrometry and *in vitro* methylation assays performed during the course of this research, failed to show methylation of SMAD3 by SET9. Nevertheless, SET9 was found to directly regulate SMAD3 protein stability and nuclear import, which required the methyltransferase activity of SET9. Cells transfected with a methyltransferase-deficient SET9 mutant showed increased SMAD3 protein turnover, increased ubiquitylation and reduced nuclear translocation of SMAD3 compared to the wild-type SET9. This suggests that a SET9 methylation event might indirectly regulate SMAD3 in order to regulate its activity. This work has shown SET9 is recruited to the *ACTA2* gene promoter by SMAD3, in response to TGF  $\beta$ -1 which is likely to result in SET9 methylation at the *ACTA2* gene promoter leading to upregulation of gene expression. Similar to previous studies showing SET9 recruitment to the pro-fibrotic gene promoters *Colla1*, *CTGF*, and *PAI-1*, in response to TGF  $\beta$ -1, resulting in increased H3K4 methylation at these gene promoters and increased transcriptional activity of these ECM-associated genes (Sun *et al.*, 2010).

Lysine methyltransferases have been shown to exert different effects depending on the type of methylation and/or their substrate. SET9 has been shown to increase the transcriptional activity of transcription factors including AR, ER and p53. The work presented here has demonstrated that SET9 also interacts with SMAD3, to enhance its transcriptional activity,

enhancing the pro-fibrotic activity of TGF  $\beta$ -1. In contrast, SET9 can also interact with SMAD7, an inhibitory SMAD, at the C terminal domain, targeting it for ubiquitylation-dependent degradation (Elkouris *et al.*, 2016). This demonstrates that SET9 can both positively and negatively regulate the transcriptional activity of different SMAD substrates. In this case, the upregulation of SMAD3 and the downregulation of SMAD7 both result in increased TGF  $\beta$ -1 signalling in renal fibrosis, further supporting the important regulatory role of SET9 in TGF  $\beta$ -1 signalling.

Another lysine methyltransferase SETDB1, is known to methylate H3K9 which is usually associated with transcriptional repression. SETDB1 is found to be upregulated in cancers such as hepatocellular carcinoma and breast cancer (Wong *et al.*, 2016; Du *et al.*, 2018) and therefore inhibition of SETDB1 could be useful in the treatment of these cancers. Conversely, the work shown here has demonstrated that SETDB1 acts as a co-repressor of SMAD3 in TGF  $\beta$ -1 signalling and its inhibition enhanced expression of pro-fibrotic markers in PRFs. These data showed suppression of SETDB1 enhanced migration and contractility of PRF cells, whereas, other research showed SETDB1 expression is upregulated in glioma cell lines and tissues and suppression of SETDB1 resulted in reduced migration of glioma cells (Spyropoulou *et al.*, 2014). This suggests that SETDB1 might have opposing roles, depending upon cell type or disease context.

This work has found migration and Collagen contractility of PRFs, both critical processes in fibrosis, are dependent upon SET9. In contrast, SETDB1 seems to act as a brake on these processes suggesting that lysine methyltransferases add an extra level of transcriptional regulation upon signalling pathways in fibrosis. More research needs to be undertaken to identify additional methyltransferases and their roles in signalling pathways and human disease.

SET9 inhibition by R-PFI-2 was effective in reducing pro-fibrotic marker expression and significantly reducing migration and contractility of PRFs, suggesting that SET9 is a valid target for the treatment of CKD. The effect of R-PFI-2 inhibitor is yet to be explored in mouse models of disease and therefore its dosage, efficacy and tolerability remain unknown. The development of other SET9 inhibitors such as DC-S238 and DC-239 is ongoing but no compound to-date has been tested in mice (Meng *et al.*, 2015a). SET9-deficient mice have a normal phenotype, which suggest that the specific SET9 inhibitor R-PFI-2 could have only negligible side-effects. However, studies of this inhibitor in mice will first enable us to

determine the effect of pharmacological inhibition of SET9 with respect to other TGF  $\beta$ -1 driven processes such as normal wound healing.

Targeting DNA and histone methylation in disease is a newly emerging field. Recently, compounds targeting histone methylation, such as an EZH2 inhibitor have entered clinical trials for cancer treatment (Morera *et al.*, 2016). Interestingly, EZH2 is a lysine methyltransferase that was identified as a potential hit by Z-score analysis from the siRNA methyltransferase screens, further indicating the important role these enzymes play in disease identifying them as attractive targets for the treatment in human disease. The accumulative effect of inhibiting several methyltransferases that upregulate TGF  $\beta$ -1 signalling in PRFs may present the best approach to reduce renal fibrosis.

It would be interesting to identify additional substrates for methylation in the TGF  $\beta$ -1/SMAD3 signalling pathway, for example by mass spectrometry. Further identification of the role of lysine methylation in the TGF  $\beta$ -1 pathway might aid the identification of additional potential therapeutic targets for the treatment of CKD.

By performing a HTS of 283 small molecule inhibitors in PRF cells, 10 AURK inhibitors were found to significantly reduce PRF proliferation. This work demonstrated that AURK inhibitors selectively inhibit proliferation and induce apoptosis in PRFs but have little effect on tubular cells. Rapidly dividing cells seem to become dependent on AURKA activity for survival making them an attractive target for AURKA inhibition (Dar *et al.*, 2010). AURKA inhibitor, MK-5108 also demonstrated a reduction in transdifferentiation of PRFs and HSCs. This work demonstrated that AURKA directly phosphorylates the C-terminus of SMAD3 at Serine 423/5 in response to TGF  $\beta$ -1 in PRFs. Treatment with MK-5108 inhibited this phosphorylation and reduced transdifferentiation of PRFs and HSCs. A significant reduction in  $\alpha$ -SMA, Collagen I and III, and total Collagen in UUO mice was observed upon MK-5108 treatment and similarly a reduction in these markers was observed in the liver injury mouse model upon MK-5108 treatment. A longer-term liver fibrosis model was not pursued due to time restraints but it is likely that a reduction in liver fibrosis would occur upon MK-5108, given the effects upon  $\alpha$ -SMA positive cells in the liver. Additionally, MK-5108 has been tested in clinical trials as an anti-cancer drug where it demonstrated effective anti-proliferative activity and has been found to be very well tolerated with minimal toxicity, further raising the prospect of AURKA as a therapeutic target in renal fibrosis (Amin *et al.*, 2016).

This research has demonstrated that there are unidentified co-factors involved in the regulation of the TGF  $\beta$ -1/SMAD3 pathway. Novel roles for SET9, SETDB1 and AURKA in the regulation of TGF  $\beta$ -1 signalling in renal fibrosis have been identified, illustrated in Figure 6.1.

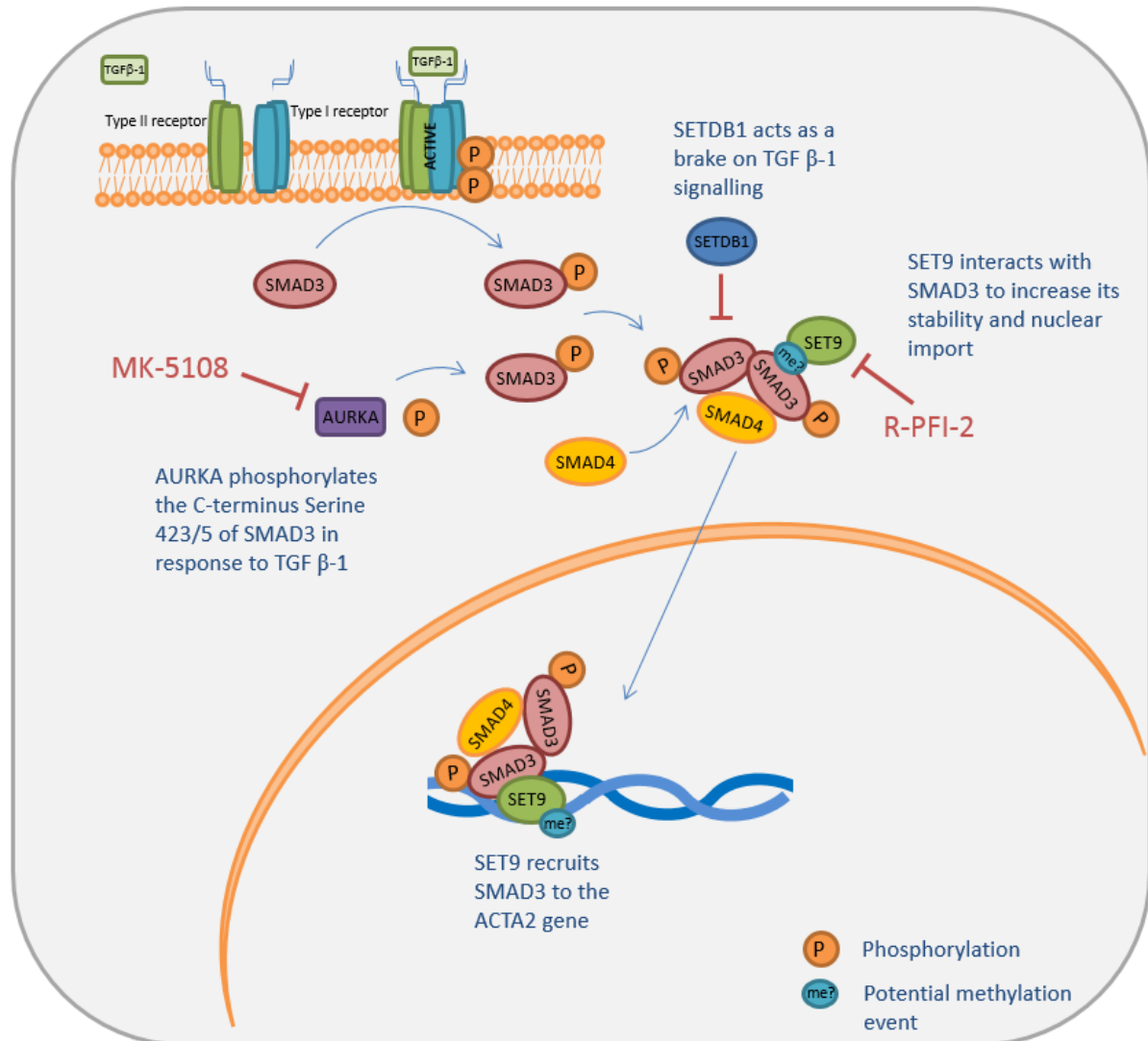


**Figure 6.1. Illustration of novel roles identified for SET9, SETDB1 and Aurora Kinase A in the TGF  $\beta$ -1 /SMAD3 signalling pathway in renal fibrosis.** SET9 interacts with SMAD3 to increase its stability and aid its nuclear translocation. SETDB1 interacts with SMAD3, acting as a brake on TGF  $\beta$ -1/SMAD3 signalling. Aurora Kinase A directly phosphorylates SMAD3 in response to TGF  $\beta$ -1.

All three proteins have been previously linked with cancer, showing upregulated expression in several human cancers. Cancer and fibrosis have many characteristics in common such as aberrant signalling resulting in uncontrolled cell proliferation and therefore these proteins may share common roles between these two diseases.

Both R-PFI-2 and MK-5108 have shown to be effective in reducing TGF  $\beta$ -1/SMAD3 signalling resulting in a significant reduction in pro-fibrotic markers and therefore could provide promising treatments for renal fibrosis. Although effective in reducing fibrosis whether these inhibitors have a detrimental effect to normal wound healing must be explored.

Another question which must be answered is what is the wider effect of targeting TGF  $\beta$ -1/SMAD3 signalling; such a central signalling pathway in many biological processes. Are the co-regulators we have identified in this pathway specific to PRFs or could the use of these inhibitors effect other cell types and biological processes?

## 6.2 Future Directions

Futher work should be undertaken to decipher the exact mechanism by which SET9 regulates SMAD3 in TGF  $\beta$ -1 signalling in renal fibrosis. Whether it is direct methylation of SMAD3 or of H3K4 at the *ACTA2* gene promoter or whether it is just the direct interaction of SET9 with SMAD3 that enables it to regulate SMAD3 function. This could be determined by the use of further methylation assays and mass spectrometry. ChIP could also be performed using an antibody against H3K4me to determine if this methylation is reduced upon SET9 knockdown at the *ACTA2* promoter. Additionally, it would be useful to perform mutagenesis on SMAD3, to introduce mutations in the lysine residues of the KKLKK motif to determine whether this would effect the interaction with SET9 and SMAD3 function.

Similarly it should be determined whether SETDB1 is also acting through its methyltransferase activity with the use of similar experiments. It would also be interesting to identify whether there are any additional SETDB1 substrates to regulate TGF  $\beta$ -1 signalling, other than SMAD3 that could be exploited as additional novel targets.

R-PFI-2 demonstrated a significant reduction in migration of PRFs, therefore it is critical to understand the effect of SET9 inhibition on normal wound healing. It would be useful to test R-PFI-2 in a UUO mouse model to determine its effect on the early developmental stages of renal fibrosis and any potential off-target effects.

To further the work on MK-5108, testing it in a longer-term liver fibrosis model would be advantageous to determine whether it has the same significant effect in reducing fibrosis in the liver as we have observed in the kidney. The effect of MK-5108 on normal wound healing must also be explored.

Finally, further siRNA and compound screening utilising our newly established PRF cell model should be undertaken for the identification of additional novel targets in TGF  $\beta$ -1 signalling to aid the discovery of much needed alternative therapeutics in renal fibrosis and CKD.

## List of Publications and Presentations

### Published Manuscripts

1. Shuttleworth, V.G., Gaughan, L., Nawafa, L., Mooney, C.A., Cobb, S.L., Sheerin, N.S. and Logan, I.R. (2018) 'The Methyltransferase SET9 Regulates TGFB1 Activation of Renal Fibroblasts via Interaction with SMAD3', *J Cell Sci*, 131(1).

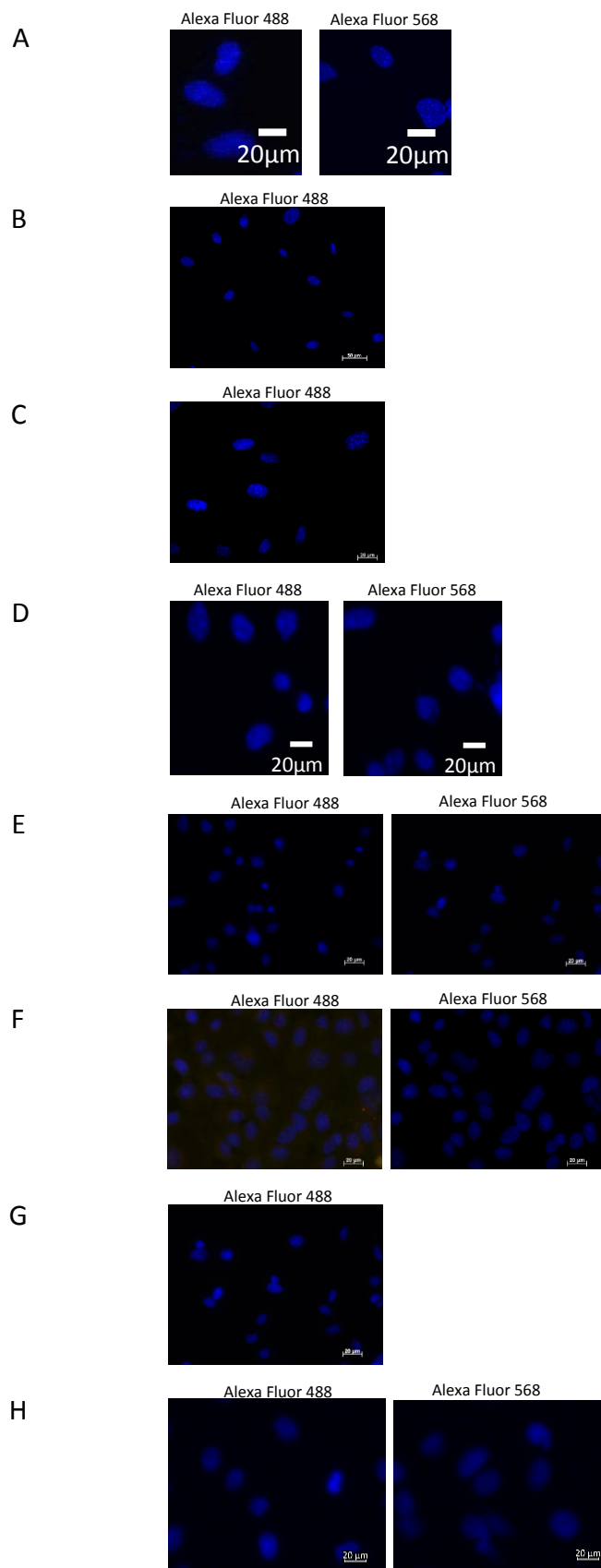
### Manuscripts in Preparation for Publication

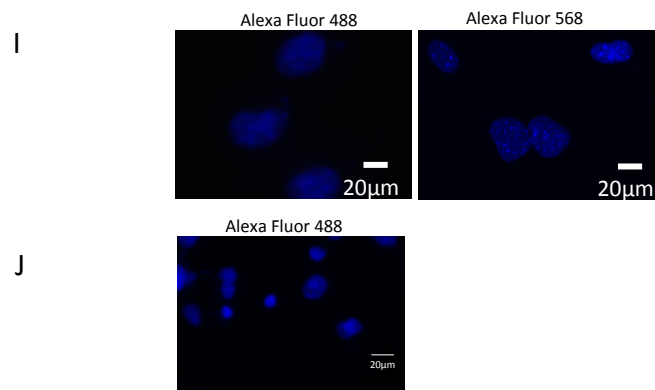
1. Shuttleworth V.G., Moles A., Ng S.W., Situmorang G., Luli S., Leslie J., Gaughan L., Fiona Oakley F., Neil S Sheerin N.S., Logan I.R. 'Aurora Kinase A Promotes Renal Fibrosis through TGFB-1 Signalling in Myofibroblasts' (submitted for publication in *Journal of The American Society of Nephrology*).
2. Shuttleworth V.G., Logan I.R., Sheerin N.S. 'The Role of Methyltransferase SETDB1 in TGFB-1 Signalling in Renal Fibroblasts'. (manuscript in preparation)
3. Shuttleworth V.G., Logan I.R., Sheerin N.S. 'Wound Healing and Collagen Contractility Assays using Primary Renal Fibroblasts' (manuscript in preparation to be submitted December 2018 to *Journal of Visualized Experiments*).

### Oral and Poster Presentations

1. Shuttleworth V.G., Logan I.R., Sheerin N.S. (2018). 'The Role of Methyltransferase SETDB1 in Chronic Kidney Disease'. Poster Presentation at UK Kidney Week (UKKW), Harrogate Conference Centre, Harrogate, United Kingdom.
2. Shuttleworth V.G., Logan I.R., Sheerin N.S. (2018). 'The Role of Methyltransferase SETDB1 in Chronic Kidney Disease'. Oral Presentation at Institute of Cellular Medicine Director's Day, Newcastle University, Newcastle Upon Tyne, United Kingdom.
3. Shuttleworth V.G., Logan I.R., Sheerin N.S. (2018). 'Methyltransferases as Therapeutic Targets in Renal Fibrosis'. Oral Presentation at Institute of Cellular Medicine Meeting, Newcastle University, Newcastle Upon Tyne, United Kingdom.

# Appendix





**Appendix Figure 1. Immunofluorescence Negative Control Slides.** Negative control immunofluorescence slides stained with secondary Alexa Fluor antibodies only, as indicated, did not exhibit fluorescence. (A) Figure 3.3A (B) Figure 3.6 (C) Figure 3.10 D, E (D) Figure 3.12C (E) Figure 4.2A (F) Figure 4.3C (G) Figure 4.3D (H) Figure 4.4C (I) Figure 5.2B, C (J) Figure 5.5B.

## Bibliography

- Adler, S.G., Schwartz, S., Williams, M.E., Arauz-Pacheco, C., Bolton, W.K., Lee, T., Li, D., Neff, T.B., Urquilla, P.R. and Sewell, K.L. (2010) 'Phase 1 study of anti-CTGF monoclonal antibody in patients with diabetes and microalbuminuria', *Clin J Am Soc Nephrol*, 5(8), pp. 1420-8.
- Ai, J., Nie, J., He, J., Guo, Q., Li, M., Lei, Y., Liu, Y., Zhou, Z., Zhu, F., Liang, M., Cheng, Y. and Hou, F.F. (2015) 'GQ5 Hinders Renal Fibrosis in Obstructive Nephropathy by Selectively Inhibiting TGF-beta-Induced Smad3 Phosphorylation', *J Am Soc Nephrol*, 26(8), pp. 1827-38.
- Amin, M., Minton, S.E., LoRusso, P.M., Krishnamurthi, S.S., Pickett, C.A., Lunceford, J., Hille, D., Mauro, D., Stein, M.N., Wang-Gillam, A., Trull, L. and Lockhart, A.C. (2016) 'A phase I study of MK-5108, an oral aurora a kinase inhibitor, administered both as monotherapy and in combination with docetaxel, in patients with advanced or refractory solid tumors', *Invest New Drugs*, 34(1), pp. 84-95.
- Angelov, D., Vitolo, J.M., Mutskov, V., Dimitrov, S. and Hayes, J.J. (2001) 'Preferential interaction of the core histone tail domains with linker DNA', *Proc Natl Acad Sci U S A*, 98(12), pp. 6599-604.
- Arnold, J.J., Hayer, M., Sharif, A., Begaj, I., Tabriez, M., Bagnall, D., Ray, D., Hoye, C., Nazir, M., Dutton, M., Fifer, L., Kirkham, K., Sims, D., Townend, J.N., Gill, P.S., Dasgupta, I., Cockwell, P. and Ferro, C.J. (2015) 'Acute Care QUALiTy in chronic Kidney disease (ACQUATIK): a prospective cohort study exploring outcomes of patients with chronic kidney disease', *BMJ Open*, 5(4), p. e006987.
- Bannister, A.J., Zegerman, P., Partridge, J.F., Miska, E.A., Thomas, J.O., Allshire, R.C. and Kouzarides, T. (2001) 'Selective recognition of methylated lysine 9 on histone H3 by the HP1 chromo domain', *Nature*, 410(6824), pp. 120-4.
- Beltran, H., Rickman, D.S., Park, K., Chae, S.S., Sboner, A., MacDonald, T.Y., Wang, Y., Sheikh, K.L., Terry, S., Tagawa, S.T., Dhir, R., Nelson, J.B., de la Taille, A., Allory, Y., Gerstein, M.B., Perner, S., Pienta, K.J., Chinnaiyan, A.M., Wang, Y., Collins, C.C., Gleave, M.E., Demichelis, F., Nanus, D.M. and Rubin, M.A. (2011) 'Molecular characterization of neuroendocrine prostate cancer and identification of new drug targets', *Cancer Discov*, 1(6), pp. 487-95.

- Benchetrit, S., Yarkoni, S., Rathaus, M., Pines, M., Rashid, G., Bernheim, J. and Bernheim, J. (2007) 'Halofuginone reduces the occurrence of renal fibrosis in 5/6 nephrectomized rats', *Isr Med Assoc J*, 9(1), pp. 30-4.
- Bischoff, J.R., Anderson, L., Zhu, Y., Mossie, K., Ng, L., Souza, B., Schryver, B., Flanagan, P., Clairvoyant, F., Ginther, C., Chan, C.S., Novotny, M., Slamon, D.J. and Plowman, G.D. (1998) 'A homologue of *Drosophila aurora* kinase is oncogenic and amplified in human colorectal cancers', *Embo j*, 17(11), pp. 3052-65.
- Black, H.R., Bakris, G.L., Weber, M.A., Weiss, R., Shahawy, M.E., Marple, R., Tannoury, G., Linas, S., Wiens, B.L., Linseman, J.V., Roden, R. and Gerber, M.J. (2007) 'Efficacy and safety of darusentan in patients with resistant hypertension: results from a randomized, double-blind, placebo-controlled dose-ranging study', *J Clin Hypertens (Greenwich)*, 9(10), pp. 760-9.
- Bommireddy, R., Saxena, V., Ormsby, I., Yin, M., Boivin, G.P., Babcock, G.F., Singh, R.R. and Doetschman, T. (2003) 'TGF-beta 1 regulates lymphocyte homeostasis by preventing activation and subsequent apoptosis of peripheral lymphocytes', *J Immunol*, 170(9), pp. 4612-22.
- Bottinger, E.P. and Bitzer, M. (2002) 'TGF-beta signaling in renal disease', *J Am Soc Nephrol*, 13(10), pp. 2600-10.
- Branski, R.C., Bing, R., Kraja, I. and Amin, M.R. (2016) 'The role of Smad3 in the fibrotic phenotype in human vocal fold fibroblasts', *Laryngoscope*, 126(5), pp. 1151-6.
- Ceol, C.J., Houvras, Y., Jane-Valbuena, J., Bilodeau, S., Orlando, D.A., Battisti, V., Fritsch, L., Lin, W.M., Hollmann, T.J., Ferre, F., Bourque, C., Burke, C.J., Turner, L., Uong, A., Johnson, L.A., Beroukhim, R., Mermel, C.H., Loda, M., Ait-Si-Ali, S., Garraway, L.A., Young, R.A. and Zon, L.I. (2011) 'The histone methyltransferase SETDB1 is recurrently amplified in melanoma and accelerates its onset', *Nature*, 471(7339), pp. 513-7.
- Chevalier, R.L., Forbes, M.S. and Thornhill, B.A. (2009) 'Ureteral obstruction as a model of renal interstitial fibrosis and obstructive nephropathy', *Kidney Int*, 75(11), pp. 1145-52.
- Cho, M.E., Smith, D.C., Branton, M.H., Penzak, S.R. and Kopp, J.B. (2007) 'Pirfenidone slows renal function decline in patients with focal segmental glomerulosclerosis', *Clin J Am Soc Nephrol*, 2(5), pp. 906-13.
- Chuikov, S., Kurash, J.K., Wilson, J.R., Xiao, B., Justin, N., Ivanov, G.S., McKinney, K., Tempst, P., Prives, C., Gamblin, S.J., Barlev, N.A. and Reinberg, D. (2004) 'Regulation of p53 activity through lysine methylation', *Nature*, 432(7015), pp. 353-60.

- Chung, A.C., Zhang, H., Kong, Y.Z., Tan, J.J., Huang, X.R., Kopp, J.B. and Lan, H.Y. (2010) 'Advanced glycation end-products induce tubular CTGF via TGF-beta-independent Smad3 signaling', *J Am Soc Nephrol*, 21(2), pp. 249-60.
- D'Assoro, A.B., Liu, T., Quatraro, C., Amato, A., Opyrchal, M., Leontovich, A., Ikeda, Y., Ohmine, S., Lingle, W., Suman, V., Ecsedy, J., Iankov, I., Di Leonardo, A., Ayers-Inglers, J., Degnim, A., Billadeau, D., McCubrey, J., Ingle, J., Salisbury, J.L. and Galanis, E. (2014) 'The mitotic kinase Aurora-a promotes distant metastases by inducing epithelial-to-mesenchymal transition in ERalpha(+) breast cancer cells', *Oncogene*, 33(5), pp. 599-610.
- Damodaran, A.P., Vaufrey, L., Gavard, O. and Prigent, C. (2017) 'Aurora A Kinase Is a Priority Pharmaceutical Target for the Treatment of Cancers', *Trends Pharmacol Sci*, 38(8), pp. 687-700.
- Dar, A.A., Goff, L.W., Majid, S., Berlin, J. and El-Rifai, W. (2010) 'Aurora kinase inhibitors-rising stars in cancer therapeutics?', *Mol Cancer Ther*, 9(2), pp. 268-78.
- de Gouville, A.C., Boullay, V., Krysa, G., Pilot, J., Brusq, J.M., Lorient, F., Gauthier, J.M., Papworth, S.A., Laroze, A., Gellibert, F. and Huet, S. (2005) 'Inhibition of TGF-beta signaling by an ALK5 inhibitor protects rats from dimethylnitrosamine-induced liver fibrosis', *Br J Pharmacol*, 145(2), pp. 166-77.
- Denton, C.P., Merkel, P.A., Furst, D.E., Khanna, D., Emery, P., Hsu, V.M., Silliman, N., Streisand, J., Powell, J., Akesson, A., Coppock, J., Hoogen, F., Herrick, A., Mayes, M.D., Veale, D., Haas, J., Ledbetter, S., Korn, J.H., Black, C.M. and Seibold, J.R. (2007) 'Recombinant human anti-transforming growth factor beta1 antibody therapy in systemic sclerosis: a multicenter, randomized, placebo-controlled phase I/II trial of CAT-192', *Arthritis Rheum*, 56(1), pp. 323-33.
- Derynck, R. and Zhang, Y.E. (2003) 'Smad-dependent and Smad-independent pathways in TGF-beta family signalling', *Nature*, 425(6958), pp. 577-84.
- Dhaun, N., Goddard, J. and Webb, D.J. (2006) 'The endothelin system and its antagonism in chronic kidney disease', *J Am Soc Nephrol*, 17(4), pp. 943-55.
- Dhayalan, A., Kudithipudi, S., Rathert, P. and Jeltsch, A. (2011) 'Specificity analysis-based identification of new methylation targets of the SET7/9 protein lysine methyltransferase', *Chem Biol*, 18(1), pp. 111-20.
- Dillon, S.C., Zhang, X., Trievel, R.C. and Cheng, X. (2005) 'The SET-domain protein superfamily: protein lysine methyltransferases', *Genome Biol*, 6(8), p. 227.
- Dobaczewski, M., Bujak, M., Li, N., Gonzalez-Quesada, C., Mendoza, L.H., Wang, X.F. and Frangogiannis, N.G. (2010) 'Smad3 signaling critically regulates fibroblast phenotype and function in healing myocardial infarction', *Circ Res*, 107(3), pp. 418-28.

- Dooley, S., Hamzavi, J., Breitkopf, K., Wiercinska, E., Said, H.M., Lorenzen, J., Ten Dijke, P. and Gressner, A.M. (2003) 'Smad7 prevents activation of hepatic stellate cells and liver fibrosis in rats', *Gastroenterology*, 125(1), pp. 178-91.
- Drake, R.L., Vogl, W. and Mitchell, A.W.M. (2009) *Gray's Anatomy For Students*. 2nd edn. Churchill Livingstone.
- Du, D., Katsuno, Y., Meyer, D., Budi, E.H., Chen, S.H., Koeppen, H., Wang, H., Akhurst, R.J. and Derynck, R. (2018) 'Smad3-mediated recruitment of the methyltransferase SETDB1/ESET controls Snail1 expression and epithelial-mesenchymal transition', *EMBO Rep*, 19(1), pp. 135-155.
- Dubey, R.K., Jackson, E.K., Rupprecht, H.D. and Sterzel, R.B. (1997) 'Factors controlling growth and matrix production in vascular smooth muscle and glomerular mesangial cells', *Curr Opin Nephrol Hypertens*, 6(1), pp. 88-105.
- Duffield, J.S. (2014) 'Cellular and molecular mechanisms in kidney fibrosis', *J Clin Invest*, 124(6), pp. 2299-306.
- Duscher, D., Maan, Z.N., Wong, V.W., Rennert, R.C., Januszyk, M., Rodrigues, M., Hu, M., Whitmore, A.J., Whittam, A.J., Longaker, M.T. and Gurtner, G.C. (2014) 'Mechanotransduction and fibrosis', *J Biomech*, 47(9), pp. 1997-2005.
- Ebisawa, T., Fukuchi, M., Murakami, G., Chiba, T., Tanaka, K., Imamura, T. and Miyazono, K. (2001) 'Smurf1 interacts with transforming growth factor-beta type I receptor through Smad7 and induces receptor degradation', *J Biol Chem*, 276(16), pp. 12477-80.
- Eddy, A.A. (1996) 'Molecular insights into renal interstitial fibrosis', *J Am Soc Nephrol*, 7(12), pp. 2495-508.
- Eddy, A.A. (2014) 'Overview of the cellular and molecular basis of kidney fibrosis', *Kidney Int Suppl (2011)*, 4(1), pp. 2-8.
- Egido, J., Rojas-Rivera, J., Mas, S., Ruiz-Ortega, M., Sanz, A.B., Gonzalez Parra, E. and Gomez-Guerrero, C. (2017) 'Atrasentan for the treatment of diabetic nephropathy', *Expert Opin Investig Drugs*, 26(6), pp. 741-750.
- Elkouris, M., Kontaki, H., Stavropoulos, A., Antonoglou, A., Nikolaou, K.C., Samiotaki, M., Szantai, E., Saviolaki, D., Brown, P.J., Sideras, P., Panayotou, G. and Talianidis, I. (2016) 'SET9-Mediated Regulation of TGF-beta Signaling Links Protein Methylation to Pulmonary Fibrosis', *Cell Rep*, 15(12), pp. 2733-44.
- Elliott, R.L. and Blobel, G.C. (2005) 'Role of transforming growth factor Beta in human cancer', *J Clin Oncol*, 23(9), pp. 2078-93.

- Fan, J.M., Ng, Y.Y., Hill, P.A., Nikolic-Paterson, D.J., Mu, W., Atkins, R.C. and Lan, H.Y. (1999) 'Transforming growth factor-beta regulates tubular epithelial-myofibroblast transdifferentiation in vitro', *Kidney Int*, 56(4), pp. 1455-67.
- Farruggio, D.C., Townsley, F.M. and Ruderman, J.V. (1999) 'Cdc20 associates with the kinase aurora2/Aik', *Proc Natl Acad Sci U S A*, 96(13), pp. 7306-11.
- Fei, Q., Shang, K., Zhang, J., Chuai, S., Kong, D., Zhou, T., Fu, S., Liang, Y., Li, C., Chen, Z., Zhao, Y., Yu, Z., Huang, Z., Hu, M., Ying, H., Chen, Z., Zhang, Y., Xing, F., Zhu, J., Xu, H., Zhao, K., Lu, C., Atadja, P., Xiao, Z.X., Li, E. and Shou, J. (2015) 'Histone methyltransferase SETDB1 regulates liver cancer cell growth through methylation of p53', *Nat Commun*, 6, p. 8651.
- Flanders, K.C. (2004) 'Smad3 as a mediator of the fibrotic response', *Int J Exp Pathol*, 85(2), pp. 47-64.
- Flanders, K.C., Sullivan, C.D., Fujii, M., Sowers, A., Anzano, M.A., Arabshahi, A., Major, C., Deng, C., Russo, A., Mitchell, J.B. and Roberts, A.B. (2002) 'Mice lacking Smad3 are protected against cutaneous injury induced by ionizing radiation', *Am J Pathol*, 160(3), pp. 1057-68.
- Fujimoto, M., Maezawa, Y., Yokote, K., Joh, K., Kobayashi, K., Kawamura, H., Nishimura, M., Roberts, A.B., Saito, Y. and Mori, S. (2003) 'Mice lacking Smad3 are protected against streptozotocin-induced diabetic glomerulopathy', *Biochem Biophys Res Commun*, 305(4), pp. 1002-7.
- Fukuchi, M., Imamura, T., Chiba, T., Ebisawa, T., Kawabata, M., Tanaka, K. and Miyazono, K. (2001) 'Ligand-dependent degradation of Smad3 by a ubiquitin ligase complex of ROC1 and associated proteins', *Mol Biol Cell*, 12(5), pp. 1431-43.
- Gao, S., Wang, Z., Wang, W., Hu, X., Chen, P., Li, J., Feng, X., Wong, J. and Du, J.X. (2017) 'The lysine methyltransferase SMYD2 methylates the kinase domain of type II receptor BMPR2 and stimulates bone morphogenetic protein signaling', *J Biol Chem*, 292(30), pp. 12702-12712.
- Gaughan, L., Stockley, J., Wang, N., McCracken, S.R., Treumann, A., Armstrong, K., Shaheen, F., Watt, K., McEwan, I.J., Wang, C., Pestell, R.G. and Robson, C.N. (2011) 'Regulation of the androgen receptor by SET9-mediated methylation', *Nucleic Acids Res*, 39(4), pp. 1266-79.
- GBD 2013 Mortality and Causes of Death Collaborators (2015) 'Global, regional, and national incidence, prevalence, and years lived with disability for 301 acute and chronic diseases and injuries in 188 countries, 1990–2013: a systematic analysis for the Global Burden of Disease Study 2013', *The Lancet*, 386(9995), pp. 743-800.

- Gordon, K.J. and Blobel, G.C. (2008) 'Role of transforming growth factor-beta superfamily signaling pathways in human disease', *Biochim Biophys Acta*, 1782(4), pp. 197-228.
- Goumans, M.J. and Mummery, C. (2000) 'Functional analysis of the TGFbeta receptor/Smad pathway through gene ablation in mice', *Int J Dev Biol*, 44(3), pp. 253-65.
- Grinnell, F., Zhu, M., Carlson, M.A. and Abrams, J.M. (1999) 'Release of mechanical tension triggers apoptosis of human fibroblasts in a model of regressing granulation tissue', *Exp Cell Res*, 248(2), pp. 608-19.
- Grunstein, M., Hecht, A., Fisher-Adams, G., Wan, J., Mann, R.K., Strahl-Bolsinger, S., Laroche, T. and Gasser, S. (1995) 'The regulation of euchromatin and heterochromatin by histones in yeast', *J Cell Sci Suppl*, 19, pp. 29-36.
- Harrington, E.A., Bebbington, D., Moore, J., Rasmussen, R.K., Ajose-Adeogun, A.O., Nakayama, T., Graham, J.A., Demur, C., Hercend, T., Diu-Hercend, A., Su, M., Golec, J.M. and Miller, K.M. (2004) 'VX-680, a potent and selective small-molecule inhibitor of the Aurora kinases, suppresses tumor growth in vivo', *Nat Med*, 10(3), pp. 262-7.
- Heldin, C.H., Miyazono, K. and ten Dijke, P. (1997) 'TGF-beta signalling from cell membrane to nucleus through SMAD proteins', *Nature*, 390(6659), pp. 465-71.
- Hewitson, T.D. and Becker, G.J. (1995) 'Interstitial myofibroblasts in IgA glomerulonephritis', *Am J Nephrol*, 15(2), pp. 111-7.
- Hinz, B., Celetta, G., Tomasek, J.J., Gabbiani, G. and Chaponnier, C. (2001) 'Alpha-smooth muscle actin expression upregulates fibroblast contractile activity', *Mol Biol Cell*, 12(9), pp. 2730-41.
- Hirota, T., Kunitoku, N., Sasayama, T., Marumoto, T., Zhang, D., Nitta, M., Hatakeyama, K. and Saya, H. (2003) 'Aurora-A and an interacting activator, the LIM protein Ajuba, are required for mitotic commitment in human cells', *Cell*, 114(5), pp. 585-98.
- Hu, B., Wu, Z. and Phan, S.H. (2003) 'Smad3 mediates transforming growth factor-beta-induced alpha-smooth muscle actin expression', *Am J Respir Cell Mol Biol*, 29(3 Pt 1), pp. 397-404.
- Hutterer, A., Berdnik, D., Wirtz-Peitz, F., Zigman, M., Schleiffer, A. and Knoblich, J.A. (2006) 'Mitotic activation of the kinase Aurora-A requires its binding partner Bora', *Dev Cell*, 11(2), pp. 147-57.
- Inazaki, K., Kanamaru, Y., Kojima, Y., Sueyoshi, N., Okumura, K., Kaneko, K., Yamashiro, Y., Ogawa, H. and Nakao, A. (2004) 'Smad3 deficiency attenuates renal fibrosis, inflammation, and apoptosis after unilateral ureteral obstruction', *Kidney Int*, 66(2), pp. 597-604.

- Iwano, M., Plieth, D., Danoff, T.M., Xue, C., Okada, H. and Neilson, E.G. (2002) 'Evidence that fibroblasts derive from epithelium during tissue fibrosis', *J Clin Invest*, 110(3), pp. 341-50.
- Jenuwein, T., Laible, G., Dorn, R. and Reuter, G. (1998) 'SET domain proteins modulate chromatin domains in eu- and heterochromatin', *Cell Mol Life Sci*, 54(1), pp. 80-93.
- Kalluri, R. and Neilson, E.G. (2003) 'Epithelial-mesenchymal transition and its implications for fibrosis', *J Clin Invest*, 112(12), pp. 1776-84.
- Kanasaki, K., Taduri, G. and Koya, D. (2013) 'Diabetic nephropathy: the role of inflammation in fibroblast activation and kidney fibrosis', *Front Endocrinol (Lausanne)*, 4, p. 7.
- Kang, H.M., Ahn, S.H., Choi, P., Ko, Y.A., Han, S.H., Chinga, F., Park, A.S., Tao, J., Sharma, K., Pullman, J., Bottinger, E.P., Goldberg, I.J. and Susztak, K. (2015) 'Defective fatty acid oxidation in renal tubular epithelial cells has a key role in kidney fibrosis development', *Nat Med*, 21(1), pp. 37-46.
- Katayama, H., Sasai, K., Kawai, H., Yuan, Z.M., Bondaruk, J., Suzuki, F., Fujii, S., Arlinghaus, R.B., Czerniak, B.A. and Sen, S. (2004) 'Phosphorylation by aurora kinase A induces Mdm2-mediated destabilization and inhibition of p53', *Nat Genet*, 36(1), pp. 55-62.
- Kavsak, P., Rasmussen, R.K., Causing, C.G., Bonni, S., Zhu, H., Thomsen, G.H. and Wrana, J.L. (2000) 'Smad7 binds to Smurf2 to form an E3 ubiquitin ligase that targets the TGF beta receptor for degradation', *Mol Cell*, 6(6), pp. 1365-75.
- Kessler, D., Dethlefsen, S., Haase, I., Plomann, M., Hirche, F., Krieg, T. and Eckes, B. (2001) 'Fibroblasts in mechanically stressed collagen lattices assume a "synthetic" phenotype', *J Biol Chem*, 276(39), pp. 36575-85.
- Khwaja, A. (1999) 'Akt is more than just a Bad kinase', *Nature*, 401(6748), pp. 33-4.
- Kimura, M., Takagi, S. and Nakashima, S. (2018) 'Aurora A regulates the architecture of the Golgi apparatus', *Exp Cell Res*, 367(1), pp. 73-80.
- Kitamura, M. and Fine, L.G. (1999) 'The concept of glomerular self-defense', *Kidney Int*, 55(5), pp. 1639-71.
- Klahr, S. and Pukerson, M.L. (1994) 'The pathophysiology of obstructive nephropathy: the role of vasoactive compounds in the hemodynamic and structural abnormalities of the obstructed kidney', *Am J Kidney Dis*, 23(2), pp. 219-23.
- Klinkhammer, B.M., Goldschmeding, R., Floege, J. and Boor, P. (2017) 'Treatment of Renal Fibrosis-Turning Challenges into Opportunities', *Adv Chronic Kidney Dis*, 24(2), pp. 117-129.
- Kondo, S., Kagami, S., Urushihara, M., Kitamura, A., Shimizu, M., Strutz, F., Muller, G.A. and Kuroda, Y. (2004) 'Transforming growth factor-beta1 stimulates collagen matrix

remodeling through increased adhesive and contractive potential by human renal fibroblasts', *Biochim Biophys Acta*, 1693(2), pp. 91-100.

Kouskouti, A., Scheer, E., Staub, A., Tora, L. and Talianidis, I. (2004) 'Gene-specific modulation of TAF10 function by SET9-mediated methylation', *Mol Cell*, 14(2), pp. 175-82.

Kramann, R., Fleig, S.V., Schneider, R.K., Fabian, S.L., DiRocco, D.P., Maarouf, O., Wongboonsin, J., Ikeda, Y., Heckl, D., Chang, S.L., Rennke, H.G., Waikar, S.S. and Humphreys, B.D. (2015) 'Pharmacological GLI2 inhibition prevents myofibroblast cell-cycle progression and reduces kidney fibrosis', *J Clin Invest*, 125(8), pp. 2935-51.

Kretzschmar, M. and Massague, J. (1998) 'SMADs: mediators and regulators of TGF-beta signaling', *Curr Opin Genet Dev*, 8(1), pp. 103-11.

Kufer, T.A., Sillje, H.H., Korner, R., Gruss, O.J., Meraldi, P. and Nigg, E.A. (2002) 'Human TPX2 is required for targeting Aurora-A kinase to the spindle', *J Cell Biol*, 158(4), pp. 617-23.

Kulkarni, A.B. and Karlsson, S. (1993) 'Transforming growth factor-beta 1 knockout mice. A mutation in one cytokine gene causes a dramatic inflammatory disease', *Am J Pathol*, 143(1), pp. 3-9.

Lan, H.Y. (2011) 'Diverse roles of TGF-beta/Smads in renal fibrosis and inflammation', *Int J Biol Sci*, 7(7), pp. 1056-67.

Lan, H.Y., Mu, W., Tomita, N., Huang, X.R., Li, J.H., Zhu, H.J., Morishita, R. and Johnson, R.J. (2003) 'Inhibition of renal fibrosis by gene transfer of inducible Smad7 using ultrasound-microbubble system in rat UUO model', *J Am Soc Nephrol*, 14(6), pp. 1535-48.

LeBleu, V.S. and Kalluri, R. (2011) 'Blockade of PDGF receptor signaling reduces myofibroblast number and attenuates renal fibrosis', *Kidney Int*, 80(11), pp. 1119-21.

LeBleu, V.S., Taduri, G., O'Connell, J., Teng, Y., Cooke, V.G., Woda, C., Sugimoto, H. and Kalluri, R. (2013) 'Origin and function of myofibroblasts in kidney fibrosis', *Nat Med*, 19(8), pp. 1047-53.

Lehnertz, B., Rogalski, J.C., Schulze, F.M., Yi, L., Lin, S., Kast, J. and Rossi, F.M. (2011) 'p53-dependent transcription and tumor suppression are not affected in Set7/9-deficient mice', *Mol Cell*, 43(4), pp. 673-80.

LeMaire, S.A., Pannu, H., Tran-Fadulu, V., Carter, S.A., Coselli, J.S. and Milewicz, D.M. (2007) 'Severe aortic and arterial aneurysms associated with a TGFBR2 mutation', *Nat Clin Pract Cardiovasc Med*, 4(3), pp. 167-71.

Levey, A.S., Eckardt, K.U., Tsukamoto, Y., Levin, A., Coresh, J., Rossert, J., De Zeeuw, D., Hostetter, T.H., Lameire, N. and Eknoyan, G. (2005) 'Definition and classification of chronic

- kidney disease: a position statement from Kidney Disease: Improving Global Outcomes (KDIGO)', *Kidney Int*, 67(6), pp. 2089-100.
- Li, B. and Wang, J.H. (2011) 'Fibroblasts and myofibroblasts in wound healing: force generation and measurement', *J Tissue Viability*, 20(4), pp. 108-20.
- Li, J., Qu, X. and Bertram, J.F. (2009) 'Endothelial-myofibroblast transition contributes to the early development of diabetic renal interstitial fibrosis in streptozotocin-induced diabetic mice', *Am J Pathol*, 175(4), pp. 1380-8.
- Li, J., Qu, X., Yao, J., Caruana, G., Ricardo, S.D., Yamamoto, Y., Yamamoto, H. and Bertram, J.F. (2010) 'Blockade of endothelial-mesenchymal transition by a Smad3 inhibitor delays the early development of streptozotocin-induced diabetic nephropathy', *Diabetes*, 59(10), pp. 2612-24.
- Li, J.H., Huang, X.R., Zhu, H.J., Oldfield, M., Cooper, M., Truong, L.D., Johnson, R.J. and Lan, H.Y. (2004) 'Advanced glycation end products activate Smad signaling via TGF-beta-dependent and independent mechanisms: implications for diabetic renal and vascular disease', *Faseb j*, 18(1), pp. 176-8.
- Lin, S.L., Kisseleva, T., Brenner, D.A. and Duffield, J.S. (2008) 'Pericytes and perivascular fibroblasts are the primary source of collagen-producing cells in obstructive fibrosis of the kidney', *Am J Pathol*, 173(6), pp. 1617-27.
- Liu, H.C., Liao, T.N., Lee, T.C., Chuang, L.Y., Guh, J.Y., Liu, S.F., Hu, M.S., Yang, Y.L., Lin, S.H., Hung, M.Y., Huang, J.S., Hung, T.J., Chen, C.D., Chiang, T.A., Chan, J.Y., Chen, S.Y. and Yang, Y.L. (2006) 'Albumin induces cellular fibrosis by upregulating transforming growth factor-beta ligand and its receptors in renal distal tubule cells', *J Cell Biochem*, 97(5), pp. 956-68.
- Liu, L., Kimball, S., Liu, H., Holowatyj, A. and Yang, Z.Q. (2015) 'Genetic alterations of histone lysine methyltransferases and their significance in breast cancer', *Oncotarget*, 6(4), pp. 2466-82.
- Liu, Q., Kaneko, S., Yang, L., Feldman, R.I., Nicosia, S.V., Chen, J. and Cheng, J.Q. (2004) 'Aurora-A abrogation of p53 DNA binding and transactivation activity by phosphorylation of serine 215', *J Biol Chem*, 279(50), pp. 52175-82.
- Liu, X., Wen, F.Q., Kobayashi, T., Abe, S., Fang, Q., Piek, E., Bottinger, E.P., Roberts, A.B. and Rennard, S.I. (2003) 'Smad3 mediates the TGF-beta-induced contraction of type I collagen gels by mouse embryo fibroblasts', *Cell Motil Cytoskeleton*, 54(3), pp. 248-53.
- Liu, Y. (2004) 'Epithelial to mesenchymal transition in renal fibrogenesis: pathologic significance, molecular mechanism, and therapeutic intervention', *J Am Soc Nephrol*, 15(1), pp. 1-12.

- Liu, Z., Huang, X.R. and Lan, H.Y. (2012) 'Smad3 mediates ANG II-induced hypertensive kidney disease in mice', *Am J Physiol Renal Physiol*, 302(8), pp. F986-97.
- Lomberk, G., Wallrath, L. and Urrutia, R. (2006) 'The Heterochromatin Protein 1 family', *Genome Biol*, 7(7), p. 228.
- Luger, K., Mader, A.W., Richmond, R.K., Sargent, D.F. and Richmond, T.J. (1997) 'Crystal structure of the nucleosome core particle at 2.8 Å resolution', *Nature*, 389(6648), pp. 251-60.
- Lyons, R.M., Keski-Oja, J. and Moses, H.L. (1988) 'Proteolytic activation of latent transforming growth factor-beta from fibroblast-conditioned medium', *J Cell Biol*, 106(5), pp. 1659-65.
- Ma, L., Li, H., Zhang, S., Xiong, X., Chen, K., Jiang, P., Jiang, K. and Deng, G. (2018) 'Emodin ameliorates renal fibrosis in rats via TGF-beta1/Smad signaling pathway and function study of Smurf 2', *Int Urol Nephrol*, 50(2), pp. 373-382.
- Masatsugu, T. and Yamamoto, K. (2009) 'Multiple lysine methylation of PCAF by Set9 methyltransferase', *Biochem Biophys Res Commun*, 381(1), pp. 22-6.
- Massague, J. (2012) 'TGFbeta signalling in context', *Nat Rev Mol Cell Biol*, 13(10), pp. 616-30.
- Massague, J., Seoane, J. and Wotton, D. (2005) 'Smad transcription factors', *Genes Dev*, 19(23), pp. 2783-810.
- Matsui, T., Leung, D., Miyashita, H., Maksakova, I.A., Miyachi, H., Kimura, H., Tachibana, M., Lorincz, M.C. and Shinkai, Y. (2010) 'Proviral silencing in embryonic stem cells requires the histone methyltransferase ESET', *Nature*, 464(7290), pp. 927-31.
- Meng, F., Cheng, S., Ding, H., Liu, S., Liu, Y., Zhu, K., Chen, S., Lu, J., Xie, Y., Li, L., Liu, R., Shi, Z., Zhou, Y., Liu, Y.C., Zheng, M., Jiang, H., Lu, W., Liu, H. and Luo, C. (2015a) 'Discovery and Optimization of Novel, Selective Histone Methyltransferase SET7 Inhibitors by Pharmacophore- and Docking-Based Virtual Screening', *J Med Chem*, 58(20), pp. 8166-81.
- Meng, X.M., Nikolic-Paterson, D.J. and Lan, H.Y. (2016) 'TGF-beta: the master regulator of fibrosis', *Nat Rev Nephrol*, 12(6), pp. 325-38.
- Meng, X.M., Tang, P.M., Li, J. and Lan, H.Y. (2015b) 'TGF-beta/Smad signaling in renal fibrosis', *Front Physiol*, 6, p. 82.
- Meraldi, P., Honda, R. and Nigg, E.A. (2002) 'Aurora-A overexpression reveals tetraploidization as a major route to centrosome amplification in p53<sup>-/-</sup> cells', *Embo j*, 21(4), pp. 483-92.
- Meran, S. and Steadman, R. (2011) 'Fibroblasts and myofibroblasts in renal fibrosis', *Int J Exp Pathol*, 92(3), pp. 158-67.

- Minkovsky, A., Sahakyan, A., Rankin-Gee, E., Bonora, G., Patel, S. and Plath, K. (2014) 'The Mbd1-Atf7ip-Setdb1 pathway contributes to the maintenance of X chromosome inactivation', *Epigenetics Chromatin*, 7, p. 12.
- Miyazono, K., Maeda, S. and Imamura, T. (2005) 'BMP receptor signaling: transcriptional targets, regulation of signals, and signaling cross-talk', *Cytokine Growth Factor Rev*, 16(3), pp. 251-63.
- Montenegro, M.F., Sanchez-Del-Campo, L., Gonzalez-Guerrero, R., Martinez-Barba, E., Pinero-Madrona, A., Cabezas-Herrera, J. and Rodriguez-Lopez, J.N. (2016) 'Tumor suppressor SET9 guides the epigenetic plasticity of breast cancer cells and serves as an early-stage biomarker for predicting metastasis', *Oncogene*, 35(47), pp. 6143-6152.
- Moon, J.A., Kim, H.T., Cho, I.S., Sheen, Y.Y. and Kim, D.K. (2006) 'IN-1130, a novel transforming growth factor-beta type I receptor kinase (ALK5) inhibitor, suppresses renal fibrosis in obstructive nephropathy', *Kidney Int*, 70(7), pp. 1234-43.
- Morera, L., Lubbert, M. and Jung, M. (2016) 'Targeting histone methyltransferases and demethylases in clinical trials for cancer therapy', *Clin Epigenetics*, 8, p. 57.
- Murray, K. (1964) 'THE OCCURRENCE OF EPSILON-N-METHYL LYSINE IN HISTONES', *Biochemistry*, 3, pp. 10-5.
- Nakao, A., Afrakhte, M., Moren, A., Nakayama, T., Christian, J.L., Heuchel, R., Itoh, S., Kawabata, M., Heldin, N.E., Heldin, C.H. and ten Dijke, P. (1997) 'Identification of Smad7, a TGFbeta-inducible antagonist of TGF-beta signalling', *Nature*, 389(6651), pp. 631-5.
- Naruganahalli, K.S., Lakshmanan, M., Dastidar, S.G. and Ray, A. (2006) 'Therapeutic potential of Aurora kinase inhibitors in cancer', *Curr Opin Investig Drugs*, 7(12), pp. 1044-51.
- Ng, Y.Y., Huang, T.P., Yang, W.C., Chen, Z.P., Yang, A.H., Mu, W., Nikolic-Paterson, D.J., Atkins, R.C. and Lan, H.Y. (1998) 'Tubular epithelial-myofibroblast transdifferentiation in progressive tubulointerstitial fibrosis in 5/6 nephrectomized rats', *Kidney Int*, 54(3), pp. 864-76.
- Nishioka, K., Chuikov, S., Sarma, K., Erdjument-Bromage, H., Allis, C.D., Tempst, P. and Reinberg, D. (2002) 'Set9, a novel histone H3 methyltransferase that facilitates transcription by precluding histone tail modifications required for heterochromatin formation', *Genes Dev*, 16(4), pp. 479-89.
- Oudhoff, M.J., Braam, M.J.S., Freeman, S.A., Wong, D., Rattray, D.G., Wang, J., Antignano, F., Snyder, K., Refaeli, I., Hughes, M.R., McNagny, K.M., Gold, M.R., Arrowsmith, C.H., Sato, T., Rossi, F.M.V., Tatlock, J.H., Owen, D.R., Brown, P.J. and Zaph, C. (2016) 'SETD7 Controls Intestinal Regeneration and Tumorigenesis by Regulating Wnt/beta-Catenin and Hippo/YAP Signaling', *Dev Cell*, 37(1), pp. 47-57.

- Pines, M. (2008) 'Targeting TGFbeta signaling to inhibit fibroblast activation as a therapy for fibrosis and cancer: effect of halofuginone', *Expert Opin Drug Discov*, 3(1), pp. 11-20.
- Preuss, H.G. (1993) 'Basics of renal anatomy and physiology', *Clin Lab Med*, 13(1), pp. 1-11.
- Pugacheva, E.N. and Golemis, E.A. (2005) 'The focal adhesion scaffolding protein HEF1 regulates activation of the Aurora-A and Nek2 kinases at the centrosome', *Nat Cell Biol*, 7(10), pp. 937-46.
- Pugacheva, E.N., Jablonski, S.A., Hartman, T.R., Henske, E.P. and Golemis, E.A. (2007) 'HEF1-dependent Aurora A activation induces disassembly of the primary cilium', *Cell*, 129(7), pp. 1351-63.
- RamachandraRao, S.P., Zhu, Y., Ravasi, T., McGowan, T.A., Toh, I., Dunn, S.R., Okada, S., Shaw, M.A. and Sharma, K. (2009) 'Pirfenidone is renoprotective in diabetic kidney disease', *J Am Soc Nephrol*, 20(8), pp. 1765-75.
- Rea, S., Eisenhaber, F., O'Carroll, D., Strahl, B.D., Sun, Z.W., Schmid, M., Opravil, S., Mechtler, K., Ponting, C.P., Allis, C.D. and Jenuwein, T. (2000) 'Regulation of chromatin structure by site-specific histone H3 methyltransferases', *Nature*, 406(6796), pp. 593-9.
- Rodon, J., Carducci, M.A., Sepulveda-Sanchez, J.M., Azaro, A., Calvo, E., Seoane, J., Brana, I., Sicart, E., Gueorguieva, I., Cleverly, A.L., Pillay, N.S., Desai, D., Estrem, S.T., Paz-Ares, L., Holdhoff, M., Blakeley, J., Lahn, M.M. and Baselga, J. (2015) 'First-in-human dose study of the novel transforming growth factor-beta receptor I kinase inhibitor LY2157299 monohydrate in patients with advanced cancer and glioma', *Clin Cancer Res*, 21(3), pp. 553-60.
- Rodriguez-Paredes, M., Martinez de Paz, A., Simo-Riudalbas, L., Sayols, S., Moutinho, C., Moran, S., Villanueva, A., Vazquez-Cedeira, M., Lazo, P.A., Carneiro, F., Moura, C.S., Vieira, J., Teixeira, M.R. and Esteller, M. (2014) 'Gene amplification of the histone methyltransferase SETDB1 contributes to human lung tumorigenesis', *Oncogene*, 33(21), pp. 2807-13.
- Ruthenburg, A.J., Li, H., Patel, D.J. and Allis, C.D. (2007) 'Multivalent engagement of chromatin modifications by linked binding modules', *Nat Rev Mol Cell Biol*, 8(12), pp. 983-94.
- Ryu, H., Lee, J., Hagerty, S.W., Soh, B.Y., McAlpin, S.E., Cormier, K.A., Smith, K.M. and Ferrante, R.J. (2006) 'ESET/SETDB1 gene expression and histone H3 (K9) trimethylation in Huntington's disease', *Proc Natl Acad Sci U S A*, 103(50), pp. 19176-81.
- Sarris, M., Nikolaou, K. and Talianidis, I. (2014) 'Context-specific regulation of cancer epigenomes by histone and transcription factor methylation', *Oncogene*, 33(10), pp. 1207-17.

- Sasaki, K., Doi, S., Nakashima, A., Irifuku, T., Yamada, K., Kokoroishi, K., Ueno, T., Doi, T., Hida, E., Arihiro, K., Kohno, N. and Masaki, T. (2016) 'Inhibition of SET Domain-Containing Lysine Methyltransferase 7/9 Ameliorates Renal Fibrosis', *J Am Soc Nephrol*, 27(1), pp. 203-15.
- Sato, M., Muragaki, Y., Saika, S., Roberts, A.B. and Ooshima, A. (2003) 'Targeted disruption of TGF-beta1/Smad3 signaling protects against renal tubulointerstitial fibrosis induced by unilateral ureteral obstruction', *J Clin Invest*, 112(10), pp. 1486-94.
- Scharer, C.D., Laycock, N., Osunkoya, A.O., Logani, S., McDonald, J.F., Benigno, B.B. and Moreno, C.S. (2008) 'Aurora kinase inhibitors synergize with paclitaxel to induce apoptosis in ovarian cancer cells', *J Transl Med*, 6, p. 79.
- Schmierer, B. and Hill, C.S. (2007) 'TGFbeta-SMAD signal transduction: molecular specificity and functional flexibility', *Nat Rev Mol Cell Biol*, 8(12), pp. 970-82.
- Schnabl, B., Kweon, Y.O., Frederick, J.P., Wang, X.F., Rippe, R.A. and Brenner, D.A. (2001) 'The role of Smad3 in mediating mouse hepatic stellate cell activation', *Hepatology*, 34(1), pp. 89-100.
- Schneider-Poetsch, T., Ju, J., Eyler, D.E., Dang, Y., Bhat, S., Merrick, W.C., Green, R., Shen, B. and Liu, J.O. (2010) 'Inhibition of eukaryotic translation elongation by cycloheximide and lactimidomycin', *Nat Chem Biol*, 6(3), pp. 209-217.
- Schultz, D.C., Ayyanathan, K., Negorev, D., Maul, G.G. and Rauscher, F.J., 3rd (2002) 'SETDB1: a novel KAP-1-associated histone H3, lysine 9-specific methyltransferase that contributes to HP1-mediated silencing of euchromatic genes by KRAB zinc-finger proteins', *Genes Dev*, 16(8), pp. 919-32.
- Science, U.N.L.o. (2015) A Randomized, Double-Masked, Placebo-Controlled, Multicenter, Phase 2 Study to Evaluate the Safety and Renal Efficacy of LY2382770 in Patients With Diabetic Kidney Disease Due to Type 1 or Type 2 Diabetes. Available at: <https://clinicaltrials.gov/ct2/show/NCT01113801>.
- Sharma, K., Ix, J.H., Mathew, A.V., Cho, M., Pflueger, A., Dunn, S.R., Francos, B., Sharma, S., Falkner, B., McGowan, T.A., Donohue, M., Ramachandrarao, S., Xu, R., Fervenza, F.C. and Kopp, J.B. (2011) 'Pirfenidone for diabetic nephropathy', *J Am Soc Nephrol*, 22(6), pp. 1144-51.
- Sharma, K., Jin, Y., Guo, J. and Ziyadeh, F.N. (1996) 'Neutralization of TGF-beta by anti-TGF-beta antibody attenuates kidney hypertrophy and the enhanced extracellular matrix gene expression in STZ-induced diabetic mice', *Diabetes*, 45(4), pp. 522-30.
- Shi, Y. and Massague, J. (2003) 'Mechanisms of TGF-beta signaling from cell membrane to the nucleus', *Cell*, 113(6), pp. 685-700.

- Shimomura, T., Hasako, S., Nakatsuru, Y., Mita, T., Ichikawa, K., Kodera, T., Sakai, T., Nambu, T., Miyamoto, M., Takahashi, I., Miki, S., Kawanishi, N., Ohkubo, M., Kotani, H. and Iwasawa, Y. (2010) 'MK-5108, a highly selective Aurora-A kinase inhibitor, shows antitumor activity alone and in combination with docetaxel', *Mol Cancer Ther*, 9(1), pp. 157-66.
- Shuttleworth, V.G., Gaughan, L., Nawafa, L., Mooney, C.A., Cobb, S.L., Sheerin, N.S. and Logan, I.R. (2018) 'The methyltransferase SET9 regulates TGFB1 activation of renal fibroblasts via interaction with SMAD3', *J Cell Sci*, 131(1).
- Siegel, P.M. and Massague, J. (2003) 'Cytostatic and apoptotic actions of TGF-beta in homeostasis and cancer', *Nat Rev Cancer*, 3(11), pp. 807-21.
- Song, Y.J., Choi, J.H. and Lee, H. (2015) 'Setdb1 is required for myogenic differentiation of C2C12 myoblast cells via maintenance of MyoD expression', *Mol Cells*, 38(4), pp. 362-72.
- Sorrell, J.M. and Caplan, A.I. (2009) 'Fibroblasts-a diverse population at the center of it all', *Int Rev Cell Mol Biol*, 276, pp. 161-214.
- Spyropoulou, A., Gargalionis, A., Dalagiorgou, G., Adamopoulos, C., Papavassiliou, K.A., Lea, R.W., Piperi, C. and Papavassiliou, A.G. (2014) 'Role of histone lysine methyltransferases SUV39H1 and SETDB1 in gliomagenesis: modulation of cell proliferation, migration, and colony formation', *Neuromolecular Med*, 16(1), pp. 70-82.
- Sraer, J.D., Delarue, F., Hagege, J., Feunteun, J., Pinet, F., Nguyen, G. and Rondeau, E. (1996) 'Stable cell lines of T-SV40 immortalized human glomerular mesangial cells', *Kidney Int*, 49(1), pp. 267-70.
- Strahl, B.D. and Allis, C.D. (2000) 'The language of covalent histone modifications', *Nature*, 403(6765), pp. 41-5.
- Strahl, B.D., Briggs, S.D., Brame, C.J., Caldwell, J.A., Koh, S.S., Ma, H., Cook, R.G., Shabanowitz, J., Hunt, D.F., Stallcup, M.R. and Allis, C.D. (2001) 'Methylation of histone H4 at arginine 3 occurs in vivo and is mediated by the nuclear receptor coactivator PRMT1', *Curr Biol*, 11(12), pp. 996-1000.
- Strutz, F., Okada, H., Lo, C.W., Danoff, T., Carone, R.L., Tomaszewski, J.E. and Neilson, E.G. (1995) 'Identification and characterization of a fibroblast marker: FSP1', *J Cell Biol*, 130(2), pp. 393-405.
- Strutz, F. and Zeisberg, M. (2006) 'Renal fibroblasts and myofibroblasts in chronic kidney disease', *J Am Soc Nephrol*, 17(11), pp. 2992-8.
- Subramanian, K., Jia, D., Kapoor-Vazirani, P., Powell, D.R., Collins, R.E., Sharma, D., Peng, J., Cheng, X. and Vertino, P.M. (2008) 'Regulation of estrogen receptor alpha by the SET7 lysine methyltransferase', *Mol Cell*, 30(3), pp. 336-47.

- Sun, G., Reddy, M.A., Yuan, H., Lanting, L., Kato, M. and Natarajan, R. (2010) 'Epigenetic histone methylation modulates fibrotic gene expression', *J Am Soc Nephrol*, 21(12), pp. 2069-80.
- Sun, Q.Y., Ding, L.W., Xiao, J.F., Chien, W., Lim, S.L., Hattori, N., Goodglick, L., Chia, D., Mah, V., Alavi, M., Kim, S.R., Doan, N.B., Said, J.W., Loh, X.Y., Xu, L., Liu, L.Z., Yang, H., Hayano, T., Shi, S., Xie, D., Lin, D.C. and Koeffler, H.P. (2015) 'SETDB1 accelerates tumorigenesis by regulating the WNT signalling pathway', *J Pathol*, 235(4), pp. 559-70.
- Sun, Y.B., Qu, X., Caruana, G. and Li, J. (2016) 'The origin of renal fibroblasts/myofibroblasts and the signals that trigger fibrosis', *Differentiation*, 92(3), pp. 102-107.
- Tachibana, K., Gotoh, E., Kawamata, N., Ishimoto, K., Uchihara, Y., Iwanari, H., Sugiyama, A., Kawamura, T., Mochizuki, Y., Tanaka, T., Sakai, J., Hamakubo, T., Kodama, T. and Doi, T. (2015) 'Analysis of the subcellular localization of the human histone methyltransferase SETDB1', *Biochem Biophys Res Commun*, 465(4), pp. 725-31.
- Takada, I., Mihara, M., Suzawa, M., Ohtake, F., Kobayashi, S., Igarashi, M., Youn, M.Y., Takeyama, K., Nakamura, T., Mezaki, Y., Takezawa, S., Yogiashi, Y., Kitagawa, H., Yamada, G., Takada, S., Minami, Y., Shibuya, H., Matsumoto, K. and Kato, S. (2007) 'A histone lysine methyltransferase activated by non-canonical Wnt signalling suppresses PPAR-gamma transactivation', *Nat Cell Biol*, 9(11), pp. 1273-85.
- Tan, S.J. and Hewitson, T.D. (2016) 'Propagation and Culture of Human Renal Fibroblasts', *Methods Mol Biol*, 1397, pp. 11-23.
- Tang, A., Gao, K., Chu, L., Zhang, R., Yang, J. and Zheng, J. (2017) 'Aurora kinases: novel therapy targets in cancers', *Oncotarget*, 8(14), pp. 23937-23954.
- Tomasek, J.J., Gabbiani, G., Hinz, B., Chaponnier, C. and Brown, R.A. (2002) 'Myofibroblasts and mechano-regulation of connective tissue remodelling', *Nat Rev Mol Cell Biol*, 3(5), pp. 349-63.
- Trachtman, H., Fervenza, F.C., Gipson, D.S., Heering, P., Jayne, D.R., Peters, H., Rota, S., Remuzzi, G., Rump, L.C., Sellin, L.K., Heaton, J.P., Streisand, J.B., Hard, M.L., Ledbetter, S.R. and Vincenti, F. (2011) 'A phase 1, single-dose study of fresolimumab, an anti-TGF-beta antibody, in treatment-resistant primary focal segmental glomerulosclerosis', *Kidney Int*, 79(11), pp. 1236-43.
- Turner, J.M., Bauer, C., Abramowitz, M.K., Melamed, M.L. and Hostetter, T.H. (2012) 'Treatment of chronic kidney disease', *Kidney Int*, 81(4), pp. 351-62.
- Vader, G. and Lens, S.M. (2008) 'The Aurora kinase family in cell division and cancer', *Biochim Biophys Acta*, 1786(1), pp. 60-72.

- Vega, G., Alarcon, S. and San Martin, R. (2016) 'The cellular and signalling alterations conducted by TGF-beta contributing to renal fibrosis', *Cytokine*, 88, pp. 115-125.
- Verrecchia, F. and Mauviel, A. (2007a) 'Transforming growth factor-beta and fibrosis', *World J Gastroenterol*, 13(22), pp. 3056-62.
- Vincenti, F., Fervenza, F.C., Campbell, K.N., Diaz, M., Gesualdo, L., Nelson, P., Praga, M., Radhakrishnan, J., Sellin, L., Singh, A., Thornley-Brown, D., Veronese, F.V., Accomando, B., Engstrand, S., Ledbetter, S., Lin, J., Neylan, J. and Tumlin, J. (2017) 'A Phase 2, Double-Blind, Placebo-Controlled, Randomized Study of Fresolimumab in Patients With Steroid-Resistant Primary Focal Segmental Glomerulosclerosis', *Kidney Int Rep*, 2(5), pp. 800-810.
- Wakabayashi, Y., Tamiya, T., Takada, I., Fukaya, T., Sugiyama, Y., Inoue, N., Kimura, A., Morita, R., Kashiwagi, I., Takimoto, T., Nomura, M. and Yoshimura, A. (2011) 'Histone 3 lysine 9 (H3K9) methyltransferase recruitment to the interleukin-2 (IL-2) promoter is a mechanism of suppression of IL-2 transcription by the transforming growth factor-beta-Smad pathway', *J Biol Chem*, 286(41), pp. 35456-65.
- Wan, X.B., Long, Z.J., Yan, M., Xu, J., Xia, L.P., Liu, L., Zhao, Y., Huang, X.F., Wang, X.R., Zhu, X.F., Hong, M.H. and Liu, Q. (2008) 'Inhibition of Aurora-A suppresses epithelial-mesenchymal transition and invasion by downregulating MAPK in nasopharyngeal carcinoma cells', *Carcinogenesis*, 29(10), pp. 1930-7.
- Wang, C., Li, Y., Zhang, H., Liu, F., Cheng, Z., Wang, D., Wang, G., Xu, H., Zhao, Y., Cao, L. and Li, F. (2014) 'Oncogenic PAK4 regulates Smad2/3 axis involving gastric tumorigenesis', *Oncogene*, 33(26), pp. 3473-84.
- Wang, G., Matsuura, I., He, D. and Liu, F. (2009) 'Transforming growth factor-beta-inducible phosphorylation of Smad3', *J Biol Chem*, 284(15), pp. 9663-73.
- Wang, H., Cao, R., Xia, L., Erdjument-Bromage, H., Borchers, C., Tempst, P. and Zhang, Y. (2001) 'Purification and Functional Characterization of a Histone H3-Lysine 4-Specific Methyltransferase', *Molecular Cell*, 8(6), pp. 1207-1217.
- Wang, W., Koka, V. and Lan, H.Y. (2005) 'Transforming growth factor-beta and Smad signalling in kidney diseases', *Nephrology (Carlton)*, 10(1), pp. 48-56.
- Watanabe, T.K., Suzuki, M., Omori, Y., Hishigaki, H., Horie, M., Kanemoto, N., Fujiwara, T., Nakamura, Y. and Takahashi, E. (1997) 'Cloning and characterization of a novel member of the human Mad gene family (MADH6)', *Genomics*, 42(3), pp. 446-51.
- Wong, C.M., Wei, L., Law, C.T., Ho, D.W., Tsang, F.H., Au, S.L., Sze, K.M., Lee, J.M., Wong, C.C. and Ng, I.O. (2016) 'Up-regulation of histone methyltransferase SETDB1 by multiple mechanisms in hepatocellular carcinoma promotes cancer metastasis', *Hepatology*, 63(2), pp. 474-87.

- Wu, J.C., Chen, T.Y., Yu, C.T., Tsai, S.J., Hsu, J.M., Tang, M.J., Chou, C.K., Lin, W.J., Yuan, C.J. and Huang, C.Y. (2005) 'Identification of V23RalA-Ser194 as a critical mediator for Aurora-A-induced cellular motility and transformation by small pool expression screening', *J Biol Chem*, 280(10), pp. 9013-22.
- Wynn, T.A. (2007) 'Common and unique mechanisms regulate fibrosis in various fibroproliferative diseases', *J Clin Invest*, 117(3), pp. 524-9.
- Xiao, Z., Liu, X., Henis, Y.I. and Lodish, H.F. (2000) 'A distinct nuclear localization signal in the N terminus of Smad 3 determines its ligand-induced nuclear translocation', *Proc Natl Acad Sci U S A*, 97(14), pp. 7853-8.
- Xu, W., Chen, H., Du, K., Asahara, H., Tini, M., Emerson, B.M., Montminy, M. and Evans, R.M. (2001) 'A transcriptional switch mediated by cofactor methylation', *Science*, 294(5551), pp. 2507-11.
- Yang, J., Shultz, R.W., Mars, W.M., Wegner, R.E., Li, Y., Dai, C., Nejak, K. and Liu, Y. (2002a) 'Disruption of tissue-type plasminogen activator gene in mice reduces renal interstitial fibrosis in obstructive nephropathy', *J Clin Invest*, 110(10), pp. 1525-38.
- Yang, L., Mei, Q., Zielinska-Kwiatkowska, A., Matsui, Y., Blackburn, M.L., Benedetti, D., Krumm, A.A., Taborsky, G.J., Jr. and Chansky, H.A. (2003) 'An ERG (ets-related gene)-associated histone methyltransferase interacts with histone deacetylases 1/2 and transcription co-repressors mSin3A/B', *Biochem J*, 369(Pt 3), pp. 651-7.
- Yang, L., Xia, L., Wu, D.Y., Wang, H., Chansky, H.A., Schubach, W.H., Hickstein, D.D. and Zhang, Y. (2002b) 'Molecular cloning of ESET, a novel histone H3-specific methyltransferase that interacts with ERG transcription factor', *Oncogene*, 21(1), pp. 148-52.
- Zakrzewicz, D., Zakrzewicz, A., Didiasova, M., Korencak, M., Kosanovic, D., Schermuly, R.T., Markart, P. and Wygrecka, M. (2015) 'Elevated protein arginine methyltransferase 1 expression regulates fibroblast motility in pulmonary fibrosis', *Biochim Biophys Acta*, 1852(12), pp. 2678-88.
- Zeisberg, E.M., Potenta, S.E., Sugimoto, H., Zeisberg, M. and Kalluri, R. (2008) 'Fibroblasts in kidney fibrosis emerge via endothelial-to-mesenchymal transition', *J Am Soc Nephrol*, 19(12), pp. 2282-7.
- Zeisberg, M. and Kalluri, R. (2013) 'Cellular mechanisms of tissue fibrosis. 1. Common and organ-specific mechanisms associated with tissue fibrosis', *Am J Physiol Cell Physiol*, 304(3), pp. C216-25.
- Zhang, J.H., Chung, T.D. and Oldenburg, K.R. (1999) 'A Simple Statistical Parameter for Use in Evaluation and Validation of High Throughput Screening Assays', *J Biomol Screen*, 4(2), pp. 67-73.

- Zhao, J., Shi, W., Wang, Y.L., Chen, H., Bringas, P., Jr., Datto, M.B., Frederick, J.P., Wang, X.F. and Warburton, D. (2002) 'Smad3 deficiency attenuates bleomycin-induced pulmonary fibrosis in mice', *Am J Physiol Lung Cell Mol Physiol*, 282(3), pp. L585-93.
- Zhou, H., Kuang, J., Zhong, L., Kuo, W.L., Gray, J.W., Sahin, A., Brinkley, B.R. and Sen, S. (1998) 'Tumour amplified kinase STK15/BTAK induces centrosome amplification, aneuploidy and transformation', *Nat Genet*, 20(2), pp. 189-93.
- Ziv, E., Cauley, J., Morin, P.A., Saiz, R. and Browner, W.S. (2001) 'Association between the T29-->C polymorphism in the transforming growth factor beta1 gene and breast cancer among elderly white women: The Study of Osteoporotic Fractures', *Jama*, 285(22), pp. 2859-63.
- Ziyadeh, F.N., Hoffman, B.B., Han, D.C., Iglesias-De La Cruz, M.C., Hong, S.W., Isono, M., Chen, S., McGowan, T.A. and Sharma, K. (2000) 'Long-term prevention of renal insufficiency, excess matrix gene expression, and glomerular mesangial matrix expansion by treatment with monoclonal anti-transforming growth factor-beta antibody in db/db diabetic mice', *Proc Natl Acad Sci U S A*, 97(14), pp. 8015-20.